C 51.17/12:992/5

Tech Notes

May 1992

PB92-925905

PENNSYLVANIA STATE UNIVERSITY
MAY 21 1992
DOCUMENTS COLLECTION
U.S. Depository Copy

Technology fact sheets from Federal laboratories

NTIS
U.S. DEPARTMENT OF COMMERCE
National Technical Information Service
Center for the Utilization of Federal Technology

U.S. DEPARTMENT OF COMMERCE
Barbara H. Franklin, Secretary of Commerce

National Technical Information Service
Donald R. Johnson, Acting Director

ISSN 0889-8464

COPYRIGHT WARNING
International Copyright © National Technical Information Service, 1992. All portions of this publication are protected against copying or other reproduction outside of the United States under the provisions of Article II of the Universal Copyright Convention. United States copyright is not asserted under the United States Copyright Law, Title 17, United States Code.

The Secretary of Commerce has determined that the publication of this periodical is necessary in the transaction of the public business required by law of this department. Use of funds for printing this periodical has been approved by the Director of the Office of Management and Budget through 1992.

Tech Notes

Highlighting Selected U.S. Government Technology & Resources

May 1992

Contents

Agriculture & Food 321
Computers 325
Electrotechnology 331
Energy 348
Engineering 351
Environmental Science & Technology 376
Manufacturing, Machinery & Tools 378
Materials 389
Medicine & Biology 394
Physical Sciences 404
Transportation & Components 409

Published monthly by the National Technical Information Service (NTIS), Tech Notes bring together individual one- to two-page fact sheets prepared by Federal agencies, their laboratories, or contractors. These fact sheets highlight current Federal technology determined to have commercial or practical application. Topics cover new processes, materials, techniques, software, instrumentation, and resources.

Some of the current sources are the Department of the Navy, Department of the Army, NASA, Department of Energy, Environmental Protection Agency, Department of the Interior, and the Department of Agriculture.

Special assistance is provided by the Federal Laboratory Consortium.

Change of address or questions concerning subscriptions should be sent to:
Subscriptions Department
National Technical Information Service
Springfield, VA 22161
(703) 487-4630

Suggestions, comments, or questions concerning Tech Notes should be directed to:
Tech Notes Editor
Room 300B F
National Technical Information Service
Springfield, VA 22161
(703) 487-4805

How to Use Tech Notes

Every Tech Notes fact sheet lists a source for additional information. The source of this information may be a special support package from the originating agency, a personal contact, a licensing opportunity, or a backup report available from NTIS.

Each fact sheet also is perforated to allow for easy removal for those subscribers who may wish to keep a special fact sheet file or route to others in their organization

Sources of Further Backup Information

Below are two representative examples of how each Tech Note fact sheet provides you with a source of further information. In most cases, this information is provided directly by the agency or its laboratory.

However, there are cases where NTIS is the source for backup documentation. In these cases, use the order form at the end.

Examples:

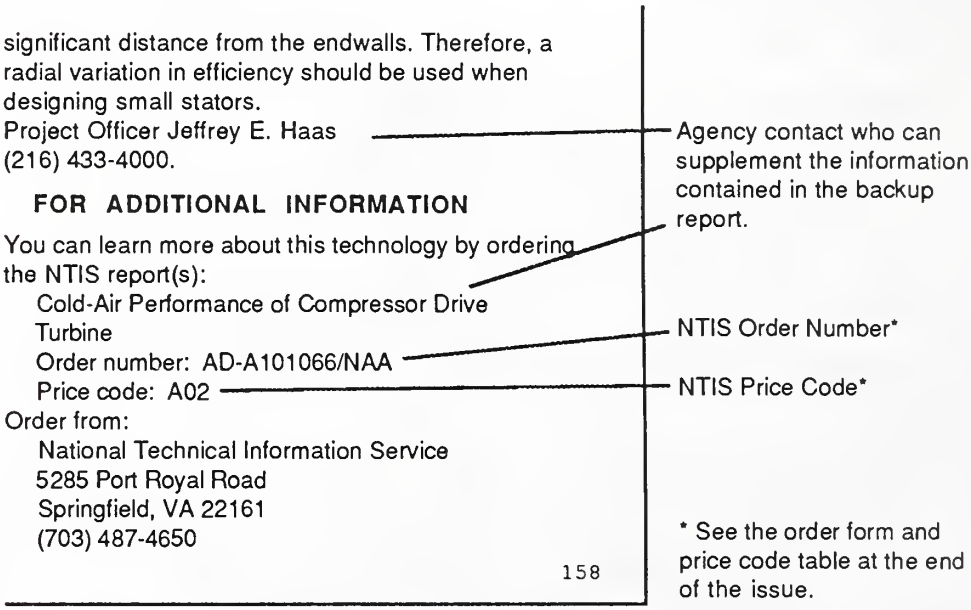
significant distance from the endwalls. Therefore, a radial variation in efficiency should be used when designing small stators.
Project Officer Jeffrey E. Haas
(216) 433-4000.
FOR ADDITIONAL INFORMATION
You can learn more about this technology by ordering the NTIS report(s):
Cold-Air Performance of Compressor Drive Turbine
Order number: AD-A101066/NAA
Price code: A02
Order from:
National Technical Information Service
5285 Port Royal Road
Springfield, VA 22161
(703) 487-4650
158
Agency contact who can supplement the information contained in the backup report.
NTIS Order Number*
NTIS Price Code*
* See the order form and price code table at the end of the issue.

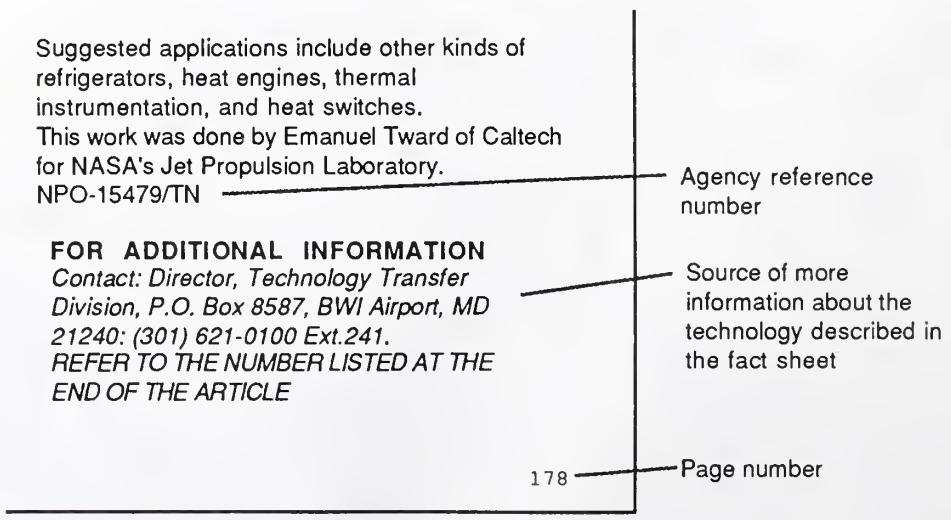
Suggested applications include other kinds of refrigerators, heat engines, thermal instrumentation, and heat switches.
This work was done by Emanuel Tward of Caltech for NASA's Jet Propulsion Laboratory.
NPO-15479/TN
FOR ADDITIONAL INFORMATION
Contact: Director, Technology Transfer Division, P.O. Box 8587, BWI Airport, MD 21240: (301) 621-0100 Ext.241.
REFER TO THE NUMBER LISTED AT THE END OF THE ARTICLE
178
Agency reference number
Source of more information about the technology described in the fact sheet
Page number

Tech Notes Title List for May 1992

Agriculture & Food

0321 Dwarf Daylily Debuts This Fall

0322 Fries From New Spud

0323 Lakebed Sediment Cut by Farming Practices

0324 Monitoring and Controlling Hydroponic Flow—A simple apparatus maintains the required slight suction while overcoming gravity effects.

Other Items of Interest

0404 Please Release Me—But Slowly

Computers

0325 SLALOM: 'Gold Standard' for Benchmarking Scientific Computers

Software

0326 Aid for Simulating Digital Flight Control Systems—A computer program translates descriptions of systems into programs for simulation.

0327 Library of Subprograms in FORTRAN 77—Subprograms can be called upon as needed to perform specific computations.

0328 Software-Design-Analyzer System—CRISP-90 provides the software designer with a medium that facilitates alterations.

0329 Software for Depiction of Three-Dimensional Objects—This program enables the user to build, manipulate, and display hierarchical three-dimensional objects.

0330 Software for Simulation of Development of Software—Personnel, resources, errors, and other realistic factors are represented in the simulation.

Other Items of Interest

0336 Knowledge-Based Flight-Status Monitor—Telemetered data from advanced aircraft would be processed automatically to detect failures.

0331 Gallium Arsenide/Germanium Solar Cells

Electrotechnology

0331 Gallium Arsenide/Germanium Solar Cells

0332 Integrated Composites Center

0333 Altering Interline Transfer in a CCD To Reduce Saturation—Charges accumulated during part of a frame period would be dumped.

0334 Automatic Rejection of Multimode Laser Pulses—Characteristic modulation is detected, enabling the rejection of multimode signals.

0335 Faster Computation of Far Fields of Dish Antennas—A modified Zernike-polynomial approach reduces the number of terms in the numerical integration.

0336 Knowledge-Based Flight-Status Monitor—Telemetered data from advanced aircraft would be processed automatically to detect failures.

0337 Lightweight, Flat Battery Case—Materials are chosen to increase strength while reducing weight and electrical resistance. (Licensing Opportunity)

0338 Rugged Direct-Current Transducer—The solid core withstands mechanical and thermal shocks. (Licensing Opportunity)

0339 Si/IrSi3 Schottky-Barrier Infrared Detectors—Ir and Si are codeposited in stoichiometric ratio to suppress mixed Ir/Si phases. (Licensing Opportunity)

0340 Solid-State Imaging Device With Carbon Film—The film reduces Fresnel reflections and dissipates static electric charges.

0341 Two-Period Gratings for Surface-Emitting Lasers—More light is reflected back into the lasers. (Licensing Opportunity)

0342 Wideband Phase-Licked Angle Modulator—The modulator can be designed independently of the phase-locked loop. (Licensing Opportunity)

Software

0343 Program Processes SAR Data—The MacMultiview program computes polarimetric and other images.

Testing & Instrumentation

0344 Holographic Wafer Inspection

0345 Characterization of Electrical Response of Photodetector—Fourier analysis of input and output yields electrical frequency response.

0346 Multiaperture Spectrometer—Advantages would be a convenient two-dimensional spectral image, fewer components, and greater efficiency.

0347 Spaceborne Microwave Imagers—Principles and practices are described.

Energy

0348 Characterizing the Solar Ultraviolet Resource

0349 NiF2 Cathodes for Rechargeable Na Batteries—Energy densities are higher than with metal chlorides.

0350 Regenerative Hydride Heat Pump—A cyclical regenerative heating scheme would increase efficiency. (Licensing Opportunity)

Engineering

0351 Artificial Intelligence in Computational Fluid Dynamics—Four AI systems are compared.

0352 Computed Hypersonic Viscous Flows Over Delta Wings—A conical Navier-Stokes algorithm accurately predicts shocks and pressure fields.

0353 Direct-Link Prehensor—An operator-powered mechanical hand gives protection, dexterity, and proximity to the work. (Licensing Opportunity)

0354 Direct Finite-Difference Simulations of Turbulent Flow—An upwind finite-difference scheme is compared with other numerical-integration schemes.

0355 Frequency-Domain Identification of Aeroelastic Modes—Data from flight tests support the choice of the frequency-sweep method.

0356 Dynamic Analyses Including Joints of Truss Structures—A straightforward method is used to determine stiffness and damping coefficients.

0357 Evaluation of Performance of a Telerobot—Various tasks were performed with and without force feedback.

0358 A General-Coordinate Formulation for Boundary-Layer Flow—The general coordinates need not be orthogonal.

0359 Generation of Surface Grids From Data Points—Grids are constructed by interpolation and blending of patches.

0360 Investigation of Tapered Tension/Torsion Strap—A tapered strap provides more torque than a parallel one does.

0361 Lightweight Valve Closes Duct Quickly—A balloon expands to block the duct. (Licensing Opportunity)

0362 Lock for Valve Stem—Readily available materials and handtools are used to make a simple but effective device. (Licensing Opportunity)

0363 Navier-Stokes Computations on Zonal Grids—Flows about a wind and an airplane are simulated.

0364 Processing Particle-Streak Imagery on a Personal Computer—Streak patterns are used to obtain maps of flow-velocity vectors.

0365 Reducing Water/Hull Drag by Injecting Air Into Grooves—A proposed method would require much less air than does the microbubble-injection method. (Licensing Opportunity)

0366 Two Techniques for Suppressing Vibrations in Structures—The techniques are based on bridge feedback and a criterion for placement of actuators.

Software

0367 Integrated Analysis Capability Program—This modular software system facilitates multidisciplinary analyses of structures and other systems.

0368 Numerical-Optimization Program—The ADS computer program is suitable for such applications as minimum-weight design.

0369 Program Calibrates Strain Gauges—Time required for acceptance tests of hardware is reduced.

0370 Tracing and Control of Engineering Requirements—Requirements and progress of an engineering project can be documented in systematic manner.

Testing & Instrumentation

0371 Liquid Level and Volume Sensor (Licensing Opportunity)

0372 Snapshots of Room Temperature and Airflow

0373 Three-Point Bend Tests Performed

0374 Experiments on Schemes for Adaptive-Wall Wind Tunnels—Ways to reduce testing time for adaptation are discused.

0375 New Sensors for Flow Velocity and Acoustics—Development programs promise more accurate measurements.

Environmental Science & Technology

0376 Hazardous and Industrial Waste Minimization

0377 Detoxifying Groundwater At a Superfund Site

Manufacturing, Machinery & Tools

0378 Manufacturing Technology for Large Aircraft Composite Primary Structure (Fuselage)

0379 Robotic Engine Manifold Cleaning Cell and Hazardous Chemical Rejuvenation

0380 New Gold Electroplating Process for Microelectronics Safer

0381 Air Driven Grinding and Polishing Tool Developed (Licensing Opportunity)

0382 Long-Lived Electrode for Arc Welding in Vacuum—Pressurized gas reduces the vaporization of the electrode.

0383 Low-Leakage Inlet Swirl Brake—Vanes change the direction of flow while giving rise to relatively low static pressure. (Licensing Opportunity)

0384 Smaller Coaxial-View Welding Torch—This torch resembles an ordinary torch without optics. (Licensing Opportunity)

0385 Testbed for Telerobotic Servicing—Various combinations of operator control and robot autonomy can be evaluated.

0386 Trailing Shield for Welding on Pipes—Weld beads remain covered with inert gas until safely cooled. (Licensing Opportunity)

Testing & Instrumentation

0387 Dynamic Tester for Rotor Seals and Bearings—A simplified apparatus measures performance under vibration. (Licensing Opportunity)

0388 Monitoring Bearing Vibrations for Signs of Damage—Real-time spectral analysis is performed to detect telltale changes in vibrations. (Licensing Opportunity)

Materials

0389 Powders Hold Promise for Capturing Market Share—Modified high pressure gas atomization.

0390 New Polymer Technology

0391 Imide/Arylene Ether Copolymers—Films cast from solution are tough and flexible, and exhibit useful thermal and mechanical properties. (Licensing Opportunity)

0392 Deposition of Diamondlike Films by ECR Microwave Plasma—Negative dc self-bias induced by radio-frequency bias appears to be essential. (Licensing Opportunity)

0393 Making Thin Laminae of Frozen Alloy Slurries—These laminae, interspersed with fiber mats, can be used to make metal/fiber composites. (Licensing Opportunity)

Other Items of Interest

0380 New Gold Electroplating Process for Microelectronics Safer

Medicine & Biology

0394 Electrostatic Discharge

0395 Boosting Immunity in the Elderly

0396 Patients Prefer Extraction

0397 3D-Mouse for Point-and-Direct Telerobotics

0398 Evaluation of DeVAR-IV with a Quadriplegic Employee

0399 An ATPase From Halobacterium Saccharovorum—The purification and subunit structure of a halobacterial enzyme are described.

0400 Deconditioning Under Prolonged, Repeated Bed Rest—Recovery takes longer than previously thought, and effects seem to be cumulative.

0401 Numerical Simulation of Flow Through an Artificial Heart—Research in both artificial hearts and fluid dynamics benefits from computational studies.

Testing & Instrumentation

0402 New Sensors with Biological Properties

0403 Non-Invasive Electromyography

Physical Sciences

0404 Please Release Me—But Slowly

Software

0405 Calculating Thermophysical Properties of 12 Fluids—Properties are expressed via equations of state.

0406 Designing Catalytic Monoliths for Closed-Cycle CO2 Lasers—The LASCAT program enables a designer to determine quickly the consequences of changes in design.

Testing & Instrumentation

0407 Wavefront Dividing Infrared Interferometer

0408 Ionizable-Substance Detector—The detector nondisruptively monitors the concentration of an ionizable substance in a stream. (Licensing Opportunity)

Other Items of Interest

0346 Multiaperture Spectrometer—Advantages would be a convenient two-dimensional spectral image, fewer components, and greater efficiency.

0347 Spaceborne Microwave Imagers—Principles and practices are described.

Transportation & Components

0409 Developing Software for a Flight-Control System—Integration of design activities reduces the incidence of errors.

0410 Langley Aircraft Landing Dynamics Facility—Aircraft landing-gear systems are tested on actual runways at operational conditions.

0411 Mechanical Backup for Fly-by-Wire Control System—A mechanical device eliminates the need for redundant fly-by-wire subsystems.

0412 Precise Autohover Control for a Helicopter—A control system attempts to maintain a constant horizontal position.

Agriculture & Food

0321 Dwarf Daylily Debuts This Fall

0322 Fries From New Spud

0323 Lakebed Sediment Cut by Farming Practices

0324 Monitoring and Controlling Hydroponic Flow—A simple apparatus maintains the required slight suction while overcoming gravity effects.

Other Items of Interest

0404 Please Release Me—But Slowly

Research Technology
Agricultural Research Service
U.S. Department of Agriculture

Dwarf Daylily Debuts This Fall

A new dwarf daylily called Yellow Tinkerbell has been developed for use both as a perennial landscape border plant and a potted plant.

Its height—only 9 inches—is the result of research to further miniaturize the dwarf daylily. The most popular dwarf variety is actually quite large, reaching a flowering height of 28 inches.

The new dwarf is identical in all traits except size to one of the shortest daylilies, which is 16 inches tall.

Yellow Tinkerbell has bright yellow, 2-1/2 inch flowers on the 9-inch stems, bearing about 7 flowers per stem. It will flower in a 4-inch pot in just 8 weeks after less than 12 hours of light daily at temperatures as low as 41°F. The new plant has survived temperatures of -15°F and will be available to plant nurseries this fall for propagation.

For further information, contact Robert J. Griesbach, USDA-ARS Florist and Nursery Crops Laboratory, 10300 Baltimore Ave., Beltsville, MD 20705-2350. Phone (301) 344-3574. ◆

Research Technology
Agricultural Research Service
U.S. Department of Agriculture

Fries From New Spud

Crisp french fries made from a new U.S. Department of Agriculture potato variety were favored over Russet Burbank in taste tests by USDA and university scientists.

A panel of trained taste testers scored Ranger Russet fries higher in flavor, color and texture than Russet Burbank, the most widely planted variety in the United States, said potato breeder Joseph J. Pavek of USDA's Agricultural Research Service in Aberdeen, Idaho.

"For flavor," Paavek said, "Ranger fries scored a 5.9 out of a possible 10, which the Burbanks scored a 4.3" in taste tests performed by scientists in Minnesota and North Dakota.

Also, the new fries were rated as having a crisper texture than Russet Burbank. "That's mainly because Ranger potatoes are 10 percent higher in solids, or dry matter, than Burbank," Pavek said. French fries with higher solids are more likely to adsorb less oil during frying and droop less after they are served, he said.

Pavek and ARS plant pathologist Dennis L. Corsini selected and bred Ranger Russet at the agency's Small Grains and Potato Germplasm Research Unit in Aberdeen. The new variety was released to growers this spring.

Local potato processors, l like J.R. Simplot Co, in Caldwell, Idaho, which provides about 60 percent of the fries sold at McDonald's nationwide, worked with the ARS scientists to evaluate Ranger potatoes and french fries. Other collaborators were university, Cooperative Extension and industry scientists in Washington, Oregon, Idaho and Colorado.

Pavek sent harvested potatoes to the ARS Potato Handling, Storage and Processing Research Unit, East Grand Forks, Minn. There, scientists prepared frozen french fries shipped to the University of North Dakota, Fargo, for the taste tests.

Potato processors also like the size of the new spuds, which weigh in at about 7 ounces, compared to an average 6 ounces for Russet Burbanks. Bigger potatoes mean less waste when they are cut into long, skinny fries, according to Glenn Vogt, manager of agricultural services at Simplot.

Ranger resembles Russet Burbank in appearance, but usually outyields it by about 28 percent, said Pavek.

Ranger potatoes are susceptible to blackspot - the formation of gray or black spots under the skin of tubers bruised during harvest, he said.

However, Corsini said, future breeding work with bruise-resistant potatoes can remedy that problem for tomorrow's new varieties.

FOR ADDITIONAL INFORMATION: For details, contact Joseph Pavek, (208)397-4181.

Research Technology
Agricultural Research Service
U.S. Department of Agriculture

Lakebed Sediment Cut by Farming Practices

Soil losses from farms around Mississippi's Moon Lake have dropped off significantly as farmers change to crops requiring less tillage. That has meant a cleaner, healthier life for the lake, a 4-square-mile body of water along the Mississippi River.

An ARS study of farm practices and 30 years of sediment deposit records documented how less intensive cropping practices can improve water quality.

Scientists found that from 1954 to 1965, about 70 percent of the lake had more than 1 inch of sediment deposited each year. But then farmers switched from cotton to soybeans and rice, which require less tillage.

Over the next 20 years, about 86 percent of the lake had less than an inch of sediment per year. This is one of the first long-term studies that proves how changing to less intensive cropping practices can greatly improve the water quality and aquatic habitat downstream.

For further information, contact Charlie Cooper, USDA-ARS National Sedimentation Laboratory, P.O. Box 1157, Oxford, MS 38655. Phone (601) 232-2935. ◆

NASA Tech Brief
National Aeronautics and Space Administration
John F. Kennedy Space Center, Florida

Monitoring and Controlling Hydroponic Flow

A simple apparatus maintains the required slight suction while overcoming gravity effects.

A pressure-monitoring and -controlling apparatus maintains the slight suction required on the nutrient solution in the apparatus described in the preceding article "Tubular Membrane Plant-Growth Unit" (KSC-11375), while overcoming gravity effects on the operation of the system on Earth. The suction helps to hold the solution in the tubular membrane (see Figure 1).

A submersible pump circulates nutrient solution from a reservoir to an inlet manifold for the growth tubes. A pair of standpipes help maintain a steady pressure in the manifold. A gauge provides a continuous indication of the pressure at the inlet of each growth tube in an array of such tubes (see Figure 2). An operator can adjust the pressure in each tube individually, by means of a needle valve, to obtain the slight negative pressure that is needed to prevent free leakage of nutrient solution. Nutrient solution flows from the manifold into the pipes according to their valve settings. A peristaltic pump on each tube draws solution through it and returns the solution to the reservoir. Unused solution in the manifold also returns to the reservoir via the standpipes.

This work was done by Thomas W. Dreschel of The Bionetics Corp. for **Kennedy Space Center.**
KSC-11416/TN

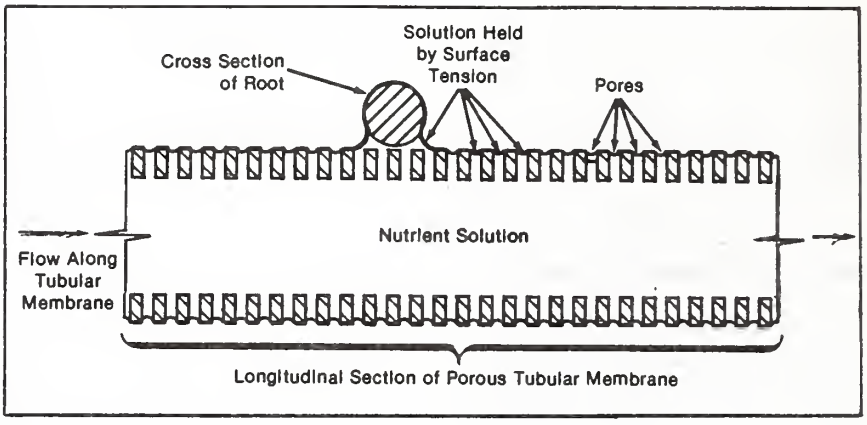

Figure 1. The **Surface Tension** of the solution seals the pores, and a slight negative gauge pressure in the solution holds the solution inside until contact with the root draws the solution out by capillary action. The negative pressure partly counteracts the capillary action, limiting the degree to which the solution flows out before surface tension takes over.

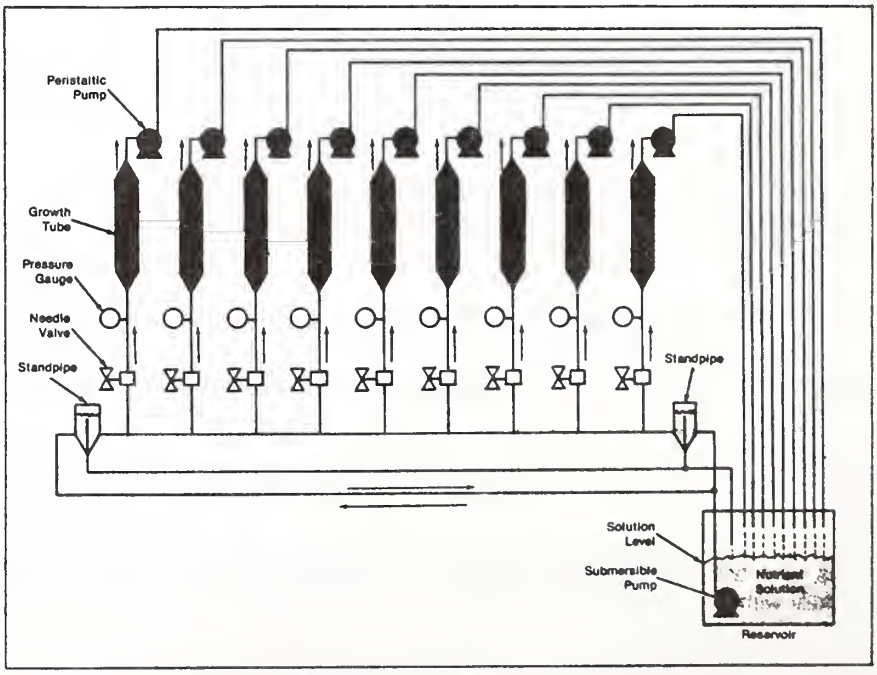

Figure 2. The **Flows of Nutrient Solution In and From Growth Tubes** are individually monitored and controlled with pressure gauges and needle valves.

FOR ADDITIONAL INFORMATION: *Contact: Director, Technology Transfer Division, P.O. Box 8757, BWI Airport, MD 21240; (301) 621-0100 Ext. 241*
REFER TO THE NUMBER LISTED AT THE END OF THIS ARTICLE

Computers

0325 SLALOM: 'Gold Standard' for Benchmarking Scientific Computers

Software

0326 Aid for Simulating Digital Flight Control Systems—A computer program translates descriptions of systems into programs for simulation.

0327 Library of Subprograms in FORTRAN 77—Subprograms can be called upon as needed to perform specific computations.

0328 Software-Design-Analyzer System—CRISP-90 provides the software designer with a medium that facilitates alterations.

0329 Software for Depiction of Three-Dimensional Objects—This program enables the user to build, manipulate, and display hierarchical three-dimensional objects.

0330 Software for Simulation of Development of Software—Personnel, resources, errors, and other realistic factors are represented in the simulation.

Other Items of Interest

0336 Knowledge-Based Flight-Status Monitor—Telemetered data from advanced aircraft would be processed automatically to detect failures.

0331 Gallium Arsenide/Germanium Solar Cells

Ames Laboratory

SLALOM: 'Gold Standard' for Benchmarking Scientific Computers

Twenty years of computer development have produced a menagerie of computer sizes, speeds, designs and architectures. Unfortunately, there has been no truly objective and generally accepted means of comparing scientific computers. The lack of such a "benchmark" has hampered progress in comparing and developing advanced computers. Now SLALOM (Scalable, Language-independent, Ames Laboratory, One-minute Measurement)--a new Ames Laboratory-developed "benchmark"--fills that void.

By coincidence, the acronym SLALOM is a double-play on its dictionary meaning because the program is, in fact, "a timed race through obstacles"; it fixes time, rather than problem size, in making comparisons. This new benchmark has received strong votes of approval from the supercomputing industry, including companies such as Intel, CRAY Research, IBM, MasPar, nCUBE, Silicon Graphics, SKY and Alliant. It has also received a 1991 R&D 100 Award, recognizing it as one of the top inventions of the year.

Existing benchmark methods fix the size of the task and measure the time it takes to solve that task. The problem with this approach is analogous to giving a tricycle and a jet a certain-distance race and timing them. If the race were 100 miles, the jet would win; if 100 feet, the tricyclist would win. Instead of using fixed distance, the SLALOM approach is "In one *hour*, how far can each go?" The ratio of distances traveled then provides a more fair measure of their relative performance.

By using fixed-time principles, SLALOM can compare Macs and CRAYs, doing justice to both. It has no preferred computer architecture or language so it can be run on scalar, vector, and parallel machines of all kinds. SLALOM is the first benchmark to include scalable tasks, so that the size of the problem can be adjusted to match the power of the computer. This feature enables SLALOM to keep pace with hardware advances, unlike other benchmarks. SLALOM is designed to remain useful for many computer generations and will be able to benchmark computers 10,000 times faster than the ones used today.

SLALOM is also the first benchmark that can evaluate an entire application (including set up and input/output) instead of an excerpt. Older benchmarks measure only simplified sections of applications, or use cases with very little input/output. Fortran, C and Pascal definitions of the revised benchmark are available, with variants for any number of processors and various means of controlling those processors.

Computers have increased in speed by a factor of perhaps a billion over the past 50 years. Even more dramatic advances in computer speed are likely to come using radical departures from traditional computer architectures. SLALOM provides the only fair means for comparing the old with the new, and tracking progress throughout this revolution.

A patent application has been filed on this benchmark.

Literature: "SLALOM-The First Scalable Supercomputing Benchmark," J. L. Gustafson, D.T. Rover, S. T. Elbert and M. B. Carter, *Supercomputing Review*, Nov. (1990) 56-61.

Patent/License Status: Application filed.

Potential Applications/Spinoffs: Can be run on scalar, vector and parallel machines and will be able to benchmark computers 10,000 times faster than ones used today.

For More Information on this Technology: Contact Daniel E. Williams, Office of Research and Technology Application, Ames Laboratory, 119 Office and Laboratory, Iowa State University, Ames, Iowa 50011 (515)294-2635.

NASA Tech Brief
National Aeronautics and Space Administration

Aid for Simulating Digital Flight Control Systems

A computer program translates descriptions of systems into programs for simulation.

The DIVERS translator is a computer program to convert descriptions of digital flight-control systems (DFCS) into a computer program written in the C language. DIVERS is language developed to represent design charts of DFCS. The DIVERS translator converts DIVERS source code into an easily transportable language, while minimizing the probability that the results will be affected by the interpretation of the programmer. The final translated program can be used as a standard of comparison to verify the operation of actual flight-control systems. DIVERS is applicable to the simulation of other control systems; for example, electrical circuits and logic processes.

The DIVERS language is designed to correspond directly to DFCS diagrams. The keywords (filter, summer, limiter, etc.) correspond to physical components. The signals (volts, flap elevation, temperature, time, etc.) are variables corresponding to lines that connect the components. The DIVERS keywords are subroutines implemented in C and stored in a dictionary and are defined by the user in terms of input signals, outputs, and lists of parameters. This enables each component to be thoroughly tested and verified before being used in an actual system. The enforced modularity reduces the risk of programmer-introduced errors. A list of parameters to each keyword can include constants and conditional expressions.

Signals are declared in terms of units, maximum and minimum values, type (real, integer, Boolean), and computer-memory requirements. The DIVERS code is translated into a C program that can be run with input signals from the terminal or an existing data file. The program cycles through a control system, prompting for input, and displaying all signals declared as "test variables". The user can alter a signal or retain its current value for the next cycle.

The DCHART program is included in the DIVERS package. Its purpose is to read DIVERS source code and make a diagram of the data flowing between components. The output is used to compare the DIVERS specifications with the original DFCS chart.

DIVERS is written in C for batch execution and is available for two different computers. The DEC VAX version has been implemented on a VAX 11/780 computer operating under VMS 4.2. The UNIX version has been implemented on a DEC PDP 11/60 with IS/1 UNIX and a central-memory requirement of approximately 99K. This program was developed in 1985.

This program was written by Richard M. Hartman of Informatics, Inc., for **Ames Research Center.**
ARC-11710/ARC-11711/TN

FOR ADDITIONAL INFORMATION

CONTACT
COSMIC®
112 Barrow Hall
University of Georgia
Athens, GA 30602

(404) 542-3265

Library of Subprograms in FORTRAN 77

Subprograms can be called upon as needed to perform specific computations.

MATH77, Release 3.17, is a library of 412 FORTRAN 77 subprograms for use in numerical computation. Researchers at the Jet Propulsion Laboratory developed the library to facilitate scientific and engineering computation.

The wide variety of computers used to perform numerical computation in scientific laboratories requires a collection of mathematical subprograms that is portable among a significant number of computing environments. The MATH77 library provides this portability. Subprograms that provide machine and system characteristic parameters make the library operational on any computer system that supports the full FORTRAN 77 standard. The portability of the library and the high quality of its subprograms and user's manual make MATH77 an extremely versatile and valuable tool for all numerical computation applications.

The library contains subprograms that perform such tasks as the computation of special functions, the generation of pseudorandom numbers, linear least-squares analysis, singular-value analysis, the solution of equations, minimization, curve fitting, Hermite cubic interpolation, quadrature, ordinary differential equations, finding the roots of polynomials, fast Fourier transforms, special arithmetic propagating derivative values, basic statistics, and printer plotting. The library, demonstration drivers, and test drivers are stored in compressed form and are expandable with a program included in the package.

MATH77 was developed during 1980–89. It is written in FORTRAN 77 and is suitable for use on any computer system that supports the full FORTRAN 77 standard. The program and documentation are copyrighted products of the California Institute of Technology.

This program was written by Charles L. Lawson, Fred T. Krogh, William Van Snyder, and Stella Y. Chiu of Caltech for **NASA's Jet Propulsion Laboratory**. *NPO-18120/TN*

FOR ADDITIONAL INFORMATION

CONTACT

COSMIC®
112 Barrow Hall
University of Georgia
Athens, GA 30602

(404) 542-3265

Software-Design-Analyzer System

CRISP-90 provides the software designer with a medium that facilitates alterations.

The CRISP-90 software-design-analyzer system, an update of CRISP-80, is a set of computer programs that constitute a software tool for the design and documentation of other software and that support top-down, hierarchical, modular, structured methodologies for design and programming. The quality of a computer program can often be influenced significantly by the design medium in which the program is developed. The medium must foster the expression of the programmer's ideas easily and quickly, and it must enable flexible and facile alterations of, additions to, and deletions from these ideas as the design evolves. The CRISP-90 software-design-analyzer system was developed to provide the programmer with such a design medium.

The design of a program in the CRISP-90 medium consists of short, English-like textual descriptions of data, interfaces, and procedures that are embedded in a simple, structured, modular syntax. The display is formatted into two-dimensional, flow-chart-like segments for a graphical presentation of the design. Together with a good interactive full-screen editing or word-processing program, CRISP-90 becomes a powerful software tool for the programmer.

In addition to being a text formatter, the CRISP-90 system prepares material, the manual extraction of which would be tedious and prone to error; examples of such material include a table of contents, a module directory, a structure (tier) chart, cross-references, and a statistical report on the characteristics of the design. Referenced modules are marked by schematic logic symbols to show conditional, iterative, and/or concurrent invocation in the program. A keyword-usage profile can be generated automatically and glossary definitions inserted into the output documentation. Another feature is the capability to detect changes that were made between versions. Thus, "change bars" can be placed in the output document along with a list of changed pages and a version-history report. Also, items can be marked as "to be determined," and each appears on a special table until the item is supplied.

The CRISP-90 software-design-analyzer system is written in Microsoft QuickBasic. The program requires an IBM-PC-compatible computer with a hard disk, 128K of random-access memory, and an ASCII printer. The program operates under MS-DOS/PC-DOS 3.10 or later. The program was developed in 1983 and updated in 1990.

Microsoft and MS-DOS are registered trademarks of Microsoft Corp. IBM PC and PC-DOS are registered trademarks of International Business Machines Corp.

This program was written by Robert C. Tausworthe of Caltech for **NASA's Jet Propulsion Laboratory**.

Inquiries concerning rights for the commercial use of this invention should be addressed to the Patent Counsel, NASA Resident Office-JPL. Refer to NPO-18212/TN.

FOR ADDITIONAL INFORMATION

CONTACT

COSMIC®
112 Barrow Hall
University of Georgia
Athens, GA 30602

(404) 542-3265

NASA Tech Brief
National Aeronautics and Space Administration

Software for Depiction of Three-Dimensional Objects

This program enables the user to build, manipulate, and display hierarchical three-dimensional objects.

The use of hierarchy in a mathematical modeling environment is critical for effective simulation of real objects. For a model that involves a combination of several moving parts, hierarchy is necessary to establish the network of dependent relationships that govern the movements of the parts and the model as a whole. HME (the Hierarchical Modeling Environment) is a three-dimensional computer-graphics software system designed to give the user complete access to the total hierarchical mathematical model.

HME enables the user to build, manipulate, and display hierarchical three-dimensional objects dynamically. The program also includes created polygons in the hierarchy. The window-oriented user interface enables the manipulation of objects by use of the mouse, windows, menus, buttons, and sliders. A hierarchy window depicts the hierarchy of the mathematical model environment. The user can point at any node on the hierarchy and use a powerful set of standard options to edit, copy, create, or save that portion of the hierarchical environment. With HME, it is easy to establish and edit the proper coordination of eye points, sources of light, and connectivity of the model necessary for accurate depiction of the model.

HME is written in C language for Silicon Graphics IRIS workstations supporting the 4Sight windowing software system and at least version 3.1 of the operating system. The program requires approximately 650 KB of memory and was developed in 1989.

This program was written by Frank Taylor and Debbi Boettger of McDonnell Douglas Corp. for **Johnson Space Center.** *MSC-21708/TN*

FOR ADDITIONAL INFORMATION

CONTACT

COSMIC®
112 Barrow Hall
University of Georgia
Athens, GA 30602

(404) 542-3265

Software for Simulation of Development of Software

Personnel, resources, errors, and other realistic factors are represented in the simulation.

SOFTREL is a prototype software package that simulates creation, detection, and repair of defects and faults during a software-development project. The user initiates the process by entering the staff and resource schedules. The factors considered in SOFTREL include (1) construction, integration, inspection, and correction of documentation; (2) construction, integration, inspection, and correction of code; (3) preparation and conduct of tests; (4) identification and repair of faults; (5) validation of repairs; and (6) retesting. Parameters include rates of building of new, reused, deleted, and added components of documentation and code; rates of generation of defects; rates and adequacies of inspections; rates and adequacies of corrections; and adequacies of validations.

SOFTREL is available in executable form only for the IBM PC under DOS 3.3 or higher. The program was developed in 1990. SOFTREL is a copyrighted work with all copyright vested in NASA.

This program was written by Robert C. Tausworthe of Caltech for **NASA's Jet Propulsion Laboratory**. *For further information, Circle 26 on the TSP Request Card. NPO-18295/TN*

FOR ADDITIONAL INFORMATION

CONTACT

COSMIC®
112 Barrow Hall
University of Georgia
Athens, GA 30602

(404) 542-3265

Electrotechnology

0331 Gallium Arsenide/Germanium Solar Cells

0332 Integrated Composites Center

0333 Altering Interline Transfer in a CCD To Reduce Saturation—Charges accumulated during part of a frame period would be dumped.

0334 Automatic Rejection of Multimode Laser Pulses—Characteristic modulation is detected, enabling the rejection of multimode signals.

0335 Faster Computation of Far Fields of Dish Antennas—A modified Zernike-polynomial approach reduces the number of terms in the numerical integration.

0336 Knowledge-Based Flight-Status Monitor—Telemetered data from advanced aircraft would be processed automatically to detect failures.

0337 Lightweight, Flat Battery Case—Materials are chosen to increase strength while reducing weight and electrical resistance. (Licensing Opportunity)

0338 Rugged Direct-Current Transducer—The solid core withstands mechanical and thermal shocks. (Licensing Opportunity)

0339 Si/IrSi3 Schottky-Barrier Infrared Detectors—Ir and Si are codeposited in stoichiometric ratio to suppress mixed Ir/Si phases. (Licensing Opportunity)

0340 Solid-State Imaging Device With Carbon Film—The film reduces Fresnel reflections and dissipates static electric charges.

0341 Two-Period Gratings for Surface-Emitting Lasers—More light is reflected back into the lasers. (Licensing Opportunity)

0342 Wideband Phase-Licked Angle Modulator—The modulator can be designed independently of the phase-locked loop. (Licensing Opportunity)

Software

0343 Program Processes SAR Data—The MacMultiview program computes polarimetric and other images.

Testing & Instrumentation

0344 Holographic Wafer Inspection

0345 Characterization of Electrical Response of Photodetector—Fourier analysis of input and output yields electrical frequency response.

0346 Multiaperture Spectrometer—Advantages would be a convenient two-dimensional spectral image, fewer components, and greater efficiency.

0347 Spaceborne Microwave Imagers—Principles and practices are described.

Wright-Patterson Air Force Base

Gallium Arsenide/Germanium Solar Cells

Applied Solar Energy Corporation was contracted to produce thin, rugged gallium arsenide solar cells on a germanium substrate for improved performance and use on Air Force and other Department of Defense satellite vehicles. This program is designed to demonstrate the production of gallium arsenide solar cells and to extend the technology from 2 cm by 2 cm cells to 4 cm by 4 cm and 6 cm by 6 cm large area cells. These larger cells offer major advantages, such as fewer parts and lower assembly costs.

The survivability of these cells has been further enhanced through development of a welded interconnect technology that can withstand the higher temperatures associated with the absorption of energy from laser and nuclear weapon exposure, in addition to reducing the mass of the contacts for higher thermal cycle life. The program will produce 20,000-square centimeters of space-qualified cells, which represent approximately 375 watts of power. Weekly production analysis indicates five thousand 4 cm by 4 cm cells can be produced. This capacity level is adequate for one or two small satellite programs and can be expanded as demand for these cells matures.

Current implementations include the Combined Release and Radiation Effects Satellite (CRRES), Living Integrated Plume Shield (LIPS) III Satellite. Future implementations include the Boost Stage Tracking Satellite and the SDIO super power demonstration managed by the Wright Laboratory Aero Propulsion and Power Directorate.

These cells have many performance improvements over existing silicon solar cells. They produce 20 to 30 percent more power at beginning of life and experience less degradation from particulate radiation at low and intermediate earth orbits. In addition, the rugged germanium substrate makes it possible to reduce the thickness, weight, and cost of these cells, and provides a more robust cell to minimize the damaging effects of thermal and mechanical strain from exposures to laser and nuclear weapons attacks.

Contract: F33615-88-C-5415, Project Engineer: Wallace Patterson, WL/MTEC, (513) 255-2461.

Wright-Patterson Air Force Base

Integrated Composites Center

The objective of the Integrated Composites Center (ICC) Program was to establish a site specific center that would result in demonstrating a significant reduction in production costs, while at the same time establishing a higher level of quality. The design of the ICC includes new process automation for the shop floor with computer integrated planning and control systems above the shop floor.

The ICC Program developed a three-tiered information management and architecture consisting of: the "enterprise" level, responsible for design and scheduling of the entire aircraft the "process center" for managing information to the ICC, and the shop-floor level, where composite parts are fabricated. Application software was developed for all three levels using a common data base. Shop-floor equipment and processes were updated and refined. A variety of equipment, including an automated packaging machine, automated ply cutters, abrasive waterjet cutting system, and robotic router was employed using the manufacturing cell concept.

After installation, the ICC became an integral part of the McAir shop floor. Production of parts for the F-15, F-18, and AV-8B aircraft are handled in this facility. In addition, ICC concepts and techniques have been made available through an Industry Review Board, implementation guide, and other technology transfer activities.

The military benefits of the ICC Program provide monitoring and control of guaranteed work order integrity for the shop floor, improved capability planning, better scheduling integration, and timely delivery of resources to the shop floor. The ICC successfully embodies the philosophy of integrated product development. Islands of automation have been transformed into resource sharing functions with major savings up to 64 percent being demonstrated in the category of nontouch labor. Potential savings for the F-15, F-16, F-18, and AV-8B aircraft exceed $95 million.

Contract: F33615-85-C-5136, Project Engineer: Paul Pirrung, WL/MTPN, (513) 255-7277.

NASA Tech Brief
National Aeronautics and Space Administration
NASA's Jet Propulsion Laboratory, Pasadena, California

Altering Interline Transfer in a CCD To Reduce Saturation

Charges accumulated during part of a frame period would be dumped.

In a proposed interline-transfer timing scheme for a charge-coupled-device (CCD) video imaging array, the charges accumulated during some fraction of a frame period would be read out in the usual way, while the charges accumulated during the remaining fraction of a frame period would be swept out and dumped to prevent overloading and saturation in intensely illuminated photosites. The excess charges would be swept out at the highest possible rate, while the charges used for imaging would be read out at a rate that was lower but that was nevertheless the highest rate that would provide complete transfer of charge on the array and that could be handled by subsequent signal-processing equipment.

In the typical operation of an interline CCD, the charges accumulated in the photosites (picture elements) are periodically transferred from rows of photosites into columns of optically masked CCD transfer gates. These charges are sequentially stepped along the columns into a row shift register so that information on the image can be extracted as a series of charges in rows of picture elements. In interlaced scanning (to which the proposed scheme applies), the complete scene is read out in frames, each of which consists of two fields. The first field consists of the odd-numbered lines; the second, of the even-numbered lines.

Figure 1 illustrates two of several versions of the proposed timing scheme. Let F denote the frame period, and let the zero of time be denoted as the leading edge of a pulse that would mark the beginning of readout of the odd field. A similar pulse would mark the beginning of readout of the even field at $F/2$. An interval of $F/4$ would be devoted to the readout of each field. In the first version of the timing scheme, the charges would be swept out of the odd (or even) field at some time during the interval of $F/4$ between the end of readout of that field and the beginning of readout of the subsequent even (or odd) field. In the second version, the charges would be swept out of each field at some time during the interval of $F/4$ that would immediately precede the readout of that field.

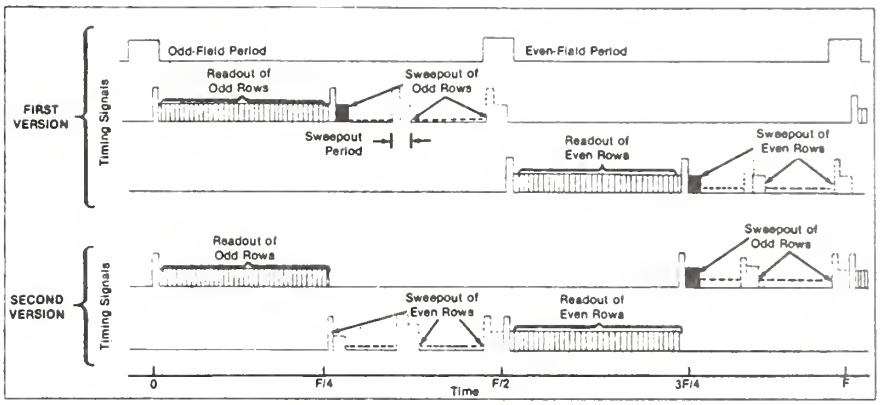

Figure 1. These **Timing Signals for Interline Transfer** of charges in a CCD would be used in two versions of the proposed scheme. In still other versions, the frame period, F, could be broken into intervals of $F/8$ or less.

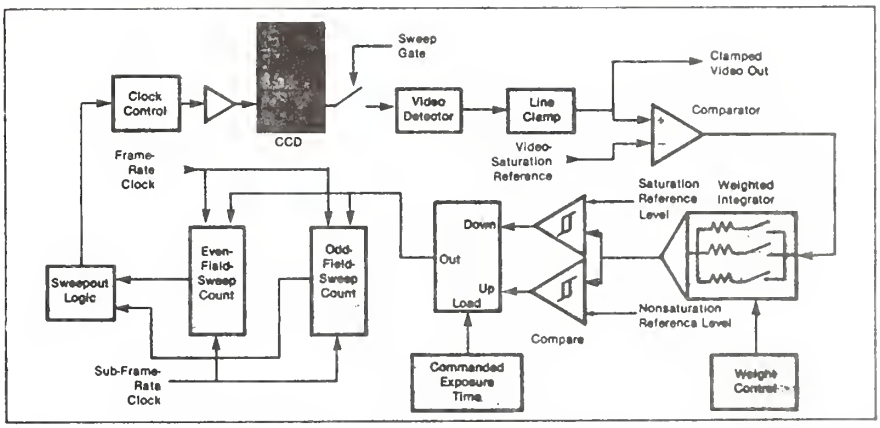

Figure 2. This **Control System** would vary the time of beginning of the last sweepout period for each field in such a way as to prevent or reduce the incidence of both overexposure and underexposure.

In both versions, the last sweepout of a field during each frame period would have to commence no later than one sweepout period before the beginning of the readout to follow. Provided that each such last sweepout occurred as late as possible and that the sweepout period was much shorter than $F/4$, the first version could dispose of as much as 1/4 the charges integrated during the frame period, F, allowing an overexposure of 4/3 the saturation intensity. The second version could allow a much greater overexposure because it would limit the charge-integration time to the time required to gain access to the photodetectors and sweep out the excess charges.

Figure 2 illustrates a scheme to control the time of the beginning of the last sweepout in response to the amount and location of overload in a scene. The readout charges would be passed from the CCD to a video detector and line clamp. The detector would filter the noise component out of the signal, while the clamp would fix the signal at a minimum dc reference level. A voltage comparator would indicate any picture elements in which the charge exceeded a reference level just below the saturation level of the CCD.

The output of the comparator would be integrated over a frame period to produce a signal indicative of the fraction of the CCD array that was saturated, if any. The integration could be weighted to emphasize the center or any other portion of the array. The output of the integrator would be applied to a pair of hysteretic voltage comparators, which would define a range of acceptable exposure. The comparators would drive the "up" and "down" control lines of a bidirectional counter, the output of which would determine the beginning of the last sweepout period. If overexposure were signaled, the counter would decrement by one count per frame until the exposure was sufficiently short or until the minimum integration time was reached. If underexposure were signaled, the counter would increment one count per frame to boost the signal. When correct exposure was signaled, no counting would occur.

This work was done by Edward M. Rentsch of General Electric Co. for **NASA's Jet Propulsion Laboratory**. *NPO-17935/TN*

FOR ADDITIONAL INFORMATION: *Contact: Director, Technology Transfer Division, P.O. Box 8757, BWI Airport, MD 21240. (301) 621-0100 Ext. 241*

REFER TO THE NUMBER LISTED AT THE END OF THIS ARTICLE

NASA Tech Brief
National Aeronautics and Space Administration
NASA's Jet Propulsion Laboratory, Pasadena, California

Automatic Rejection of Multimode Laser Pulses

Characteristic modulation is detected, enabling the rejection of multimode signals.

A monitoring circuit senses multiple longitudinal mode oscillation of a transversely excited, atmospheric-pressure (TEA) CO_2 laser. This facility was specifically developed for inclusion into a coherent detection laser radar (LIDAR) system. However, the circuit described would be of use in any experiment where it is desirable to record data only when the laser operates in a single longitudinal mode. In the case of the LIDAR application for which this device was originally conceived, received signals, derived from multimode transmitted pulses, exhibit a much broader frequency bandwidth than that of the receiver electronics in a typical heterodyne (coherent) detection configuration. They, therefore, contribute little or nothing to the detected signal. Although control circuitry usually enforces single-mode operation, the subject laser can occasionally revert to multimode operation. When this occurs, the monitoring circuit causes the data-acquisition system to ignore the incoming signal, thereby optimizing the signal-to-noise ratio in a signal averaging situation.

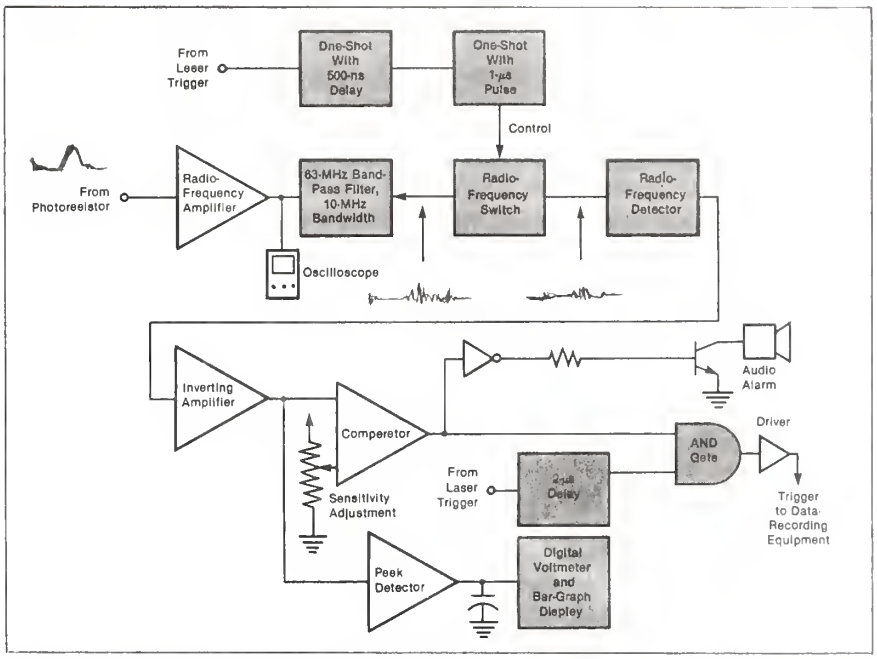

Amplitude Modulation at the Intermode-Separation Frequency during the laser pulse causes this circuit to suppress the data system trigger.

Multimode oscillation causes the laser pulse to be strongly amplitude-modulated at the frequency of separation between the longitudinal modes. This intermode-separation frequency is the reciprocal of the period required by light to make one round trip within the laser cavity, so that the modulation is easily detectable as long as the laser pulse duration exceeds this round-trip period. The monitoring circuit (see figure) senses this modulation and processes it to determine whether the detected data should be rejected.

A low-reflectivity beam splitter samples a portion of the subject laser beam and directs it onto an HgCdTe photoresistor. The output of this photoresistor is band-pass-filtered at the intermode-separation frequency (63 MHz in the original application). The resultant filtered signal is then amplified and sent to a radio-frequency switch controlled by the laser trigger via a delay circuit. The switch blocks the burst of broadband excitation noise that occurs before the laser pulse and that can trigger a false multimode-operation alarm. The switch passes the signal during the time window containing the main part of the laser pulse, then shuts off to block the "tail" of the pulse, which occasionally contains modulation that could also trigger a false multimode alarm.

After passing through the switch, the signal is envelope-detected, amplified, and fed to a comparator. If the signal exceeds a preset value, the comparator sends a pulse to an AND gate. The other input to the AND gate is derived from the laser trigger, but delayed so as to render it synchronous with the output of the comparator. The AND gate is configured so that if a multimode laser pulse has been detected, then the data system trigger (the output from the AND gate) is inhibited and the multimode data thus rejected.

This work was done by David M. Tratt and Robert T. Menzies of Caltech and Carlos Esproles of Ball Systems for **NASA's Jet Propulsion Laboratory.**
NPO-17777/TN

FOR ADDITIONAL INFORMATION: *Contact: Director, Technology Transfer Division, P.O. Box 8757, BWI Airport, MD 21240; (301) 621-0100 Ext. 241*
REFER TO THE NUMBER LISTED AT THE END OF THIS ARTICLE

NASA Tech Brief
National Aeronautics and Space Administration
NASA's Jet Propulsion Laboratory, Pasadena, California

Faster Computation of Far Fields of Dish Antennas

A modified Zernike-polynomial approach reduces the number of terms in the numerical integration.

A method of computing the far electromagnetic field radiated by a paraboloidal-dish-reflector or other circular antenna incorporates an improved series expansion and numerical-integration scheme. In comparison with prior methods, this one yields greater or equal accuracy with fewer terms in the series expansion and fewer sampling points across the aperture and, consequently, less computation. In a representative calculation of the far field of an offset-reflector antenna, the computing time of this method was only about one-thirtieth that of prior methods (see figure).

This method is one of few based on the Jacobi–Bessel-expansion concept, according to which the distribution of electrical current (or a physical-optics approximation thereof) across a circular aperture is represented by an infinite series (or a finite-series approximation) of basis functions that are orthogonal and integrable over the aperture. In this method, the basis functions are the circle polynomial functions introduced by Zernike in 1934. These functions are related to the well-known Bessel functions and the Jacobi hypergeometric polynomials. The Zernike-polynomial approach confers three important advantages:

(1) The infinite series equivalent to the radiation integral converges rapidly. The leading term in the series represents the pattern of radiation from an undistorted uniform-amplitude distribution across the aperture. Along the polar axis (in the direction of maximum intensity of the beam), the contribution of all the other terms in the series is zero. In other directions at small polar angles, the terms of higher order are the corrections over the leading term and in most practical cases are relatively small. Thus, relatively few terms are needed.

(2) The coefficients of the series expansion are independent of the observation angles. Therefore, once the coefficients are determined, the series can be rapidly computed for any observation point in the region of validity of the radiation integral.

(3) The Bessel-function terms, the calculation of which is relatively time-consuming, are inside the first of two summations in the series expansion and are decoupled from a second summation over harmonic exponential functions. This feature helps to reduce the computation time.

The coefficients of the series expansion are obtained by an improved numerical-integration scheme. For the integration over the azimuthal angle, the samples are taken at uniform intervals via the trapezoidal rule. The integration over the diameter is performed by use of a new Gaussian quadrature scheme. This scheme requires one-sixth to one-fourth the number of integration points needed in other currently available numerical-integration schemes developed for the same purpose.

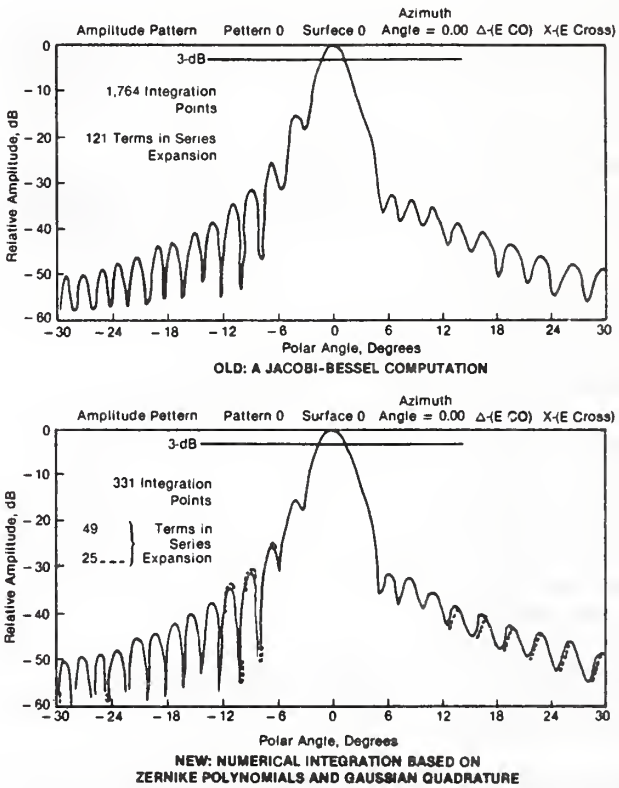

Far-Field Radiation Patterns computed by a more-conventional Jacobi-Bessel series expansion and the new method are similar, but the new method requires fewer integration points and fewer terms in the series expansion.

This work was done by Vahraz Jamnejad of Caltech for **NASA's Jet Propulsion Laboratory.** *NPO-18055/TN*

FOR ADDITIONAL INFORMATION: *Contact: Director, Technology Transfer Division, P.O. Box 8757, BWI Airport, MD 21240; (301) 621-0100 Ext. 241*
REFER TO THE NUMBER LISTED AT THE END OF THIS ARTICLE

NASA Tech Brief
National Aeronautics and Space Administration
Ames Research Center, Moffett Field, California

Knowledge-Based Flight-Status Monitor

Telemetered data from advanced aircraft would be processed automatically to detect failures.

A conceptual digital computing system is intended to monitor and interpret telemetered data on the health and status of a complicated avionic system in an advanced experimental aircraft. When fully developed, the monitor would be programmed with expert-system software to interpret the data in real time. The software would include a rule-based model of the failure-management system of the aircraft that would process fault-indicating signals from the avionic system to give timely advice to human operators in the mission-control room on the ground. A prototype of the expert-system software was developed via the MUSE system, which is a software toolkit for the development of real-time applications of artificial intelligence.

In the flight-status monitor (see Figure 1), the telemetered data would be translated into digital words, then fed into the expert system, which would determine whether any changes in the data had occurred since the previous sample. The expert system would evaluate the effects of any such changes. A data-driven foreground loop would determine the state of the system and inform the user — in this case the systems engineer — of the changes and consequences. If a failure were detected, a warning or caution would be issued along with corrective or emergency procedures, when required. As a part of this evaluation, the expert system might ask the user questions on the state of the aircraft. A background task would allow the user to query the monitor for information on the state of the flight-control system or the rationale used to reach its conclusions. The expert system would interrupt the background task, when necessary, to evaluate new data, but if the state of the flight-control system had not changed between inputs, the expert system would not reevaluate that state.

The knowledge base would contain both rules specific to the aircraft and metarules, which are the rules that the systems engineer uses to determine the correct response to a failure. The flight-status monitor would use these rules to model the failure-detection subsystem of the flight-control system and compare the modeled state with that of the aircraft. If the conclusions of the monitor disagreed with the state of the aircraft, a warning would be issued, and the user could ask the system to resolve the conflict. The conflict would be resolved as part of the background task so as not to interfere with the higher-priority task of evaluating the aircraft data as they were received.

The prototype software consists of several separate expert systems, each with its own inference mechanism. The internal structure of the flight-status monitor, as represented in the software, is shown in Figure 2. The inference mechanisms involve predominantly forward-chaining, data-driven processes. The aircraft sensor-and-failure-management (ASFM) expert system uses a forward-chaining logic mechanism to model the failure-management system of the aircraft and to deduce conditions of concern or danger based on the failure-indicator information. A metamonitor expert system deduces situations of concern based on knowledge of deductions from the ASFM expert system and the failure-management system. The situations of concern deduced by the metamonitor are analyzed by a fault-isolation expert system that deduces probable causes of conflicts, recommends corrective actions, and issues warnings.

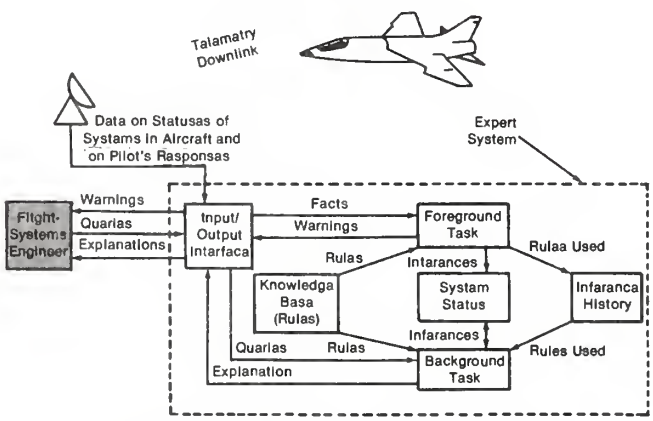

Figure 1. The **Flight-Status Monitor** would alert the flight-systems engineer to the need for corrective action in the event of a failure during flight.

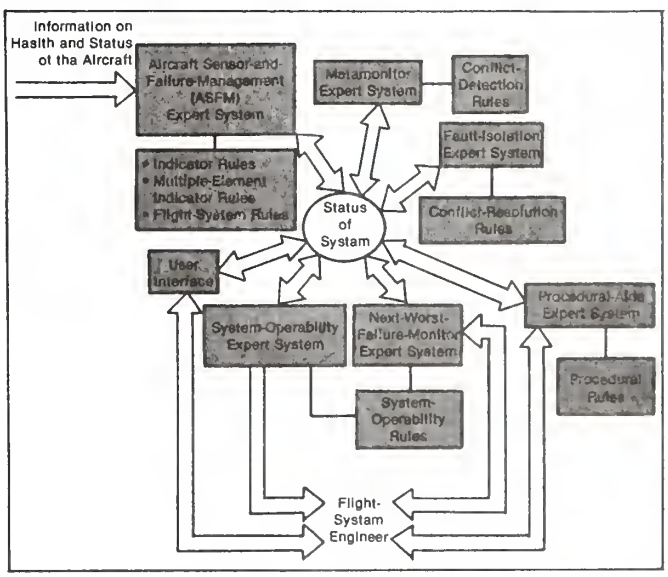

Figure 2. The **Internal Structure of the Flight-Status Monitor**, as envisioned in its software, includes several different representations of expert-system rules.

These expert systems provide detailed information on the status of the aircraft systems and perform a function comparable to that of an expert in flight systems.

The system-operability expert system uses knowledge of the effectiveness of the system and the detailed data on the status of the system to provide a high-level assessment of the ability of the flight-control system to control the aircraft, complete a specific mission, or function in a given mode. This assessment is performed by a backward-chaining mechanism, using hypotheses in an order established by the user. The order of the hypotheses is important because it provides a means for the expert system to determine priorities; the system uses this knowledge of priorities to determine the highest level at which the system is operable and provides this information to the user. The system-operability rules are also used to establish the worst consequences of any additional failure.

This work was done by E. L. Duke of **Ames Research Center**, *J.D. Disbrow of PRC Systems Services, Inc., and G. F. Butler of the Royal Aerospace Establishment. Further information may be found in NASA TM-101710 [N90-13995], "A Knowledge Based Flight Status Monitor for Real-Time Application in Digital Avionics Systems."*

Copies may be purchased [prepayment required] from the National Technical Information Service, Springfield, Virginia 22161, Telephone No. (703) 487-4650. Rush orders may be placed for an extra fee by calling (800) 336-4700. ARC-12712/TN

FOR ADDITIONAL INFORMATION: *Contact: Director, Technology Transfer Division, P.O. Box 8757, BWI Airport, MD 21240; (301) 621-0100 Ext. 241*

REFER TO THE NUMBER LISTED AT THE END OF THIS ARTICLE

NASA Tech Brief
National Aeronautics and Space Administration
NASA's Jet Propulsion Laboratory, Pasadena, California

Licensing Opportunity

Lightweight, Flat Battery Case

Materials are chosen to increase strength while reducing weight and electrical resistance.

The case of a low-profile bipolar battery is designed to be strong, rigid, and light in weight. It also has low-resistance terminals.

A prototype of the case was demonstrated by using it to construct a sealed lead/acid bipolar battery in which six stacked flat cells produced a 12-volt output (see figure). The end plates of the case are made of fiber honeycomb panels that restrain the stacked cells and prevent them from being warped or distorted by internal and external stresses. The positive and negative terminals, located at opposite edges of the case, are made of solid copper rods instead of the usual lead. The weight and the electrical resistance of the copper are less than those of lead.

This work was done by John J. Rowlette of Caltech for **NASA's Jet Propulsion Laboratory**. *For further information, Circle 66 on the TSP Request Card.*

In accordance with Public Law 96-517, the contractor has elected to retain title to this invention. Inquiries concerning rights for its commercial use should be addressed to

Edward Ansell
Director of Patents and Licensing
Mail Stop 305-6
California Institute of Technology
1201 East California Boulevard
Pasadena, CA 91125

Refer to NPO-17605/TN.

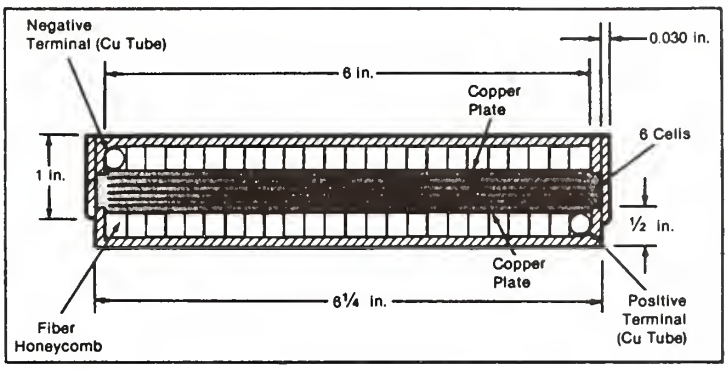

This **Cross Section of the Case** emphasizes its low ratio of height to width. The number of cells in the stack can be reduced or increased; the height will shrink or grow accordingly.

Jet Propulsion Lab.
NASA Resident Office
Technology Utilization Officer: Arif Husain
Mail Stop 180-801
4800 Oak Grove Drive
Pasadena, CA 91109
(818) 354-4862
Patent Counsel: Thomas H. Jones
Mail Code 180-801
4800 Oak Grove Drive
Pasadena, CA 91109
(818) 354-5179
Technology Utilization Mgr. for JPL: Dr. Norman L. Chalfin
Mail Stop 156-211
4800 Oak Grove Drive
Pasadena, CA 91109
(818) 354-2240

FOR ADDITIONAL INFORMATION: *Contact: Director, Technology Transfer Division, P.O. Box 8757, BWI Airport, MD 21240; (301) 621-0100 Ext. 241*
REFER TO THE NUMBER LISTED AT THE END OF THIS ARTICLE

NASA Tech Brief
National Aeronautics and Space Administration
NASA's Jet Propulsion Laboratory, Pasadena, California

Licensing Opportunity

Rugged Direct-Current Transducer

The solid core withstands mechanical and thermal shocks.

A direct-current transducer withstands thermal and mechanical shocks. It operates from a single, nominally 15-V power supply and is nearly insensitive to both large variations in temperature and variations of as much as ±5 V in the supply voltage. Its output voltage is a highly linear function of the sensed current, with a full-scale value of about 3 Vdc and an offset of about 0.1 Vdc at 0 sensed current.

The ruggedness of the transducer is due in large part to the novel magnetic core, which is machined from a solid block of a nickel/iron high-permeability, low-hysteresis alloy. This kind of core can withstand more mechanical and thermal abuse than can the tape-wound and sintered cores used in older transducers. The core includes mounting tabs and a gap that accommodates a Hall-effect sensor (see Figure 1). The wire carrying the current to be sensed is wrapped around part of the core.

The Hall-effect sensor is connected to an instrumentation amplifier (see Figure 2). This sensor puts out a voltage proportional to the current to be sensed and to the constant current I_c that is supplied to it. I_c is generated by part of the instrumentation amplifier; namely, the combination of Zener diode CR_2, constant-current diode CR_1, and operational amplifier U_A, which is part of a quad operational amplifier that also includes operational amplifiers U_B, U_C, and U_D.

The output voltage V_H from the Hall-effect sensor is fed to U_B and U_C. The outputs of U_B and U_C are fed to U_D, which serves as the output amplifier. Resistor R_{13} is selected to provide the desired output-voltage offset, and R_{14} is selected in conjunction with the number of turns in the coil on the core to provide the desired gain. Three units were built, 1 turn for 20 A, 2 turns for 10 A, and 20 turns for 1 A.

This work was done by Colonel W.T. McLyman of Caltech for **NASA's Jet Propulsion Laboratory.**

In accordance with Public Law 96-517, the contractor has elected to retain title to this invention. Inquiries concerning rights for its commercial use should be addressed to

Edward Ansell
Director of Patents and Licensing
Mail Stop 305-6
California Institute of Technology
1201 East California Boulevard
Pasadena, CA 91125
Refer to NPO-17957/TN.

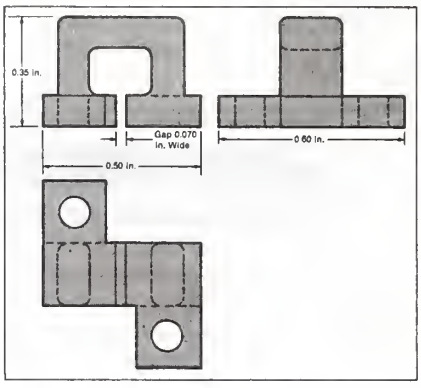

Figure 1. The **Magnetic Core** is machined from a solid block of high-permeability nickel/iron alloy.

Jet Propulsion Lab.
NASA Resident Office
Technology Utilization Officer Gordon S. Chapman
Mail Stop 180-801
4800 Oak Grove Drive
Pasadena, CA 91109
(818) 354-4849
Patent Counsel Paul F. McCaul
Mail Code 180-801
4800 Oak Grove Drive
Pasadena, CA 91109
(818) 354-2734
Technology Utilization Mgr. for JPL Norman L. Chalfin
Mail Stop 156-211
4800 Oak Grove Drive
Pasadena, CA 91109
(818) 354-2240

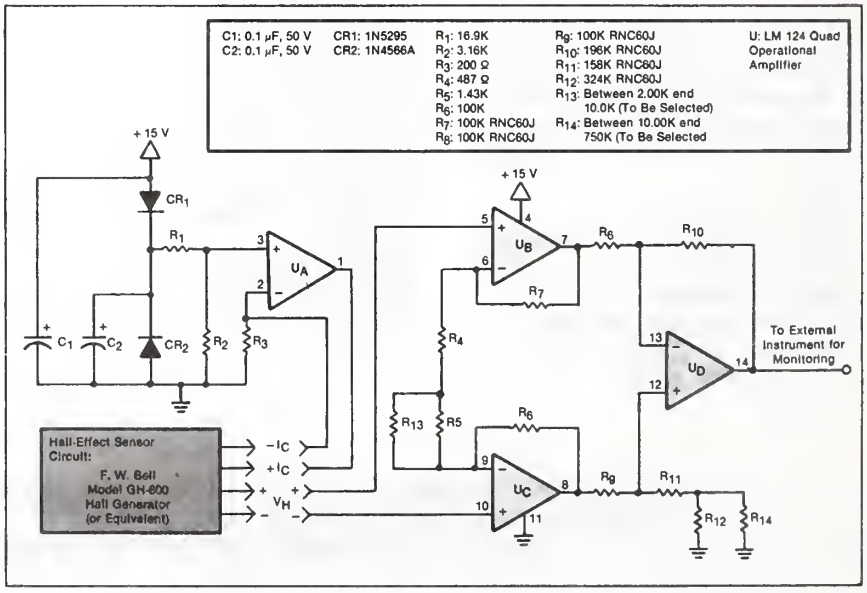

Figure 2. The **Transducer Circuit** excites a Hall-effect sensor and puts out a voltage that varies linearly with the sensed current.

FOR ADDITIONAL INFORMATION: *Contact: Director, Technology Transfer Division, P.O. Box 8757, BWI Airport, MD 21240; (301) 621-0100 Ext. 241*
REFER TO THE NUMBER LISTED AT THE END OF THIS ARTICLE

NASA Tech Brief
National Aeronautics and Space Administration
NASA's Jet Propulsion Laboratory, Pasadena, California

Licensing Opportunity

Si/IrSi$_3$ Schottky-Barrier Infrared Detectors

Ir and Si are codeposited in stoichiometric ratio to suppress mixed Ir/Si phases.

Silicon/iridium silicide Schottky-barrier detectors that have cutoff wavelengths from about 9 to about 14 μm have been fabricated with the help of an improved Ir/Si-codeposition process. This is part of a continuing effort to develop imaging arrays of Schottky-barrier detectors that operate at far-infrared wavelengths. Imaging arrays of 512×512 silicon/iridium silicide Schottky-barrier detectors with a cutoff wavelength of 7.3 μm had been fabricated previously, but these and other devices made of silicon/iridium silicide had exhibited poor and unreproducible diode characteristics, and their quantum efficiencies have been lower than those of silicon/platinum silicide Schottky-barrier detectors. (Silicon/platinum silicide detectors exhibit a cutoff wavelength of 5.6 μm, and the technology of these devices is relatively mature.)

Previously, silicon/metal silicide Schottky-barrier devices were fabricated by depositing metals on silicon substrates, then annealing to form the silicides by chemical reactions between the metals and the silicon. In the case of silicon/iridium silicide, the poor quality of the resulting devices has been attributed partly to contamination — primarily oxygen — at the silicon/silicide interfaces. In addition, iridium tends to react with the oxygen at the interfaces to form iridium oxide, which impedes diffusion across the interfaces, thereby impeding the formation of iridium silicide. The products of the reactions are mixtures of the IrSi, IrSi$_{1.75}$, and IrSi$_3$ phases. Either IrSi or IrSi$_3$ (not both) is preferred. Undesirably, the presence of the three phases in varying amounts causes variations in the heights of the Schottky barriers (with corresponding variations in cutoff wavelengths), and IrSi$_{1.75}$ contributes to high series resistances.

Both Si/IrSi and Si/IrSi$_3$ detectors (see Figure 1) have been fabricated by the improved process. In this process, the silicon substrate is oriented for deposition on the (100) surface, and prior to deposition, the surface is cleaned. In a vacuum chamber, Ir and Si are codeposited by molecular-beam epitaxy in the stoichiometric ratio of 1:1 or 1:3 from two electron-gun

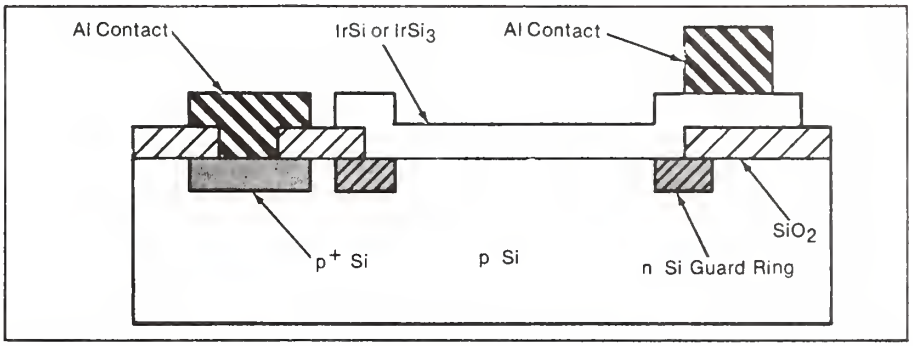

Figure 1. The **Si/IrSi or Si/IrSi$_3$ Schottky-Barrier Detector** is fabricated by the stoichiometric codeposition of Ir and Si on the p Si substrate. It includes a p$^+$ substrate contact, the silicide electrode, and an n Si guard ring, which suppresses leakage around the periphery of the silicide electrode.

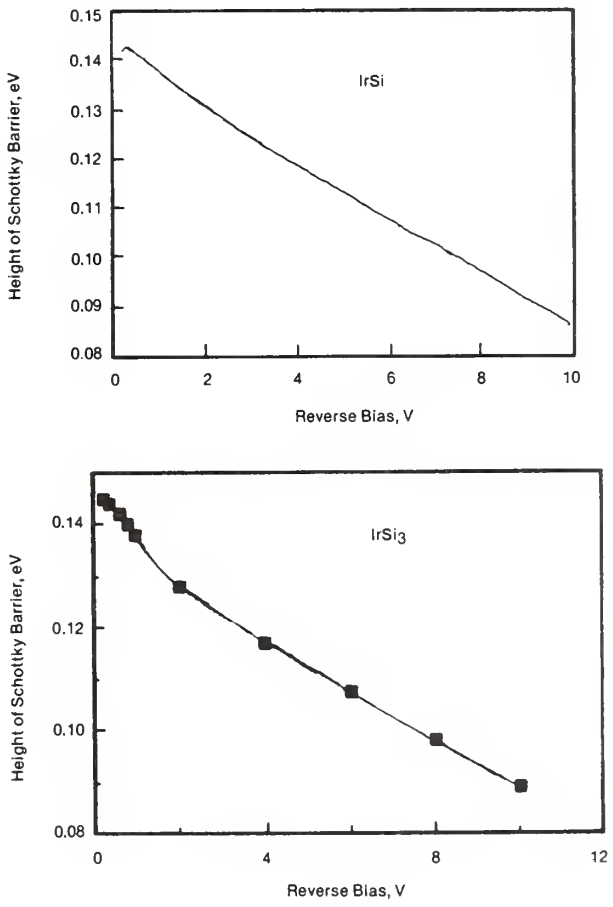

Figure 2. The **Heights of Schottky Barriers** as functions of reverse bias were determined by activation-energy analysis.

sources. The thickness of the deposit is about 50 Å. The substrate is heated to a temperature between 200 and 500 °C or between 680 and 800 °C for the deposition of IrSi or $IrSi_3$, respectively. The IrSi or $IrSi_3$ is then patterned by ion milling. Aluminum contacts are then deposited on the silicide and substrate.

Experimental devices fabricated by this process have been characterized by current-vs.-voltage measurements and activation-energy analysis. In addition, the cutoff wavelength of an $Si/IrSi_3$ detector was determined independently by measuring its photoresponse. For $Si/IrSi_3$, the measured heights of the Schottky barriers ranged from 0.138 eV to 0.089 eV as the reverse bias voltage ranged from −1 to −10 V; this represents a range of cutoff wavelengths from 9 to 14 m. Similar results were obtained for Si/IrSi (see Figure 2).

This work was done by True-Long Lin of Caltech for **NASA's Jet Propulsion Laboratory.**

In accordance with Public Law 96-517, the contractor has elected to retain title to this invention. Inquiries concerning rights for its commercial use should be addressed to

Edward Ansell
Director of Patents and Licensing
Mail Stop 305-6
California Institute of Technology
1201 East California Boulevard
Pasadena, CA 91125

Refer to NPO-18027/TN and NPO-17946/TN.

Jet Propulsion Lab.
NASA Resident Office
Technology Utilization Officer Gordon S. Chapman
Mail Stop 180-801
4800 Oak Grove Drive
Pasadena, CA 91109
(818) 354-4849
Patent Counsel Paul F. McCaul
Mail Code 180-801
4800 Oak Grove Drive
Pasadena, CA 91109
(818) 354-2734
Technology Utilization Mgr. for JPL Norman L. Chalfin
Mail Stop 156-211
4800 Oak Grove Drive
Pasadena, CA 91109
(818) 354-2240

FOR ADDITIONAL INFORMATION: *Contact: Director, Technology Transfer Division, P.O. Box 8757, BWI Airport, MD 21240; (301) 621-0100 Ext. 241*
REFER TO THE NUMBER LISTED AT THE END OF THIS ARTICLE

NASA Tech Brief
National Aeronautics and Space Administration
NASA's Jet Propulsion Laboratory, Pasadena, California

Solid-State Imaging Device With Carbon Film

The film reduces Fresnel reflections and dissipates static electric charges.

The performance of a solid-state imaging device (e.g., a charge-coupled device) can be enhanced by coating the surface through which photons enter with a thin film of carbon or diamondlike carbon. The film is beneficial in two ways: it acts as an antireflection coat, and it helps to dissipate undesired static electric charges that would otherwise accumulate on the surface.

Typically, a solid-state imaging device resides on a silicon substrate, and light is directed into the substrate through the back surface — that is, the surface opposite the one that holds the circuitry. An antireflection coat is desirable because the relatively high index of refraction of silicon gives rise to large Fresnel reflections of the incident light.

Some incident photons give rise to photoelectrons that are ejected from the surface, and because the electrical resistivity of the silicon substrate is high, this phenomenon causes the undesired accumulation of positive charges on the surface. The accumulated charges can reach levels great enough to alter the desired transfers of charges among the picture elements of the imaging device. Metallic films have been deposited on back surfaces of such devices in the attempt to conduct static charges away. However, metal films are disadvantageous in several ways: some metals diffuse into silicon, others absorb gases and behave anomalously, and most absorb photons, attenuating the light on its way to the sensing elements.

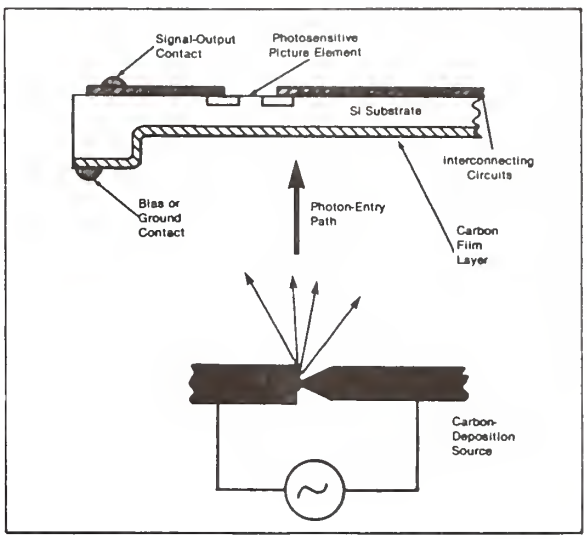

Carbon is Evaporated onto the back surface of a solid-state imaging device. The carbon film acts as an antireflection and antistatic coat.

Carbon is a good choice for the back-surface film for three reasons: (1) It is sufficiently electrically conductive to drain away the static charges but not so conductive as to attenuate light severely when deposited in thin layers. (2) Its index of refraction approximates the square root of the index of refraction of silicon, which is the optimum value for an antireflection coat. (3) It is chemically inert at the operating temperatures of the imaging device.

Carbon can be deposited on an imaging device by any of a number of established methods, and preferably by evaporation (see figure). The carbon film will be maximally effective as an antireflection coat if its thickness is an odd integral multiple of a quarter wavelength of the incident light (preferably ¼ or ¾ wavelength). In contrast, a typical metal film thicker than 1,000 Å would be opaque at most wavelengths.

This work was done by Robert E. Frazer of Caltech for **NASA's Jet Propulsion Laboratory.** *NPO-18201/TN*

FOR ADDITIONAL INFORMATION: *Contact: Director, Technology Transfer Division, P.O. Box 8757, BWI Airport, MD 21240; (301) 621-0100 Ext. 241*
REFER TO THE NUMBER LISTED AT THE END OF THIS ARTICLE

NASA Tech Brief
National Aeronautics and Space Administration
NASA's Jet Propulsion Laboratory, Pasadena, California

Licensing Opportunity

Two-Period Gratings for Surface-Emitting Lasers

More light is reflected back into the lasers.

Solid-state lasers of the type that emit light perpendicularly to their broad surfaces can be made more efficient by use of two-period surface diffraction gratings. Heretofore, a typical device of this type has been made with two gratings, both of which have a single spatial period equal to the wavelength of the light.

In such a device with a single-period grating, the same gratings serve both to couple light out from the surface and to reflect light back into the laser resonator (see Figure 1). To obtain high efficiency and low threshold current, it is necessary to reflect most of the light back inside and couple out only a small fraction. It is difficult to fabricate a single-period grating in such a way as to attain the desired ratio of output coupling to reflection; as a result, the proportion coupled out is too large, the proportion reflected back in is too small, and consequently the single-period devices tend to exhibit low efficiencies and high threshold currents.

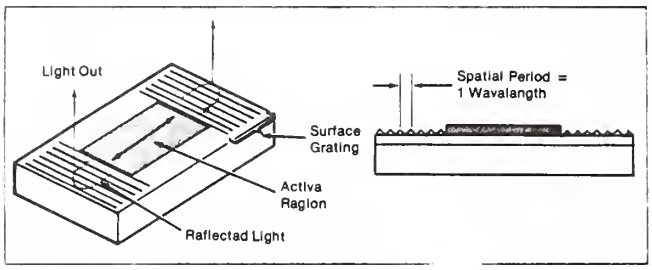

Figure 1. In a **Surface-Emitting Laser With Single-Period Gratings**, the same gratings both couple light out and reflect light back inside.

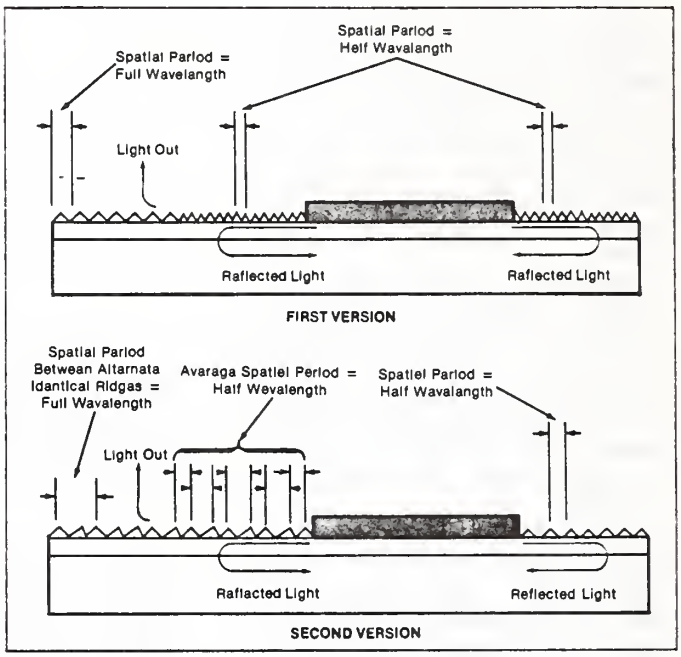

Figure 2. **Grating Surfaces That Have Two Spatial Periods** can be tailored to obtain the desired proportions of output coupling and inward reflection.

Figure 2 illustrates two versions of a rectangular two-period-grating surface-emitting laser. In the first version, one of the gratings is divided into two adjacent parts: an output part in which the spatial period is equal to or slightly less than the wavelength and a reflecting part in which the spatial period is half the wavelength. By separating the output-coupling portion from the reflecting portion, one can tailor each independently of the other to optimize the structure of the device to obtain low threshold current. This device has been demonstrated to give a 40 percent reduction in threshold current compared to conventional devices.

In the second version, the grating on the reflecting (only) surface has a spatial period of half the wavelength, while the grating on the output surface has a single pattern characterized by two spatial periods. The average distance between adjacent ridges is half the wavelength. The even- and odd-numbered ridges have slightly different shapes and/or are displaced toward or away from each other by a small fraction of the wavelength; this amounts to a slight perturbation in the half-wavelength pattern, with a spatial period equal to the full wavelength. The strength of the output coupling from this grating increases with the amount of full-wavelength perturbation from the half-wavelength pattern.

The same principle should also be applicable to an annular-Bragg-reflector-grating surface-emitting laser described in *NASA Tech Briefs* Vol. 14, No. 10 (1990), page 20 (NPO-17912). In this case, the annular grating would be divided into two parts: an inner first-order grating (with radial period ≈ half the wavelength) for reflection and an outer second-order grating (with radial period ≈ the wavelength) for output coupling.

This work was done by Robert J. Lang of Caltech for **NASA's Jet Propulsion Laboratory**.

This invention is owned by NASA, and a patent application has been filed. Inquiries concerning nonexclusive or exclusive license for its commercial development should be addressed to the Patent Counsel, NASA's Resident Office-JPL. Refer to NPO-18054/TN.

Jet Propulsion Lab.
NASA Resident Office
Technology Utilization Officer Gordon S. Chapman
Mail Stop 180-801
4800 Oak Grove Drive
Pasadena, CA 91109
(818) 354-4849
Patent Counsel Paul F. McCaul
Mail Code 180-801
4800 Oak Grove Drive
Pasadena, CA 91109
(818) 354-2734
Technology Utilization Mgr. for JPL Norman L. Chaffin
Mail Stop 156-211
4800 Oak Grove Drive
Pasadena, CA 91109
(818) 354-2240

NASA Tech Brief
National Aeronautics and Space Administration
NASA's Jet Propulsion Laboratory, Pasadena, California

Licensing Opportunity

Wideband Phase-Locked Angle Modulator

The modulator can be designed independently of the phase-locked loop.

A modified configuration for a phase-locked angle modulator circuit makes it possible to design the filters in the modulating portion of the circuit independently of the filter in the phase-locked-loop portion (the "loop filter"). The bandwidth of the phase- or frequency-modulated output is not limited by the low-pass nature of the loop filter, as it is in a typical conventional phase-locked angle modulator.

The figure illustrates the conventional and modified phase-locked angle modulators. In the conventional circuit, the phase- or frequency-modulating signal, whichever the case may be, is applied at one of the two baseband positions of the feedback arm of the phase-locked loop. These are, respectively, the position immediately preceding or the position immediately following the loop filter. In the modified circuit, the modulating signal is applied through modulation filters to both baseband positions, so that the design of the modulator can be freed of the constraints that would otherwise be imposed by the loop filter.

An analysis of the transfer functions of the modified circuit shows that an appropriate choice of the modulation filters makes the output phase or frequency modulation independent of the transfer function of the loop filter. For phase modulation, this choice is $P(s) = s/K_O K_D$ and $Q(s) = 1$, where the symbols have the meanings indicated in the figure. The modulation filter denoted by this $P(s)$ is a differentiator with a time constant equal to $1/K_O K_D$. This choice makes the phase modulation of the output signal equal to $1/K_D \times$ the input modulating signal.

For frequency modulation, the choice is $P(s) = 1$ and $Q(s) = K_O K_D/s$. The modulation filter denoted by this $Q(s)$ is an integrator with a time constant equal to $1/K_O K_D$. This choice makes the frequency modulation of the output signal equal to $K_O \times$ the input modulating signal. As one can determine by examining the figure, the frequency modulator can be derived from the phase modulator by inserting an integrator in each of the modulating-signal-injecting arms.

This scheme is subject to the requirement to constrain the peak modulation index so that the total phase error at the input of the phase detector does not exceed the linear range of the phase detector. Also, because the phase-locked loop is a carrier-tracking loop, the modulation index must be constrained to prevent a carrier null at the input of the phase detector and to prevent saturation of the integrator or differentiator.

This scheme was applied to phase-mod-

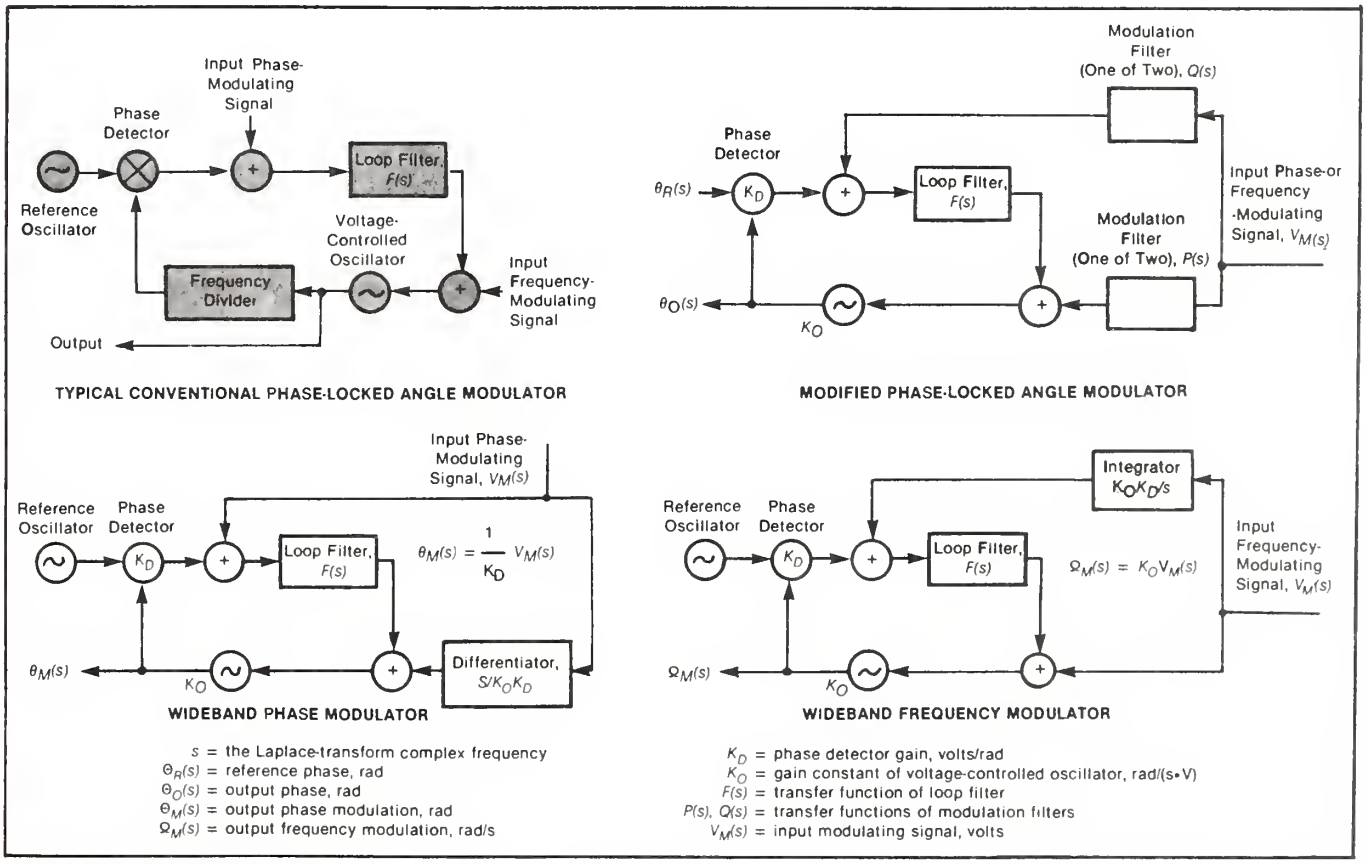

In the Modified Phase-Locked Angle Modulator, the modulating signal is applied at two points instead of at one point as it is in the conventional version. The wideband phase and frequency modulators are examples of the modified phase-locked angle modulator.

ulate a phase-locked oscillator designed for low-noise performance at a carrier frequency of 2,290 MHz. Measurements showed that the 3-dB bandwidth of the output modulation spectrum was about 1.50 MHz, even though that of the phase-locked loop was only 75 kHz.

This work was done by Lim Nguyen of Caltech for **NASA's Jet Propulsion Laboratory.**

Inquiries concerning rights for the commercial use of this invention should be addressed to the Patent Counsel, NASA Resident Office-JPL. Refer to NPO-18047/TN.

Jet Propulsion Lab.
NASA Resident Office
Technology Utilization Officer Gordon S. Chapman
Mail Stop 180-801
4800 Oak Grove Drive
Pasadena, CA 91109
(818) 354-4849
Patent Counsel Paul F. McCaul
Mail Code 180-801
4800 Oak Grove Drive
Pasadena, CA 91109
(818) 354-2734

Technology Utilization Mgr. for JPL Norman L. Chalfin
Mail Stop 156-211
4800 Oak Grove Drive
Pasadena, CA 91109
(818) 354-2240

FOR ADDITIONAL INFORMATION: *Contact: Director, Technology Transfer Division, P.O. Box 8757, BWI Airport, MD 21240; (301) 621-0100 Ext. 241*
REFER TO THE NUMBER LISTED AT THE END OF THIS ARTICLE

Program Processes SAR Data

The MacMultiview program computes polarimetric and other images.

MacMultiview is an interactive software tool for the Macintosh II family of computers that enables one to display, and make computations that use, polarimetric radar data collected by the Jet Propulsion Laboratory's imaging SAR (synthetic-aperture radar) polarimeter system. The system includes the single-frequency L-band sensor mounted on the NASA CV990 aircraft and its replacement, the multifrequency P-, L-, and C-band sensors mounted on the NASA DC-8 airplane.

MacMultiview provides two basic functions: synthesis of polarimetric images and computation of polarization signatures. The radar data can be used to compute a variety of images. The total-power image displays the sum of the polarized and unpolarized components of the backscatter for each picture element. The magnitude/phase-difference image displays the difference between the phases of the HH (horizontal transmitting and horizontal receiving polarization) signals and the VV (vertical transmitting and vertical receiving polarization) signals by use of color. Magnitude is displayed as intensity. The user may also select any combination of transmitting and receiving polarizations from which an image is synthesized. This image displays the backscatter that would have been observed, had the sensor been configured to use the selected transmitting and receiving polarizations.

MacMultiview can also be used to compute polarization signatures, which are three-dimensional plots of backscatter versus transmitting and receiving polarizations. The standard copolarization signatures (transmitting and receiving polarizations the same) and cross-polarization signatures (transmitting and receiving polarizations orthogonal) can be plotted for any rectangular subset of picture elements within a set of radar data. In addition, the ratio of copolarization and cross-polarization signatures computed from different subsets within the same set of data can also be computed.

Computed images can be saved in a variety of formats: byte format (headerless format, which saves the image as a string of byte values), MacMultiview (a byte image preceded by an ASCII header), and PICT2 format (standard format readable by MacMultiview and other image-processing programs for the Macintosh computer). Images can also be printed on PostScript output devices.

Polarization signatures can be saved in either a PICT format or a text file containing PostScript commands and can be printed on any QuickDraw output device. The associated Stokes matrices can be stored in a text file.

The only computers on which MacMultiview can be executed are those of the Macintosh II family that are equipped with 8-bit video (gray shades or color). The program also requires a minimum configuration of System 6.0, Finder 6.1, and 1 megabyte of memory. Macintosh Programmer's Workshop and Macintosh Programmer's Workshop C (version 3.0) are required for recompiling and relinking. The program is written in C and was developed in 1989.

This program was written by Lynne Norikane and Howard Zebker of Caltech for **NASA's Jet Propulsion Laboratory.**
NPO-18048/TN

FOR ADDITIONAL INFORMATION

CONTACT
COSMIC®
112 Barrow Hall
University of Georgia
Athens, GA 30602

(404) 542-3265

Wright-Patterson Air Force Base

Holographic Wafer Inspection

Integrated circuit wafer size and density have increased substantially in recent years, which has necessitated advances in inspection equipment. Historically, the optical microscope has been the primary tool for defect detection and process evaluation. However, due to the ever increasing magnification required, the inspection area continues to decrease when using this method. Other automated methods also are inadequate for present and future wafer technology. Holographic inspection techniques offer the best solution to this problem—they are fast, and they can highlight defects over a major portion of the wafer surface.

A holographic inspection technique, developed by Insystems of San Jose, California and optimized by the National Semiconductor Corporation, provides a permanent, three-dimensional record of process anomalies. Inspection can be performed in line, on line, in process, or off line in more detail. A new wafer inspection philosophy is emerging through the success of this program. Unlike the traditional "defect accounting" methods, process improvement emphasis has shifted to the detection of whole wafer defect patterns and process signatures, which can lead directly to specific process control problems. Faster and earlier detection of process problems means lower cost and shorter lead times for integrated circuits and, thus, military devices.

The system has been implemented at National Semiconductor's facility and further transfer of these improvements within the integrated circuit industry is being accomplished using Sematech, a consortium of 14 U.S. semiconductor manufacturers and the Department of Defense. A follow-on effort for whole wafer inspection is being pursued for a FY 1992 start.

The benefits of this improvement include reduced wafer inspection time, which reduces cost and increases yield, real-time and in-process control, early identification of process problems for increased yield, and extensive transfer of these improvements within the industry.

Contract: F33615-88-C-5442, Project Engineer: Mary Kinsella, WL/MTEM, (513) 255-2142.

NASA Tech Brief
National Aeronautics and Space Administration
Goddard Space Flight Center, Greenbelt, Maryland

Characterization of Electrical Response of Photodetector

Fourier analysis of input and output yields electrical frequency response.

Fourier analysis is the basis of a method of characterizing the electrical frequency or time response of a photodetector. In this method, the detector is stimulated by an optical input signal, the intensity of which is modulated with a square wave or other repetitive waveform of known frequency spectrum, and the output of the detector is recorded. The electro-optical transfer function, which characterizes the frequency response of the detector, is then computed as the ratio between the discrete Fourier transforms of the output and input waveforms (see figure).

The real and imaginary components of the discrete Fourier transform $S(k)$ at the kth point in frequency space are given by

$$S(k)_{real} = \frac{1}{N}\sum_{i=0}^{N-1} X(i)\cos\left(\frac{2\pi ik}{N}\right)$$

$$S(k)_{imaginary} = \frac{1}{N}\sum_{i=0}^{N-1} X(i)\sin\left(\frac{2\pi ik}{N}\right)$$

where N is the number of samples, k can be any integer from 0 through $N-1$, and $X(i)$ is the instantaneous amplitude of the signal in question at the time of the ith sample. The sampling period, T_s, must be an integral submultiple of the period of the waveform, and the reciprocal of the sampling period must be at least twice the highest frequency present in the waveform. The frequency resolution, Δf, becomes finer as the number of samples increases:

$$\Delta f = 1/NT_s$$

The method has been applied successfully to Golay-cell and bolometer detectors and is applicable to any detector system, the ac component of the electrical response of which is linear. The principal advantage of this method is speed; because the input waveform contains many frequencies spanning the entire spectral range of interest, one set of measurements serves to characterize the response of the detector at all of these frequencies. On the other hand, in the traditional method, the frequency response of a detector is measured by exciting it with a sinusoidally modulated signal, one frequency at a time, and measuring the output with a lock-in amplifier or spectrum analyzer. This is a time-consuming and tedious process in which accuracy depends on stability in both the output of the modulated source and the sensitivity of the detector. Changes in either the source or the detector (e.g., temperature dependence of the sensitivity of a bolometer) during a series of measurements can render the calibration invalid.

In one instance of the method, a Golay cell was illuminated by an infrared light-emitting diode powered by square wave with a period of 2.048 s. A digital oscilloscope sampled the input and output waveforms at 4,096 equal intervals (1/2 ms) during one cycle. The waveform data were transferred to a computer, where they were processed via an algorithm that first computed a modified binary Fourier transform, then computed the electro-optical transfer function by taking the ratio between the nonzero terms of the discrete Fourier transforms of the output and input waveforms.

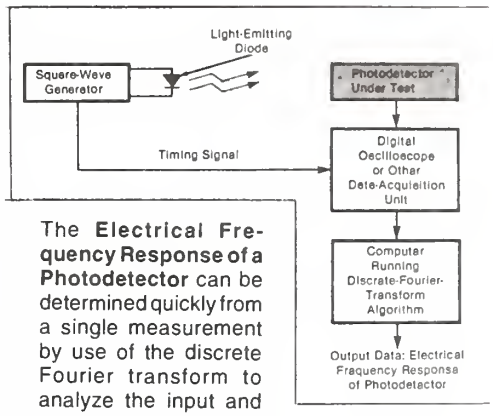

The **Electrical Frequency Response of a Photodetector** can be determined quickly from a single measurement by use of the discrete Fourier transform to analyze the input and output waveforms.

This work was done by John G. Hagopian and William Eichorn of **Goddard Space Flight Center.** *GSC-13349/TN*

FOR ADDITIONAL INFORMATION: *Contact: Director, Technology Transfer Division, P.O. Box 8757, BWI Airport, MD 21240; (301) 621-0100 Ext. 241*
REFER TO THE NUMBER LISTED AT THE END OF THIS ARTICLE

NASA Tech Brief
National Aeronautics and Space Administration
NASA's Jet Propulsion Laboratory, Pasadena, California

Multiaperture Spectrometer

Advantages would be a convenient two-dimensional spectral image, fewer components, and greater efficiency.

A proposed multiaperture spectrometer containing a single grating would provide high spectral resolution over a broad spectrum. In comparison with a more-conventional cross-dispersing spectrometer (containing two crossed gratings), this spectrometer would be simpler and more efficient and would provide greater flexibility in the detector format.

Heretofore, cross-dispersing spectrometers have been used to obtain wide-band, high-resolution spectral coverage. However, each grating acts as a partial polarizer, and therefore the two crossed gratings in a cross-dispersing spectrometer act partly like cross-polarizers, blocking much of the light that is needed to display the spectrum. In addition, the various orders of the spectrum in the output of a cross-dispersing spectrometer are not parallel.

The proposed multiaperture spectrometer (see figure) would use the available light more efficiently and display the various orders of the spectrum parallel to each other. To ensure that each entrance slit is illuminated by the same scene, the entrance pupil of the telescope that supplies the light to be analyzed would be made oversized and reimaged onto the plane of the entrance slits of the spectrometer. Inasmuch as the entrance pupil of the telescope and the entrance slits would be located at conjugate points with respect to each other, spectral-order-sorting bandpass filters could be placed at either location. Thus, the entrance aperture of the telescope would, in effect, be made into a series of apertures, each with its own filter.

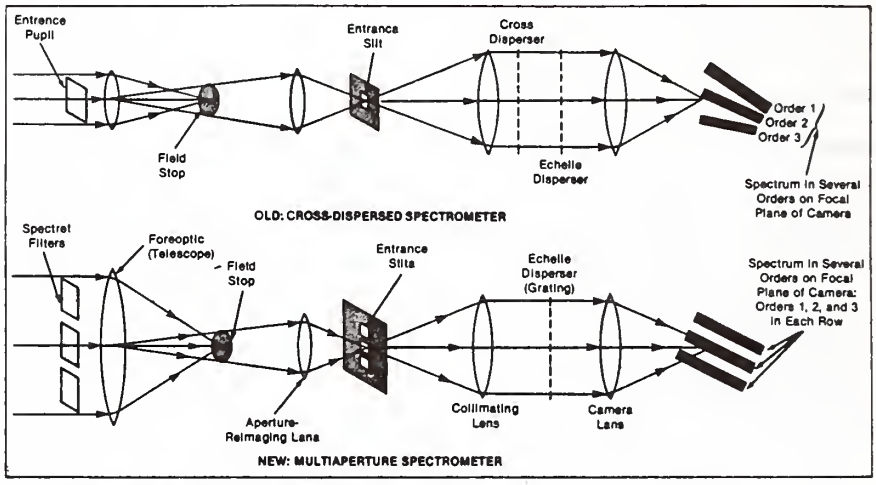

The **Multiaperture Spectrometer** would produce parallel line images, each of which would be a highly spectrally resolved display of intensity vs. wavelength in the wavelength band of one of the orders of the spectrum produced by the grating.

This work was done by Rudolf A. Schindler, Robert J. Pagano, and Fred G. O'Callaghan of Caltech for **NASA's Jet Propulsion Laboratory.**
NPO-18011/TN

FOR ADDITIONAL INFORMATION: *Contact: Director, Technology Transfer Division, P.O. Box 8757, BWI Airport, MD 21240; (301) 621-0100 Ext. 241*
REFER TO THE NUMBER LISTED AT THE END OF THIS ARTICLE

NASA Tech Brief
National Aeronautics and
Space Administration

Spaceborne Microwave Imagers

Principles and practices are described.

A monograph presents a comprehensive overview of the science and technology of spaceborne microwave-imaging systems. Microwave imagers are used as versatile orbiting, remote-sensing systems to investigate the atmospheres and surfaces of planets. For example, they can detect surface objects through canopies of clouds, measure distributions of raindrops in the clouds that their views penetrate, find meandering rivers in rain forests and underground water in arid regions, and provide information on ocean currents, wakes, ice/water boundaries, aircraft, ships, buoys, and bridges.

The document begins by presenting general background information on the nature and capabilities of spaceborne microwave imagers. This is followed by a general description of microwave-imaging equipment, with emphasis on antennas, scanning mechanisms, and receivers. The geometrical and functional relationships between an orbiting imager and the scene under observation, and the use of both horizontally and vertically polarized microwave radiation are discussed.

The equations that describe the radiative transfer of power are derived from basic physical principles. The thermodynamic temperature (an effective microwave-brightness temperature of the scene viewed by the microwave imager, and distinguished from the thermometric temperature, which would be measured by a thermometer in contact with an object in the scene) is expressed in closed form as a sum of cosmic, surface, and upwelling contributions. The equivalence between microwave power and thermodynamic temperature is established. The laws of thermodynamics are then applied to show the directions and amounts of flow of microwave energy among multiple bodies.

Examples are presented to illustrate the detection of such surface features as emitting (warm) objects, cold objects, and metal objects (which stand out in microwave scenes because their high electrical conductivities alter radiation patterns). The bistatic (forward- and back-scattering) cross sections of aircraft, ships, and metal buoys are discussed, with descriptions of a mathematical model, calculations, and the underlying theory. Examples of the detection of ships, aircraft, and buoys in images produced by orbiting microwave radiometers are presented, along with computed signal-to-clutter ratios for these objects.

The main text concludes with a general discussion of concepts of spaceborne microwave imagers. Examples of existing and contemplated planetary imagers are presented. Principal elements of microwave technology that are essential for remote sensing of the surfaces and atmospheres of planets are identified.

This work was done by J.M. Stacey of Caltech for **NASA's Jet Propulsion Laboratory.** *"Spaceborne Microwave Imagers—Principles and Practices."*
NPO-17094/TN

FOR ADDITIONAL INFORMATION: *Contact: Director, Technology Transfer Division, P.O. Box 8757, BWI Airport, MD 21240; (301) 621-0100 Ext. 241*
REFER TO THE NUMBER LISTED AT THE END OF THIS ARTICLE

Energy

0348 Characterizing the Solar Ultraviolet Resource

0349 NiF2 Cathodes for Rechargeable Na Batteries—Energy densities are higher than with metal chlorides.

0350 Regenerative Hydride Heat Pump—A cyclical regenerative heating scheme would increase efficiency. (Licensing Opportunity)

Department of Energy

Technology Application

National Renewable Energy Laboratory

Characterizing the Solar Ultraviolet Resource

The high-energy photons found in ultraviolet (UV) light play an important role in the performance of solar detoxification systems and multilayered photovoltaic devices. For the past year, SERI researchers have been collecting UV data that will allow more accurate performance predictions for these technologies.

The study, which took place at SERI's Solar Radiation Resource Laboratory in Golden, involved the use of spectroradiometers to measure the amount of UV radiation in the global-horizontal and direct-normal components of sunlight (see page 4). Results show that the ratio of global-horizontal UV varies only slightly with the position of the sun, forming about 4%-6% of the full-spectrum, global-horizontal radiation received throughout the day and year. Direct-normal UV is more dependent on sun angle and cloud cover.

Results also indicate that current models for predicting the performance of solar detoxification systems underestimate the amount of direct-normal UV radiation received under clear skies.

Until this study, most UV resource data have been limited to global-horizontal measurements. In addition to developing technologies, the new data can be used to validate models for estimating spectral solar radiation resources for areas where actual measurements aren't available.

For Additional Information:

Steve Rubin
National Renewable Energy Laboratory
1617 Cole Boulevard
Golden, CO 80401-3393
(303) 231-7303

Refer to Volume XII, Number 2/TN

NASA Tech Brief
National Aeronautics and Space Administration
NASA's Jet Propulsion Laboratory, Pasadena, California

NiF_2 Cathodes for Rechargeable Na Batteries

Energy densities are higher than with metal chlorides.

The use of NiF_2 cathodes in place of $NiCl_2$ cathodes in medium-to-high-temperature rechargeable sodium batteries increases energy and power densities by 25 to 30 percent without detracting from the potential advantage of safety that this type of sodium battery offers over sodium batteries that have sulfur cathodes. High-energy-density sodium batteries with metal fluoride cathodes could be used in electric vehicles and for leveling loads on powerlines.

Cathodes made of transition-metal chlorides ($FeCl_2$ and $NiCl_2$) have been used as alternatives to sulfur cathodes in rechargeable sodium batteries that are now approaching commercialization. These metal chlorides are typically insoluble in the molten-$NaAlCl_4$ catholytes of these cells. Apart from several potential safety and operational advantages, these systems have theoretical energy densities almost comparable to those of Na/S batteries. However, the practical energy and power densities attainable in these batteries are slightly lower than those of Na/S batteries. This fact has stimulated modifications to enhance the practically attainable energy and power densities.

The use of nickel fluoride in place of nickel chloride would reduce the weight of an energy-equivalent cathode by 25 percent. Assuming that the electrochemical potential is the same as for $NiCl_2$ (it could be higher), the theoretical energy density of NiF_2 is about 1,436 Wh/kg — 34 percent greater than the energy density of $NiCl_2$, which is 1,070 Wh/kg.

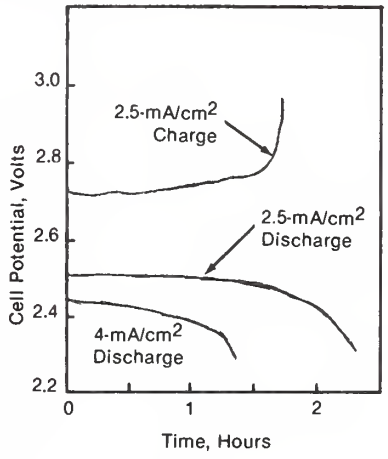

These Charge/Discharge Curves were obtained from measurements on a sodium cell with a 48-mAh NiF_2 cathode at a temperature of 230 °C.

In an experiment, nickel fluoride was impregnated from a concentrated aqueous solution into a sintered nickel matrix of the type used as plaques in Ni/Cd batteries. The impregnated matrix was then dried. On the basis of the gain in weight, the amount of NiF_2 in the electrode thus fabricated corresponded to about 48 mAh. The NiF_2 electrode was then tested in a laboratory cell, the configuration of which was Na(molten)/β''-Al_2O_3/$NaAlCl_4$(molten)/NiF_2(solid); this configuration is similar to that of a sodium/metal chloride cell.

The cell was tested at an operating temperature of about 230 °C. It exhibited charge/discharge curves that resemble those of an Na/$NiCl_2$ cell in that they are relatively flat, and the voltages are about the same (see figure). However, the electrochemical equivalent of the cathode of this cell (0.55 Ah/g) was greater than that of a representative Na/$NiCl_2$ cell (0.41 Ah/g). The coulombic yields in discharge exceeded 90 percent at current densities of 2 to 4 mA/cm^2. The cell exhibited a high degree of reversibility in charge/discharge cycling.

This work was done by Ratnakumar Bugga, Salvador Di Stefano, and Gerald Halpert of Caltech for **NASA's Jet Propulsion Laboratory.**
NPO-18119/TN

FOR ADDITIONAL INFORMATION: *Contact: Director, Technology Transfer Division, P.O. Box 8757, BWI Airport, MD 21240; (301) 621-0100 Ext. 241*
REFER TO THE NUMBER LISTED AT THE END OF THIS ARTICLE

NASA Tech Brief
National Aeronautics and Space Administration
NASA's Jet Propulsion Laboratory, Pasadena, California

Licensing Opportunity

Regenerative Hydride Heat Pump

A cyclical regenerative heating scheme would increase efficiency.

A proposed hydride chemisorption heat pump would be based on a cyclical regenerative heating scheme. In this scheme, over 90 percent of the sensible heat necessary to desorb hydrogen from each chemisorption unit during one phase of the cycle of operation would be supplied by recycling sensible heat from a similar chemisorption unit that was heated during the preceding phase. The portion of heat recycled in previous regenerative hydride heat pumps has been limited to about 50 percent. The cooling coefficient of performance of the proposed heat pump is expected to be about 0.9, which is 40 to 50 percent greater than that of present hydride heat pumps. Another important advantage is that unlike the chlorofluorocarbon working fluids used in conventional mechanical heat pumps, the hydrogen working fluid does not damage the ozone layer of the atmosphere.

The proposed heat pump would include four FeTi and four $LaNi_{4.7}Al_{0.3}$ chemisorption units, which would operate in a four-phase cycle. In the air-conditioning version shown in the figure, a coolant, such as oil or water, would be circulated among the sorption units and associated heat exchangers, radiators, and other heat-transfer units by a pump and a system of cyclically switched valves. The main input power would be supplied in the form of heat from natural gas, the Sun, or an external source of waste heat, for example.

When the main input power was directed to one of the $LaNi_{4.7}Al_{0.3}$ units, it would raise the temperature of the unit to 110 °C, causing it to desorb hydrogen at a pressure of 10 atm (1 MPa). Simultaneously, hydrogen would be absorbed exothermally in one of the FeTi units, and the large heat of this reaction would be transferred to the environment via a radiator at a temperature of about 50 °C. When the $LaNi_{4.7}Al_{0.3}$ unit was cooled to 50 °C, it would reabsorb the hydrogen from the FeTi, causing the FeTi to cool a great deal — down to 10 °C at 2 atm (0.2 MPa) hydrogen pressure. More heat would then be absorbed from the room at 10 °C to release more hydrogen from the FeTi, thereby cooling the room.

This **Hydride Heat Pump** would feature regenerative heating and a single circulation loop. Counterflow heat exchangers would accommodate the different temperatures of the FeTi and $LaNi_{4.7}Al_{0.3}$ subloops.

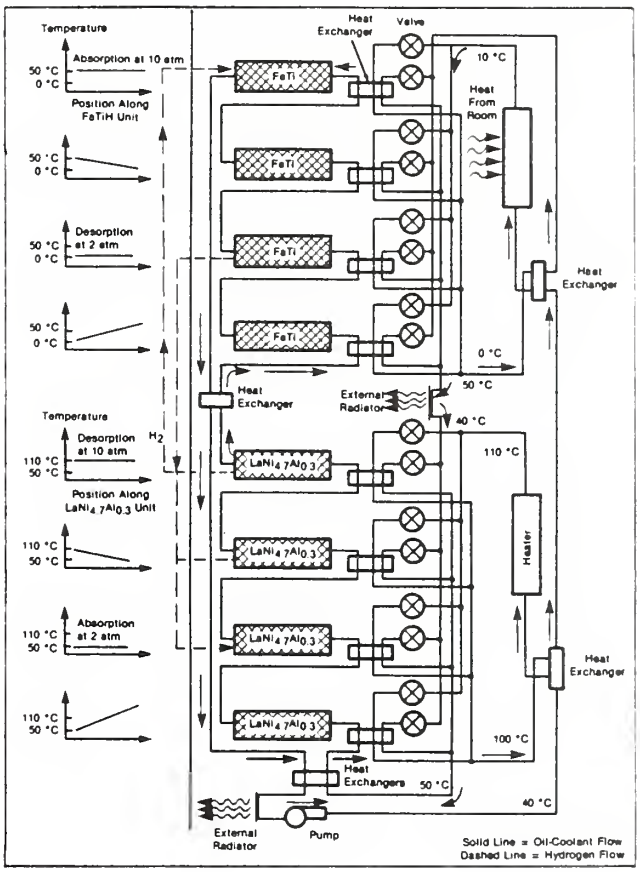

Jet Propulsion Lab.
NASA Resident Office
Technology Utilization Officer: Arif Husain
Mail Stop 180-801
4800 Oak Grove Drive
Pasadena, CA 91109
(818) 354-4862
Patent Counsel: Thomas H. Jones
Mail Code 180-801
4800 Oak Grove Drive
Pasadena, CA 91109
(818) 354-5179
Technology Utilization Mgr. for JPL: Dr. Norman L. Chalfin
Mail Stop 156-211
4800 Oak Grove Drive
Pasadena, CA 91109
(818) 354-2240

The valve-switching sequence would be set so that each $LaNi_{4.7}Al_{0.3}$ and each FeTi unit would be at one of the four phases of the cycle. Thus, a cyclic wave of heating and cooling would travel around the fluid-flow circuit (upward along the sequence of sorption units in the figure), each unit being warmed up to its next hot phase or cooled down to its next cold phase partly by the flow of working fluid from the preceding hot or cold unit, respectively.

This work was done by Jack A. Jones of Caltech for **NASA's Jet Propulsion Laboratory**.

In accordance with Public Law 96-517, the contractor has elected to retain title to this invention. Inquiries concerning rights for its commercial use should be addressed to
Edward Ansell
Director of Patents and Licensing
Mail Stop 305-6
California Institute of Technology
1201 East California Boulevard
Pasadena, CA 91125
Refer to NPO-18104/TN.

Engineering

0351 Artificial Intelligence in Computational Fluid Dynamics—Four AI systems are compared.

0352 Computed Hypersonic Viscous Flows Over Delta Wings—A conical Navier-Stokes algorithm accurately predicts shocks and pressure fields.

0353 Direct-Link Prehensor—An operator-powered mechanical hand gives protection, dexterity, and proximity to the work. (Licensing Opportunity)

0354 Direct Finite-Difference Simulations of Turbulent Flow—An upwind finite-difference scheme is compared with other numerical-integration schemes.

0355 Frequency-Domain Identification of Aeroelastic Modes.—Data from flight tests support the choice of the frequency-sweep method.

0356 Dynamic Analyses Including Joints of Truss Structures—A straightforward method is used to determine stiffness and damping coefficients.

0357 Evaluation of Performance of a Telerobot—Various tasks were performed with and without force feedback.

0358 A General-Coordinate Formulation for Boundary-Layer Flow—The general coordinates need not be orthogonal.

0359 Generation of Surface Grids From Data Points—Grids are constructed by interpolation and blending of patches.

0360 Investigation of Tapered Tension/Torsion Strap—A tapered strap provides more torque than a parallel one does.

0361 Lightweight Valve Closes Duct Quickly—A balloon expands to block the duct. (Licensing Opportunity)

0362 Lock for Valve Stem—Readily available materials and handtools are used to make a simple but effective device. (Licensing Opportunity)

0363 Navier-Stokes Computations on Zonal Grids—Flows about a wind and an airplane are simulated.

0364 Processing Particle-Streak Imagery on a Personal Computer—Streak patterns are used to obtain maps of flow-velocity vectors.

0365 Reducing Water/Hull Drag by Injecting Air Into Grooves—A proposed method would require much less air than does the microbubble-injection method. (Licensing Opportunity)

0366 Two Techniques for Suppressing Vibrations in Structures—The techniques are based on bridge feedback and a criterion for placement of actuators.

Software

0367 Integrated Analysis Capability Program—This modular software system facilitates multidisciplinary analyses of structures and other systems.

0368 Numerical-Optimization Program—The ADS computer program is suitable for such applications as minimum-weight design.

0369 Program Calibrates Strain Gauges—Time required for acceptance tests of hardware is reduced.

0370 Tracing and Control of Engineering Requirements—Requirements and progress of an engineering project can be documented in systematic manner.

Testing & Instrumentation

0371 Liquid Level and Volume Sensor (Licensing Opportunity)

0372 Snapshots of Room Temperature and Airflow

0373 Three-Point Bend Tests Performed

0374 Experiments on Schemes for Adaptive-Wall Wind Tunnels—Ways to reduce testing time for adaptation are discused.

0375 New Sensors for Flow Velocity and Acoustics—Development programs promise more accurate measurements.

NASA Tech Brief
National Aeronautics and Space Administration

Artificial Intelligence in Computational Fluid Dynamics

Four AI systems are compared.

A paper compares four first-generation artificial-intelligence (AI) software systems for computational fluid dynamics. On the basis of that comparison, the paper concludes that AI is most successful when it is applied to well-formulated problems that are solved by classifying or selecting preenumerated solutions. In contrast, the application of AI to poorly understood or poorly formulated problems generally results in a long development time and a large investment of effort, with no guarantee of success.

The paper focuses on knowledge-based ("expert") software systems. It analyzes their intended tasks, the kinds of knowledge they possess, the magnitude of effort required to codify the knowledge, how quickly they were constructed, their performances, and the return on investment.

The four software systems are the following:

1. The Expert Cooling Fan Design System (EXFAN) computes aerodynamical portions of the designs of turbomachinery components by starting with initial designs and repeatedly analyzing and revising until the design goals are met.
2. The PAN AIR Knowledge System (PAKS) aids users of PAN AIR, a panel-method program widely used in the design of airplanes. PAKS takes the user's goals and the geometry defined by the user and constructs a PAN AIR input deck.
3. The grid-adaptation program MITOSIS (referred to as "ADAPT" in this study since the actual name was unknown) adds robust failure recovery to a successive grid refinement/coarsening procedure, which depends on the local flow field.
4. The Expert Zonal Grid Generation (EZGrid) program partitions a two-dimensional flow field into four-sided, well-shaped zones that are then individually discretized.

The paper rates each system graphically with respect to several criteria. For example, it finds that the knowledge-amplification factor of EXFAN is quite high, while that of MITOSIS is rather low, and those of EZGrid and PAKS lie between the two extremes.

Three challenges for future development are proposed. The first is to identify additional aspects of computational fluid dynamics to which AI can be applied, and to refine or build on existing first-generation systems. The second is to increase the understanding and formalization of various aspects of computational fluid dynamics with a view toward the benefits that can be obtained in the long term by automating those aspects via AI. The third challenge is to identify the aspects of computational fluid dynamics that can be automated (for example, definition of geometry, design, generation of code, and selection of methodology), but the automation of which requires AI techniques that are still being developed (for example, geometric reasoning, representation of perceptual knowledge, constructive problem solving, learning, automatic programming, and qualitative physics). Starting work on this third challenge early will likely produce results sooner and will produce valuable feedback for researchers in AI.

This work was done by Alison Andrews Vogel of **Ames Research Center**. *Further information may be found in AIAA Journal 88A28036, Volume 26, No. 1, (January, 1988), pages 40 through 46, "Progress and Challenges in the Application of Artificial Intelligence to Computational Fluid Dynamics."*

Copies may be purchased [prepayment required] from AIAA Technical Information Service Library, 555 West 57th Street, New York, New York 10019, Telephone No. (212) 247-6500. ARC-12445/TN

FOR ADDITIONAL INFORMATION: *Contact: Director, Technology Transfer Division, P.O. Box 8757, BWI Airport, MD 21240; (301) 621-0100 Ext. 241*
REFER TO THE NUMBER LISTED AT THE END OF THIS ARTICLE

NASA Tech Brief
National Aeronautics and
Space Administration

Computed Hypersonic Viscous Flows Over Delta Wings

A conical Navier–Stokes algorithm accurately predicts shocks and pressure fields.

A report describes the development of an algorithm for the finite-volume (a type of finite-difference) solution of the conical Navier–Stokes equations of hypersonic viscous flow over a conical delta wing. The conical Navier–Stokes equations involve an approximation in which derivatives along rays that pass through the apex of the cone are set to zero. This approximation is justified by previous experimental observations that the viscous regions of supersonic flows over conical bodies are strongly dominated by the surrounding conical inviscid flows.

The conical Navier–Stokes equations in conservation-law form are derived, and the thin-layer approximation is introduced. The fluid is assumed to be a perfect gas similar to air, with viscosity, thermal conductivity, and Prandtl number dependent upon temperature according to Sutherland's formulas for the first two of these quantities.

The thin-layer Navier–Stokes equations are solved via a finite-volume formulation with state vectors stored at the centers of cells and fluxes defined at the faces of cells. Upwind differences are used for the inviscid flux derivatives, while central differences are used for the viscous flux vector. The initial conditions are chosen simply by setting all state vectors to free-stream values. This corresponds to an impulsively accelerated body in a supersonic flow. The solution is advanced to a steady state by an explicit, multistage scheme.

The conical Navier–Stokes equations and the algorithm were tested by using them to compute the mach 1.8 flow over an elliptical delta wing. The computation predicted primary and secondary leading-edge vortexes. The calculated pressure coefficient on the wing compared favorably with experimental data. Mach 10.17 flow over an isothermal flat delta wing was computed for angles of attack from 0° through 15°, and the extent of the viscous layer was predicted accurately for all angles of attack.

In the cases of hypersonic flow over an adiabatic wing, the calculation yielded spurious total temperatures in the boundary layer. This error is due to the van Leer flux-split formulation used in the algorithm. However, the overall comparison with experimental data in these cases was good. The conical Navier–Stokes equations can thus be expected to provide a good approximation for the flow over simple delta wings in supersonic and hypersonic flow.

A von Neumann stability analysis based on a one-dimensional flux-split model is used to predict the stability boundaries of the scheme. One-, two-, and three-stage schemes are considered for both first-order-accurate and second-order-accurate upwind formulations. The one-dimensional analysis shows that for the first-order-accurate formulation, the two-stage scheme is the most efficient. However, for the second-order-accurate formulation, the three-stage scheme is more efficient and is used in all the calculations. Also, the Courant-number restriction is strongly dependent on the stage coefficients and order of accuracy. In this study, a switch that involves a second difference in pressure was found to give sharp shocks while allowing nearly-second-order-accurate differencing in the boundary layer.

This work was done by Stephen M. Ruffin of **Ames Research Center** *and Earll M. Murman of the Massachusetts Institute of Technology. "Solutions for Hypersonic Viscous Flow Over Delta Wings."* *ARC-12179/TN*

FOR ADDITIONAL INFORMATION: *Contact: Director, Technology Transfer Division, P.O. Box 8757, BWI Airport, MD 21240; (301) 621-0100 Ext. 241*
REFER TO THE NUMBER LISTED AT THE END OF THIS ARTICLE

NASA Tech Brief
National Aeronautics and Space Administration
Ames Research Center, Moffett Field, California

Licensing Opportunity

Direct-Link Prehensor

An operator-powered mechanical hand gives protection, dexterity, and proximity to the work.

A mechanical prehensor replicates the movements of an operator's hand and fingers just a few centimeters from the hand. Because it encloses the operator's hand in a protective shroud, the prehensor enables the operator to grasp, hold, and manipulate nearby objects in a hostile or hazardous environment. The operator moves the prehensor through direct mechanical linkages; no electric motors or electronic circuits are needed.

The prehensor has a "ring" finger, an "index" finger, and a thumb, mounted on a supporting frame (see figure). The ring and index fingers consist of three jointed links each, and the thumb consists of two jointed links. The thumb is positioned opposite the fingers in an anthropomorphic arrangement. A palm assistor — a disk projecting from the support frame — helps the mechanical fingers to hold objects, much like the palm of a human hand.

The shroud is made of a rigid, gas-impermeable material such as aluminum or molded fiberglass. It is joined to the supporting frame by welding, bonding, or other means that produce a gas-tight seal. At its wrist end, the shroud is joined to a sleeve of the operator's protective suit by a seal.

Within the shroud, rings engage the various phalanges of the operator's fingers. The operator's middle and ring fingers are used in tandem to move the mechanical ring finger of the prehensor, and the operator's index finger and thumb are used independently to move the mechanical index finger and thumb, respectively, of the prehensor.

When the operator moves part of a finger, the movement is translated by mechanical linkages into similar movement of the corresponding part of the mechanical prehensor. For example, when the operator rotates the distal phalange of the thumb about its joint, the distal-control link rotates about the distal-control joint on the thumb mechanism. This actuates a distal-control pushrod, the action of which rotates the distal thumb link about the distal link joint on the mechanical thumb.

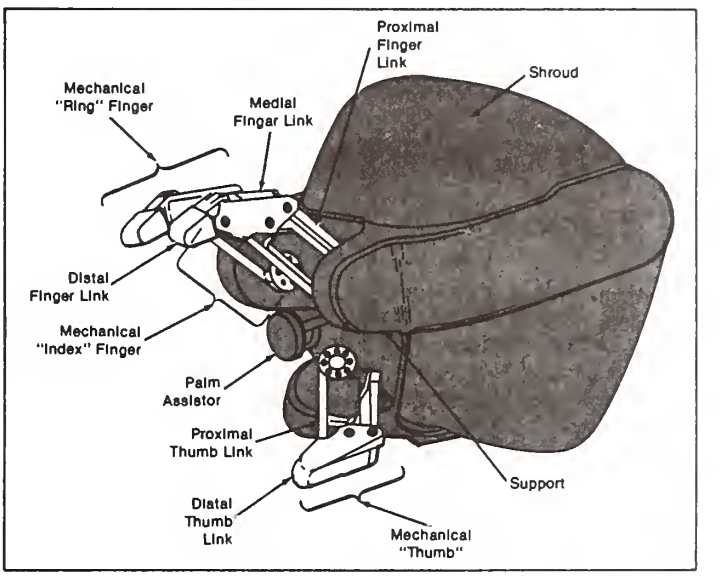

A Shroud Encloses the Operator's Hand, protecting it from vacuum, high pressure, or hazardous materials. The external mechanical fingers are made of materials compatible with the external environment.

The ratio of motion of the mechanical finger links to the corresponding control links is 1 to 1.1. With this ratio, the mechanical links can reach useful positions that would otherwise result in collisions between components of the control linkages.

This work was done by John W. Jameson of **Ames Research Center.**

In accordance with Public Law 96-517, the contractor has elected to retain title to this invention. Inquiries concerning rights for its commercial use should be addressed to

Stanford University
Office of Technology Licensing
3500 Cambridge Avenue, Suite 250
Palo Alto, CA 94306

Refer to ARC-11666/TN.

Ames Research Ctr.
Technology Utilization Officer: Laurance Milov
Mail Code 223-3
Moffett Field, CA 94035
(415) 694-4044
Patent Counsel:
Darrell G. Brekke
Mail Code 200-11
Moffett Field, CA 94035
(415) 694-5104

FOR ADDITIONAL INFORMATION: *Contact: Director, Technology Transfer Division, P.O. Box 8757, BWI Airport, MD 21240; (301) 621-0100 Ext. 241*
REFER TO THE NUMBER LISTED AT THE END OF THIS ARTICLE

NASA Tech Brief
National Aeronautics and
Space Administration

Direct Finite-Difference Simulations of Turbulent Flow

An upwind finite-difference scheme is compared with other numerical-integration schemes.

A report discusses the use of an upwind-biased finite-difference numerical-integration scheme to simulate the evolution of small disturbances and fully developed turbulence in the three-dimensional flow of a viscous, incompressible fluid in a channel. In contrast with simulations involving approximate mathematical models of turbulence, direct simulation involves the use of a computational grid sufficiently fine to resolve the motion of the fluid at all relevant length scales. This study was motivated partly by the need to simulate turbulent flows bounded by complicated shapes and partly by the observation that the main advantage of finite-difference schemes over the highly accurate spectral methods lies in the relative ease with which finite-difference schemes can be applied to complicated shapes. The purpose of this study was to demonstrate the superior performance of high-order-accurate upwind-biased finite-difference numerical-integration schemes in simulating turbulent flows and accurately predicting the higher-order statistics of such flows.

The main text begins by presenting the Navier–Stokes equations of flow and an upwind-biased finite-difference scheme for solving them. The scheme uses a staggered grid and is a variant of a partially implicit, fractional-step scheme used in a previous study. The accuracy of the integration method is first tested by computing the evolution of small-amplitude disturbances in channel flow. The scheme is then used to compute fully developed channel flow at a Reynolds number of 180 (based on wall shear velocity and the half width of the channel). The results of these calculations are compared with experimental data and with spectral calculations of the same flow in a previous study, and the agreement is found to be good. The dissipative nature of the upwind-biased scheme is found to control aliasing error without unduly affecting the accuracy of the solution for grids of reasonable size.

The results of simulations using a second-order-accurate central-difference numerical-integration scheme are also presented. The inadequacy of the second-order accuracy of the scheme (for the grid size chosen) is demonstrated using the test cases mentioned above. An additional limitation of this scheme is that its stability is ensured only because it conserves kinetic energy. Deviations in the differencing technique that retained second-order accuracy but not the energy-conservation principle resulted in unstable solutions.

The report ends by stating several conclusions, including the following: While the shortcoming of the upwind method (numerical dissipation) can be overcome by use of additional grid points, the limitations of the spectral method are more fundamental in nature. The use of central-difference schemes depends on whether general-purpose aliasing-error-control procedures can be found. The upwind-difference code requires approximately the same amount of computing time per grid point for each substep in the Runge–Kutta numerical-integration scheme as spectral simulations do. At present, it appears that the high-order-accurate upwind-biased method is a good candidate for direct simulations of turbulent flows associated with complicated shapes.

This work was done by Man Mohan Rai of **Ames Research Center** *and Parviz Moin of Stanford University. Further information may be found in AIAA paper 89A-25312, "Direct Simulations of Turbulent Flow Using Finite-Difference Schemes."*

Copies may be purchased [prepayment required] from AIAA Technical Information Service Library, 555 West 57th Street, New York, New York 10019, Telephone No. (212) 247-6500. ARC-12463/TN

FOR ADDITIONAL INFORMATION: *Contact: Director, Technology Transfer Division, P.O. Box 8757, BWI Airport, MD 21240; (301) 621-0100 Ext. 241*
REFER TO THE NUMBER LISTED AT THE END OF THIS ARTICLE

NASA Tech Brief
National Aeronautics and Space Administration

Frequency-Domain Identification of Aeroelastic Modes

Data from flight tests support the choice of the frequency-sweep method.

A report describes flight measurements and frequency-domain analyses of aeroelastic vibrational modes of the wings of the XV-15 tilt-rotor aircraft. The main text of the report begins with a description of flight-test methods. This is followed by a brief discussion of the methods of analysis, which include Fourier-transform computations using chirp *z* transforms, the use of coherence and other spectral functions, and methods and computer programs to obtain frequencies and damping coefficients from measurements. This is followed by a brief description of the results of flight tests and comparisons among various experimental and theoretical results. The report ends with a section on conclusions and recommended improvements in techniques.

The measurements were taken during flight tests in which dual flaperon exciters with automatic frequency-sweep controls were used to excite individual modes precisely. During the tests, the aircraft was equipped with the original metal rotor blades (as distinguished from new composite-material blades, with which subsequent tests are to be performed).

After the wing modes were excited with flaperon frequency sweeps, the frequency spectra of the resulting time-history data were generated with the chirp *z* transforms. Modal frequencies and damping were determined by fitting curves to frequency-response magnitude and phase data. In addition, theoretical analyses were performed with the help of the CAMRAD and ASAP computer progams to predict the modes by use of mathematical models of the aircraft. Estimates of frequency and damping were plotted and compared with values predicted by both CAMRAD and ASAP.

From the results of the measurements and analyses, the authors conclude that the combination of frequency-sweep excitation with frequency-domain analysis provides a reliable and efficient method for the determination of the aeroelastic modes of the XV-15 aircraft from flight data. Because of its good analytical results and its reduced flight time in comparison with other methods, the frequency-sweep method has been chosen to support flight tests of the aircraft equipped with the new composite blades.

This work was done by C. W. Acree, Jr., and Mark B. Tischler of **Ames Research Center**. *Further information may be found in NASA TM-101021 [N90-21756], "Identification of XV-15 Aeroelastic Modes Using Frequency-Domain Methods."*

Copies may be purchased [prepayment required] from the National Technical Information Service, Springfield, Virginia 22161, Telephone No. (703) 487-4650. Rush orders may be placed for an extra fee by calling (800) 336-4700. ARC-12407/TN

FOR ADDITIONAL INFORMATION: *Contact: Director, Technology Transfer Division, P.O. Box 8757, BWI Airport, MD 21240; (301) 621-0100 Ext. 241*

REFER TO THE NUMBER LISTED AT THE END OF THIS ARTICLE

NASA Tech Brief
National Aeronautics and Space Administration
Langley Research Center, Hampton, Virginia

Dynamic Analyses Including Joints of Truss Structures

A straightforward method is used to determine stiffness and damping coefficients.

Space structures larger than 300 ft (91 m) in diameter, such as the hoop-column antenna and proposed Space-Station structures (see figure), are being designed. These include truss substructures to span large distances because trusses provide high stiffness with low mass. The designs of many of these structures require accurate, dynamic analyses for prediction of loads, stability, shape control, and accuracy of orientation.

The designs of truss structures proposed for use in outer space specify joints that enable the erection or deployment of the truss members. Unlike in civil engineering structures, the designs of joints for space structures include finite tolerances between mating surfaces to enable the joints to rotate or to be latched. A tolerance results in a dead band within which a joint can be made to move with nearly zero applied force. The dead bands of joints are believed to affect the vibrational response of truss structures significantly, and detailed mathematical modeling may be necessary to incorporate these effects in the overall, or global, analysis. The joints influence the dynamic response of a truss in two major ways: first, by reducing the effective stiffness of the truss; and second, by introducing additional damping beyond that of a structure in which the members are rigidly connected but that is otherwise identical. Therefore, a method for mathematically modeling joints to assess the influences of joints on the dynamic response of truss structures was developed in a study. Only structures with low-frequency oscillations were considered in this study; thus, only Coulomb friction and viscous damping were included in the analysis.

The focus of this effort was to obtain finite-element mathematical models of joints that exhibited load-vs.-deflection behavior similar to the measured load-vs.-deflection behavior of real joints. Experiments were performed to determine stiffness and damping nonlinearities typical of joint hardware. An algorithm for computing coefficients of analytical joint models based on test data was developed to enable the study of linear and nonlinear effects of joints on global structural response.

Spring, viscous-damper, and friction-damper elements were formulated and included in an existing finite-element computer code. Beams with joints were loaded, and their transient vibrational response was simulated with the finite-element program. The effects of linear and nonlinear joint stiffnesses on the amplitudes and frequencies of vibrations of beams were then studied. A truss structure with 32 joints was analyzed to study the effect of joints on its global vibrational response. Equations for predicting the sensitivities of deformations of beams to changes in stiffness of joints were derived. In addition, random perturbations were used to evaluate the effects of changes in stiffness of joints on the frequency of a bending vibrational mode of a truss.

The results of these analyses indicate that nonlinearities in the stiffnesses of the joints produced nonlinear dynamic response in beam and truss structures at certain values of these stiffnesses. For vibrations of constant amplitude, nonlinearities in the stiffnesses of the joints produced sinusoidal vibrational responses in beams and trusses, and the frequencies of vibration could be simulated with linearized stiffness of the joints. The random perturbations of these stiffnesses produced small changes in the global frequency, indicating that the average value of stiffness may be adequate to predict the global vibrational behavior of a structure. Sensitivity analyses of beams with joints were used to develop equations that show that there exist values of stiffnesses of joints above which the flexibilities of the affected joints can be neglected in analyses of the vibrations of truss structures that contain them. The relative stiffnesses of the joints compared with those of truss members are major parameters that determine the need for mathematical modeling of the joints.

The results of this study would be of value to designers of truss structures and framed structures in which the properties of joints have large effects, especially for cases in which deflection and vibration characteristics are major considerations in design. Besides the intended application to large space structures, applications in the nonaerospace community could include ground-based antennas and earthquake-resistant steel-framed buildings.

This work was done by W. Keith Belvin of **Langley Research Center**. *Further information may be found in NASA TP-2661 [N87-20567], "Modeling of Joints for the Dynamic Analysis of Truss Structures."*

Copies may be purchased [prepayment required] from the National Technical Information Service, Springfield, Virginia 22161, Telephone No. (703) 487-4650. Rush orders may be placed for an extra fee by calling (800) 336-4700. LAR-14306/TN

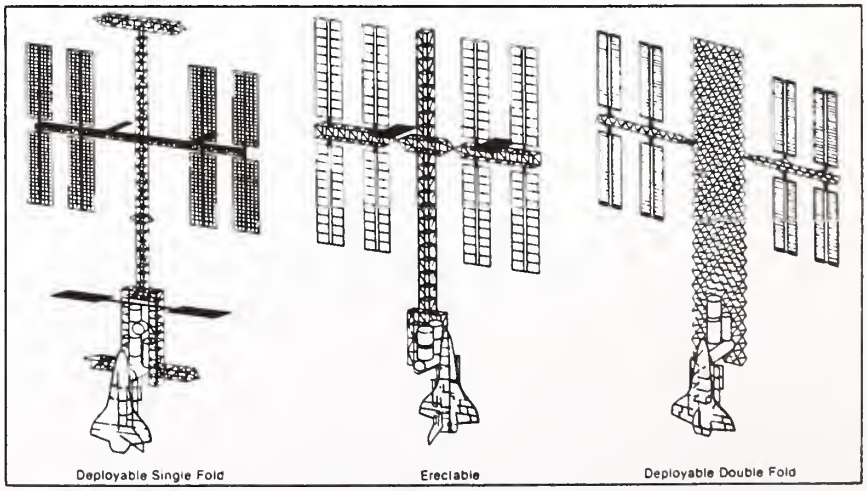

Proposed Space-Station Configurations make extensive use of large truss structures.

FOR ADDITIONAL INFORMATION: *Contact: Director, Technology Transfer Division, P.O. Box 8757, BWI Airport, MD 21240; (301) 621-0100 Ext. 241*
REFER TO THE NUMBER LISTED AT THE END OF THIS ARTICLE

NASA Tech Brief
National Aeronautics and Space Administration

Evaluation of Performance of a Telerobot

Various tasks were performed with and without force feedback.

A paper presents an evaluation of the performance of a six-axis telerobot system with shared control and advanced modes of force feedback. The evaluation is based on manipulation experiments in which the system was operated in two modes: with position control only and with position control and force feedback. To establish an additional basis for comparison, tests were also conducted in a third mode in which technicians performed the same manipulations with their hands. The experiments consisted of the following four tasks:

- Exchange the positions of two differently shaped blocks attached to a task board with Velcro hook-and-pile material. The objective is to attach the blocks securely while minimizing unnecessary force.
- Insert pegs in designated holes in a square matrix of nine holes. The holes in each succeeding row present a larger clearance, while those in each succeeding column present a different chamfer.
- Mate and unmate 3 standard electrical connectors — a 3-prong chassis power-cord connector, a 25-pin signal connector, and a 1/4-in. (6.35-mm) telephone plug.
- Unlock, unmate, mate, and lock a bayonet-style electrical connector.

The performance of the system in each of the tasks was evaluated on the basis of the forces, torques, and time required. The performance clearly improved as the level of sensitivity progressed from position control to position control with force reflection to barehanded operation: the average time to complete the first three tasks was 92 s with position control only, 63 s with position control and force feedback, and only 14 s for the bare-handed technicians. The average number of errors in the completion of the first three tasks was about three with position control only, about one with position control and force feedback, and zero for the barehanded operators. The sum of squared forces, a measure of the force or torque required for a task, fell even more dramatically in the progression through the three modes. (The fourth task was not included in the calculations because it took much longer than the other tasks did and often could not be completed because of its difficulty.)

Overall, the study found that force feedback reduced the average time required to complete a task by about 30 percent. It reduced sum of squared forces by a factor of 7 and errors by 63 percent.

This work was done by Blake Hannaford and Laurie A. Wood of Caltech for **NASA's Jet Propulsion Laboratory.** *"Performance Evaluation of a 6 Axis High Fidelity Generalized Force Reflecting Teleoperator."* *NPO-17924/TN*

FOR ADDITIONAL INFORMATION: *Contact: Director, Technology Transfer Division, P.O. Box 8757, BWI Airport, MD 21240; (301) 621-0100 Ext. 241*
REFER TO THE NUMBER LISTED AT THE END OF THIS ARTICLE

NASA Tech Brief
National Aeronautics and Space Administration
Ames Research Center, Moffett Field, California

A General-Coordinate Formulation for Boundary-Layer Flow

The general coordinates need not be orthogonal.

A formulation for the solution of the equations of boundary-layer flow in general body-fitted curvilinear coordinates retains the velocities in Cartesian coordinates. This formulation may increase the stability of numerical simulations by avoiding coordinate source terms. Moreover, in this formulation, the curvilinear coordinates do not have to be orthogonal, and much of the software (including that for grids and boundary conditions) developed previously for use in numerical simulations of flow based on the Navier–Stokes equations can be used.

The equations in the new formulation express the conservation of momentum along and perpendicular to the surface, the conservation of energy, and the conservation of mass, and include an equation of state for a perfect gas that has a constant ratio of specific heats. For example, the equation for the conservation of momentum perpendicular to the surface is $p_\eta = 0$, while the equations for the conservation of momentum along the surface are

$$\rho u_t + \rho U u_\xi + \rho V u_\eta + \rho W u_\zeta + (\xi_x p_\xi + \eta_x p_\eta + \zeta_x p_\zeta) = J\partial_\eta \{J^{-1}[\mu m_1 u_\eta + (\mu/3) m_2 \eta_x]\}$$

$$\rho v_t + \rho U v_\xi + \rho V v_\eta + \rho W v_\zeta + (\xi_y p_\xi + \eta_y p_\eta + \zeta_y p_\zeta) = J\partial_\eta \{J^{-1}[\mu m_1 v_\eta + (\mu/3) m_2 \eta_y]\}$$

$$\rho w_t + \rho U w_\xi + \rho V w_\eta + \rho W w_\zeta + (\xi_z p_\xi + \eta_z p_\eta + \zeta_z p_\zeta) = J\partial_\eta \{J^{-1}[\mu m_1 w_\eta + (\mu/3) m_2 \eta_z]\}$$

In these equations, the curvilinear coordinates are ξ, η and ζ; ρ denotes density; u, v, and w denote the Cartesian components of velocity along the x, y, and z axes, respectively; p denotes pressure, μ denotes viscosity; subscripts denote partial derivations with respect to the coordinates they represent;

$$m_1 = \eta_x^2 + \eta_y^2 + \eta_z^2;\ m_2 = \eta_x u_\eta + \eta_y v_\eta + \eta_z w_\eta$$

J is the transformation Jacobian and U, V, and W are contravariant velocities given by

$$\begin{pmatrix} U \\ V \\ W \end{pmatrix} = \begin{pmatrix} \xi_x & \xi_y & \xi_z \\ \eta_x & \eta_y & \eta_z \\ \zeta_x & \zeta_y & \zeta_z \end{pmatrix} \begin{pmatrix} u \\ v \\ w \end{pmatrix}$$

These six equations can be used to determine p, u, w, the specific total enthalpy H, ρ, and v. Generally, p is uncoupled and determined from $p_\eta = 0$ and an outer-edge boundary condition so that $p = p_{edge}$ along η coordinates. In more general cases, pressure is weakly coupled and can be determined from

$$s_\eta + \nabla\eta \cdot (\nabla\xi p_\xi + \nabla\eta p_\eta + \nabla\zeta p_\zeta) = 0$$

using the same outer-edge condition with the source term defined as

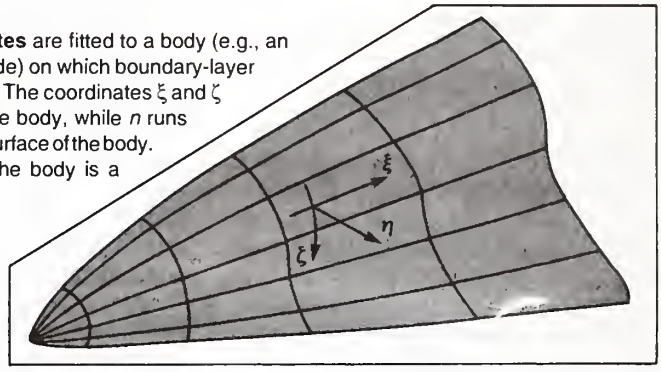

Curvilinear Coordinates are fitted to a body (e.g., an aircraft or a turbine blade) on which boundary-layer flow is to be computed. The coordinates ξ and ζ lie on the surface of the body, while n runs perpendicularly to the surface of the body. Thus, the surface of the body is a surfact of constant n.

$$\begin{aligned} s_\eta &= -\rho U (u\partial_\xi \bar{\eta}_x + v\partial_\xi \bar{\eta}_y + w\partial_\xi \bar{\eta}_z) \\ &= -\rho V (u\partial_\eta \bar{\eta}_x + v\partial_\eta \bar{\eta}_y + w\partial_\eta \bar{\eta}_z) \\ &= -\rho W (u\partial_\zeta \bar{\eta}_x + v\partial_\zeta \bar{\eta}_y + w\partial_\zeta \bar{\eta}_z) \end{aligned}$$

where the overbar denotes scaling of metrics, e.g.,

$$\bar{\xi}_x = \xi_x / \sqrt{\xi_x^2 + \xi_y^2 + \xi_z^2}$$

In this case, pressure varies throughout the boundary layer.

This work was done by Joseph L. Steger, William R. Van Dalsem, Argyris G. Panaras, and K. V. Rao of **Ames Research Center.** *Further information may be found in NASA TM-100079 [N88-24600], "A Formulation for the Boundary-Layer Equations in General Coordinates."*

Copies may be purchased [prepayment required] from the National Technical Information Service, Springfield, Virginia 22161, Telephone No. (703) 487-4650. Rush orders may be placed for an extra fee by calling (800) 336-4700.

ARC-12465/TN

FOR ADDITIONAL INFORMATION: *Contact: Director, Technology Transfer Division, P.O. Box 8757, BWI Airport, MD 21240; (301) 621-0100 Ext. 241*

REFER TO THE NUMBER LISTED AT THE END OF THIS ARTICLE

NASA Tech Brief
National Aeronautics and Space Administration
Ames Research Center, Moffett Field, California

Generation of Surface Grids From Data Points

Grids are constructed by interpolation and blending of patches.

A computational procedure generates grids on complicated three-dimensional surfaces (e.g., those of airplanes) from sets of data points (e.g., those generated by computer-aided design systems) that lie on and specify those surfaces. Such grids are needed to compute flows over the surfaces. Starting with grouping of possibly sparse surface points into lines and/or patches, the procedure involves interpolation within and blending of lines and/or patches and possibly the redistribution and reassembly of patches to obtain a finished system of zonal patch grids that match at the boundaries between them. The procedure can be semiautomated via a computer program that performs all steps except the selection of patches and interpolation points, which are left to the discretion of the user.

The original data on the surface points cannot usually be used in raw form and must be preprocessed. For example, a fuselage might be represented by sets of points that vary widely among different cross sections, wing/fuselage intersections may be undefined, and there may not be enough points to represent the surface accurately in areas of large curvature. In addition, it is necessary to group the data into the network of patches, which is to serve later as the basis for a global block structure. To perform the necessary preprocessing, the procedure includes an algorithm, called the "geometry data processor," which acts like a data editor in that it provides for the insertion, deletion, and redistribution of surface data points. It can also smooth a sectional curve by interpolating and segmenting it into any number of pieces. These functions are all performed in conjunction with interpolation between data points on curves via piecewise parametric cubic polynomials.

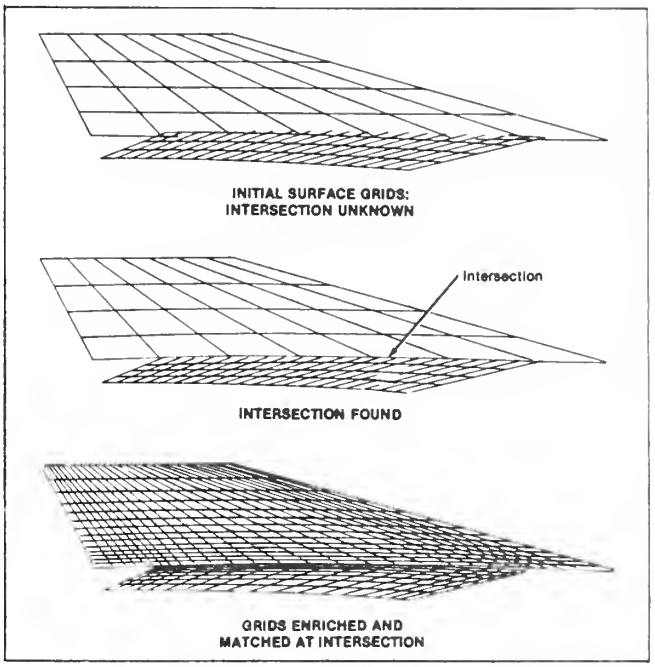

The **Curve of Intersection** of a vertical surface grid of 8 by 5 points with a horizontal surface grid of 21 by 5 points is initially unknown. An iterative procedure finds the curve of intersection. Additional grid points and lines are then interpolated and matched at the intersection.

Once the initial geometric data have been preprocessed, an algorithm called the "surface grid generator" interpolates each patch to a grid of m by n points with distribution functions on its boundaries (m, n, and the distribution functions are specified by the user). Here, the interpolation technique of the geometry data preprocessor is extended to bicubic parametric interpolation. The surface grid generator also finds the intersection of two surfaces via a parametric equation, based on the interpolation scheme, for the intersection of one surface with a curve in the other surface (see figure). The equation is solved by the Newton–Raphson method; convergence is usually obtained within three to four iterations.

This work was done by Raymond Ching-Chung Luh of **Ames Research Center.** *Further information may be found in NASA TM-101046 [N89-13747], "Surface Grid Generation for Complex Three-Dimensional Geometries."*

Copies may be purchased [prepayment required] from the National Technical Information Service, Springfield, Virginia 22161, Telephone No. (703) 487-4650. Rush orders may be placed for an extra fee by calling (800) 336-4700.

ARC-12481/TN

FOR ADDITIONAL INFORMATION: *Contact: Director, Technology Transfer Division, P.O. Box 8757, BWI Airport, MD 21240; (301) 621-0100 Ext. 241*

REFER TO THE NUMBER LISTED AT THE END OF THIS ARTICLE

NASA Tech Brief
National Aeronautics and
Space Administration

Investigation of Tapered Tension/Torsion Strap

A tapered strap provides more torque than a parallel one does.

A report describes the theoretical and experimental investigation of a simplified model of a tension/torsion strap. A tension/torsion strap has been proposed for use in a helicopter rotor blade to hold an otherwise freely pitching blade tip inward against centrifugal force and to apply torque about the pitch axis to regulate the pitching motions of the tip. This kind of design is intended to improve the aerodynamic performances of rotors and to reduce vibrations.

According to a previous concept, a tension/torsion strap would be made by arranging thin wires side by side in parallel and embedding them in an elastomeric filler. The torsional moment would be derived mainly from a component of the tensile load in the wires. Ignoring the aerodynamic effects, the strap and pitching blade tip would function analogously to a torsion pendulum except that the tensile load on the strap would be caused by the centrifugal force of the tip instead of by the weight of the pendulum.

The tapered tension/torsion strap was proposed to increase the torque generated by this type of strap (by increasing the torsional stiffness). According to this concept, the wires would be fanned out so that the strap would be wider at the inboard (anchored) end than at the outboard (pitching-tip) end. In this investigation, a two-wire torsional pendulum was used as the simplified model of a strap. When the suspension wires of such a pendulum are parallel in the steady state, it becomes a bifilar pendulum representing a constant-width tension/torsion strap. When the suspension wires are spread further apart at the upper (anchor) ends to form a V-shape, it represents the tapered tension/torsion strap.

The characteristics of the torsion-pendulum model were investigated by use of a simple mathematical model (small-angle approximation, no torsional stiffness in the wires, no stretching of the wires) and by measurements of the damping and of the torsional stiffness and natural frequency as a function of the separation between the wires at the upper ends. The results showed that, as expected, the torsional stiffness increases with the separation. The reason for this is that as the taper increases, so does the component of tension in the plane of rotation.

This work was done by Alexander Louie of **Ames Research Center**. *Further information may be found in NASA TM-101049 [N89-13746], "An Experimental and Analytical Evaluation of the Tapered Tension-Torsion Strap Concept."*

Copies may be purchased [prepayment required] from the National Technical Information Service, Springfield, Virginia 22161, Telephone No. (703) 487-4650. Rush orders may be placed for an extra fee by calling (800) 336-4700.
ARC-12480/TN

FOR ADDITIONAL INFORMATION: *Contact: Director, Technology Transfer Division, P.O. Box 8757, BWI Airport, MD 21240; (301) 621-0100 Ext. 241*
REFER TO THE NUMBER LISTED AT THE END OF THIS ARTICLE

NASA Tech Brief
National Aeronautics and Space Administration
Marshall Space Flight Center, Alabama

Licensing Opportunity

Lightweight Valve Closes Duct Quickly

A balloon expands to block the duct.

An expanding balloon serves as a lightweight emergency valve to close a wide duct. The balloon valve weighs much less than does a conventional butterfly, hot-gas, or poppet valve capable of closing a duct of equal diameter.

The balloon is initially folded like an accordion in a housing on the side of the duct (see figure). When it is necessary to close the duct, a control system injects a suitable gas into the balloon. The balloon expands, bursting through a protective diaphragm in the wall of the duct. The balloon fully inflates in less than a second, pressing against the inner surface of the duct and thereby sealing it.

After use, the housing is removed temporarily. The balloon is checked under pressure to ensure that it has not been punctured, then packed in the housing for reuse. The burst diaphragm is replaced, and the housing is reinstalled on the duct.

The housing can be made of the same material as that of the duct or of a lightweight composite; e.g., glass-, graphite-, or boron-reinforced epoxy. The balloon can be made of a material such as aluminized Mylar (or equivalent) polyethylene terephthalate.

This work was done by Walter L. Fournier and N. Frank Burgy of United Technologies Corp. for **Marshall Space Flight Center.**

Inquiries concerning rights for the commercial use of this invention should be addressed to the Patent Counsel, Marshall Space Flight Center. Refer to MFS-28511/TN.

George C. Marshall Space Flight Center
Technology Utilization Officer Ismail Akbay
Code AT01
Marshall Space Flight Center,
AL 35812
(205) 544-2223
Patent Counsel
Leon D. Wofford, Jr.
Mail Code CC01
Marshall Space Flight Center,
AL 35812
(205) 544-0024

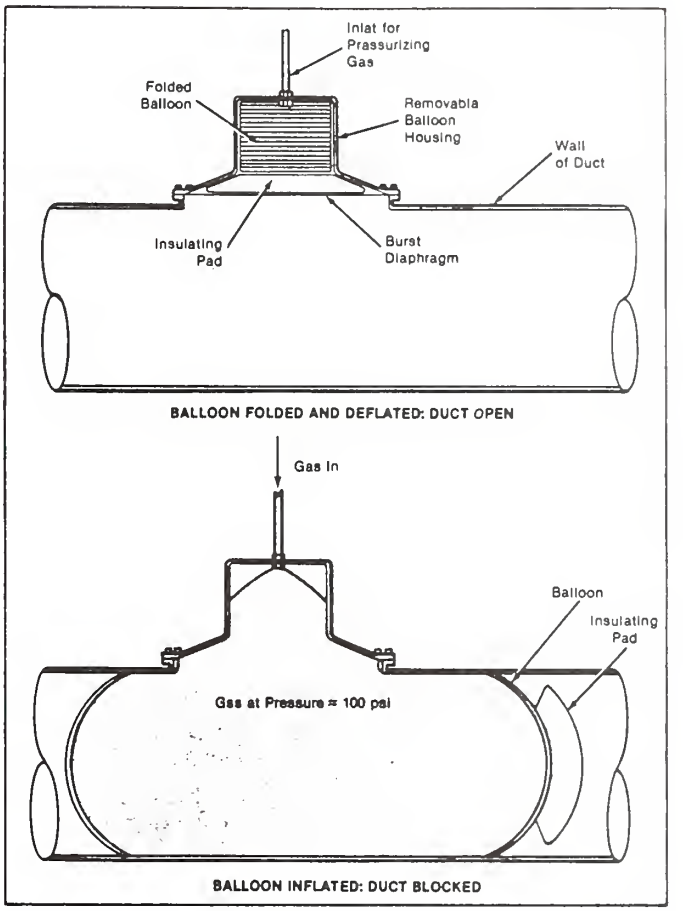

The **Uninflated Balloon is Stored** in a housing on the duct. A pad resting on the burst diaphragm protects the balloon from the hot gases in the duct. Once the control system triggers a valve, the balloon inflates rapidly to block the duct.

FOR ADDITIONAL INFORMATION: *Contact: Director, Technology Transfer Division, P.O. Box 8757, BWI Airport, MD 21240; (301) 621-0100 Ext. 241*
REFER TO THE NUMBER LISTED AT THE END OF THIS ARTICLE

NASA Tech Brief
National Aeronautics and Space Administration
Marshall Space Flight Center, Alabama

Licensing Opportunity

Lock for Valve Stem

Readily available materials and handtools are used to make a simple but effective device.

A simple, cheap device locks a valve stem so that its setting cannot be changed by unauthorized people. The device covers the valve stem; the cover is locked in place with a standard padlock. Only someone with a key to the padlock can then gain access to the valve and open, close, or otherwise change it.

The device is intended for use on a double-union polyvinyl chloride (PVC) ball valve. It is made from a piece of 1-in. (2.5-cm)-diameter schedule-40 PVC pipe and a strip of 1/2-in. (1.3-cm)-wide band (of a type ordinarily used for shipping). The device is fabricated by use of standard handtools.

The pipe is cut to lengths and opposing slits are sawed in its wall (see figure). The shipping band, cut to length and with holes punched or drilled in its ends, is inserted through the slits. A metal rod is inserted in the pipe to form the band so that it can fit over the valve stem. The valve handle is removed from the valve stem, and the pipe-and-band assembly is slipped over the stem. The band is wrapped around the valve body so that its ends meet, and a padlock is slipped through the holes and locked. The valve is now secure.

This work was done by Richard K. Burley and Kamal S. Guirguis of Rockwell International Corp. for **Marshall Space Flight Center.**

Inquiries concerning rights for the commercial use of this invention should be addressed to the Patent Counsel, Marshall Space Flight Center. Refer to MFS-29764/TN.

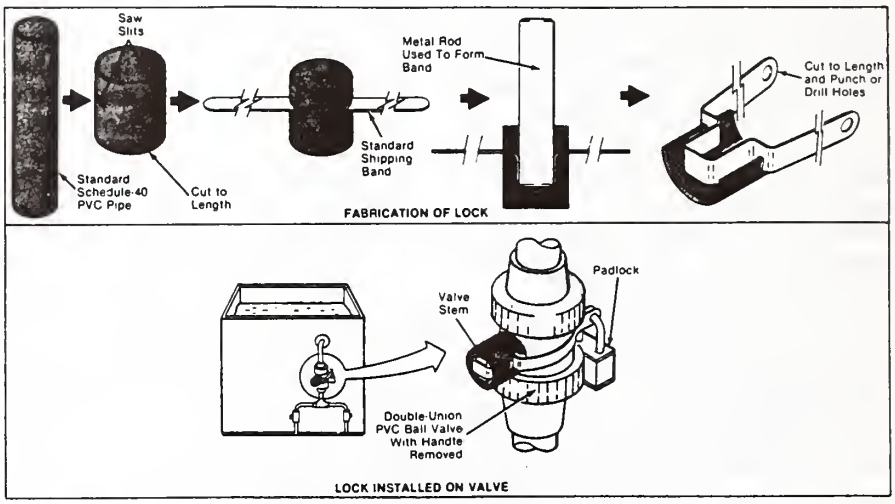

The **Valve Lock** is made of PVC pipe and a packing band. Shears, a drill or punch, and a forming rod are the only tools needed.

George C. Marshall Space Flight Center
Technology Utilization Officer Ismail Akbay
Code AT01
Marshall Space Flight Center,
AL 35812
(205) 544-2223
Patent Counsel
Leon D. Wofford, Jr.
Mail Code CC01
Marshall Space Flight Center,
AL 35812
(205) 544-0024

FOR ADDITIONAL INFORMATION: *Contact: Director, Technology Transfer Division, P.O. Box 8757, BWI Airport, MD 21240; (301) 621-0100 Ext. 241*
REFER TO THE NUMBER LISTED AT THE END OF THIS ARTICLE

NASA Tech Brief
National Aeronautics and Space Administration

Navier-Stokes Computations on Zonal Grids

Flows about a wing and an airplane are simulated.

A report describes numerical simulations of the transonic flow of air about an isolated wing and about the wing and fuselage (but not the tail assembly) of the F-16A aircraft. A fast, diagonalized Beam–Warming numerical-integration algorithm for the solution of the Euler and Navier–Stokes equations was applied via the Transonic Navier–Stokes computer program, using computational grids divided into zones of coarse and finer meshes.

As in previous studies, the thin-layer Navier–Stokes equations with no-slip surface conditions were applied on solid surfaces, while the Euler equations (of inviscid flow), which are simpler, are used elsewhere. The regions where viscosity is important also tend to involve high gradients of flow variables. To reduce the amount of computation required, the meshes were refined only to the degrees necessary in the near-surface, high-gradient regions.

The base grid was generated by an algorithm based on Poisson's equation and was divided into zones by a zoning algorithm. The grid about the wing consisted of four zones. The first included all points except those in the vicinity of the wing, which were contained in the second through fourth zones. The second zone, with a mesh finer than that of the first zone, contained all points in the vicinity of the wing except those in still finer meshes in the third and fourth zones, which were attached to the upper and lower surfaces respectively.

The grid about the airplane was divided into a total of 19 zones. These zones were essentially of three types; inviscid zones, viscous zones with clustering of the grids on faces that correspond to wing or fuselage no-slip surfaces, and viscous zones with clustering on pairs of adjacent faces that correspond to the wing/fuselage juncture.

The simulation for the wing was conducted both with and without inclusion of the effects of wind-tunnel walls, and the results of the two cases were compared with those of an experiment. The simulation with wall effects agreed well with the experiment, and the results show that when the effects of the wall are not considered, the predicted position of the shock is too far upstream.

The results of simulation for the aircraft are presented in plots of pressure coefficients as functions of position along various coordinate axes. For the most part, these plots show good agreement with experimental data.

This work was done by Jolen Flores of **Ames Research Center**. *Further information may be found in NASA TM-100080 [N88-24602], "Applications of the Navier–Stokes Equations to Wings and Complex Configurations Using a Zonal Approach."*

Copies may be purchased [prepayment required] from the National Technical Information Service, Springfield, Virginia 22161, Telephone No. (703)487-4650. Rush orders may be placed for an extra fee by calling (800) 336-4700. ARC-12447/TN

FOR ADDITIONAL INFORMATION: *Contact: Director, Technology Transfer Division, P.O. Box 8757, BWI Airport, MD 21240; (301) 621-0100 Ext. 241*
REFER TO THE NUMBER LISTED AT THE END OF THIS ARTICLE

NASA Tech Brief
National Aeronautics and
Space Administration

Processing Particle-Streak Imagery on a Personal Computer

Streak patterns are used to obtain maps of flow-velocity vectors.

A report describes a simple flow experiment in which the streak images of particles suspended in the fluid and illuminated for short times were processed into maps of velocity vectors. The particle-streak concept is simple and dates back to the early part of this century but has not been considered viable until recently because the manipulation of the images to extract the velocity data has required excessive time and effort.

Advances in the digital processing of images have revived interest in the particle-streak method. In some applications, excessive emphasis has been placed on the automatic reduction of data, and a large portion of the significant image data is typically discarded to avoid the inclusion of erroneous data. To accumulate a sufficient number of data points to map a velocity field, repeated detection of a specific state in the image is required. Such repetition is, in practice, feasible only for steady flow. In the experiment described in this report, the authors used a semiautomatic data-reduction scheme, which can recover significant image data much more efficiently than a currently available automatic scheme can.

The experiment was performed in a towing tank filled with water seeded with neutrally buoyant particles. A circular cylinder 0.5 in. (12.7 mm) in diameter was moved along the tank at 0.31 in./s (0.79 cm/s) with its axis perpendicular to the motion. The flow around the cylinder was illuminated with a sheet of laser light and was photographed in 0.5-s exposures to obtain the streak images of the particles.

The photographs were acquired by a video camera, digitized, and stored in the memory and on the hard disk of a personal computer connected with the computer network at Ames Research Center. The image was then enhanced by manipulation of contrast, noise cleaning, filtering, statistical differencing, thresholding, and other techniques. The enhanced images of the streaks were examined by the experimenters; those judged to represent valid data were traced semiautomatically with a "mouse" to generate their binary images for use in calculating the velocity vectors. Coordinate transformations were applied to correct for distortions in the image, and velocity vectors at locations other than those of streaks were interpolated via a simple convolution with an adaptive Gaussian window.

The velocity-vector map was found to agree fairly well with the results of a Navier-Stokes calculation of the flow. Even in regions where the magnitude of the streak-image velocity did not agree with that of the Navier-Stokes velocity, the directions of the velocities agreed well. The discrepancy is attributed partly to errors in the processing of the images and partly to that there were not enough streaks in regions of large gradients in the velocity.

This work was done by Y.C. Cho and B.G. McLachlan of **Ames Research Center**. *"Personal computer (PC) based image processing applied to fluid mechanics research."*
ARC-12267/TN

FOR ADDITIONAL INFORMATION: *Contact: Director, Technology Transfer Division, P.O. Box 8757, BWI Airport, MD 21240; (301) 621-0100 Ext. 241*
REFER TO THE NUMBER LISTED AT THE END OF THIS ARTICLE

NASA Tech Brief
National Aeronautics and Space Administration
Langley Research Center, Hampton, Virginia

Licensing Opportunity

Reducing Water/Hull Drag by Injecting Air Into Grooves

A proposed method would require much less air than does the microbubble-injection method.

The concept of reducing the drag on a water vehicle by placing air in the boundary layer between the vehicle and the water is not new but has been unworkable because of the difficulty of stabilizing a layer of air on the surface of the hull. Attempted solutions to the air-stability problem required changes in the basic configuration of the hull to trap air — an approach not practical for most oceangoing vessels.

Previous work has shown that air in the boundary layer of a waterflow can, indeed, greatly reduce the skin friction. One technique consisted of the injection of microbubbles through a porous plate into a boundary layer. Although this technique has reduced friction by as much as 80 percent, the required flow of air is so large that it negates the drag-reduction benefits in practical situations. The disadvantage of microbubbles is that they are easily dispersed and fill the entire boundary layer. In theory, only the portion of air nearest the wall acts as a drag-reduction agent. Therefore, most of the air injected in the microbubble technique is wasted.

A proposed technique for the reduction of friction drag on a hydrodynamic body involves the use of grooves and combinations of surfactants to control the motion of a layer on the surface of such a body. The surface would contain many rows of side-by-side, evenly spaced, longitudinal grooves. These grooves would be generally triangular, with tip-to-tip spacing between 0.040 in. (1.0 mm) and 0.010 in. (0.25 mm) and depth from 0.10 in. (2.5 mm) to 0.010 in. (0.25 mm). The dimensions of grooves and sharpnesses of tips in a specific case would depend on the conditions of flow about the vessel.

Air-injection ports would be either drilled holes in the valleys of the grooves or thin slots, each reaching across several valleys to distribute air more evenly. Air injectors would be angled as tangentially to the surface as possible. Injection of air would be repeated downstream several unit lengths, depending on the particular type of vessel.

The ribbed surface would be roughened deliberately during fabrication or coated before use with an antiwetting surfactant to enhance its air-trapping ability. Polytetrafluoroethylene is the most-desirable coating material, although such other antiwetting agents as those based on hydrocarbons would also be effective.

In operation, the air would be injected continuously through the ports. The ribs would act to hold the injected air in a connecting sheet that would fill the grooves via transverse surface tension forces. The depth and spacing of the ribs would alter the interfacial tension at the surface, favorably controlling the gas phase, or air sheet, by holding a thin sheet of air at the wall, where it is most likely to be effective in reducing drag. At slow speeds of vessels through water, this technique would likely require approximately one-tenth or less of the amount of air required in the injection of microbubbles.

This work was done by Jason C. Reed of Old Dominion University and Dennis M. Bushnell and Leonard M. Weinstein of **Langley Research Center.**

This invention is owned by NASA, and a patent application has been filed. Inquiries concerning nonexclusive or exclusive license for its commercial development should be addressed to the Patent Counsel, Langley Research Center. Refer to LAR-14078/TN.

Langley Research Ctr.
Technology Utilization
Officer John Samos
Mail Stop 139A
Hampton, VA 23665
Patent Counsel
George F. Helfrich
Mail Code 279
Hampton, VA 23665
(804) 864-3523

FOR ADDITIONAL INFORMATION: *Contact: Director, Technology Transfer Division, P.O. Box 8757, BWI Airport, MD 21240; (301) 621-0100 Ext. 241*
REFER TO THE NUMBER LISTED AT THE END OF THIS ARTICLE

NASA Tech Brief
National Aeronautics and Space Administration
NASA's Jet Propulsion Laboratory, Pasadena, California

Two Techniques for Suppressing Vibrations in Structures

The techniques are based on bridge feedback and a criterion for placement of actuators.

Two techniques intended to be used together to suppress vibrations in a large, complicated truss structure involve a combination of active and passive damping. Research continues to develop a system that would use these and other techniques to suppress vibrations in, and help control the shape of, a truss structure in outer space that would support the precise, segmented reflector of a communication antenna. On Earth, the developmental techniques should be applicable to the suppression of vibrations in bridges and tall buildings.

In addition to or in place of ordinary structural members, the truss or other structure includes active and passive damping members. Each active member includes a piezoelectric or other actuator collocated with a force sensor and a vibrational-velocity sensor (see figure). The first of the two new techniques calls for the use of the active damping members (which, by itself, is not new) in a bridge-feedback control scheme (which is new in this application). This scheme involves the concept of mechanical impedance of a member, defined as the Laplace transform of the ratio between the axial force applied to the member and the difference between the velocities of its ends. The mechanical impedance of an active member is analogous to the electrical output impedance of an amplifier.

In this scheme, local feedback is used to control the mechanical impedance, Z_m, of each active member in such a way as to effectively make it less stiff (and possibly more or less damping). The member could dissipate incident vibrational energy maximally if its mechanical impedance were the complex conjugate of

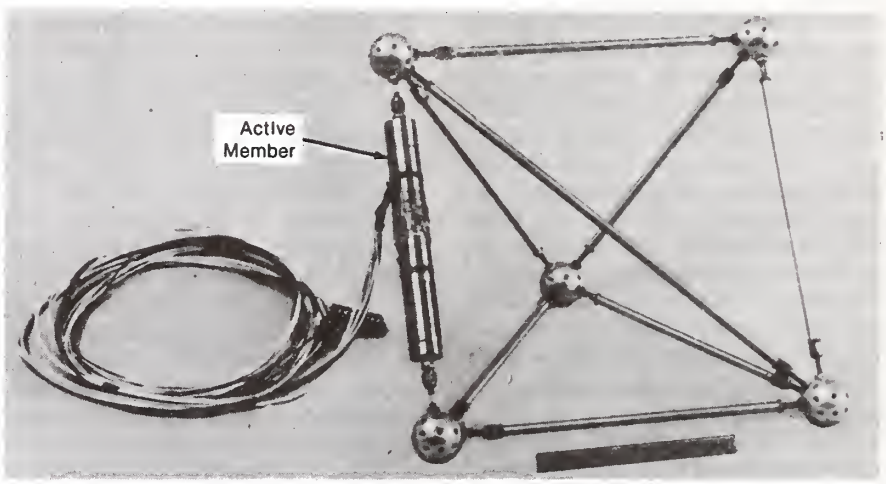

Part of a Truss Structure contains an active damping member, which is a stainless-steel tube 8 in. (20.3 cm) long and 1 in. (2.5 cm) in diameter with an embedded stack of concentric piezoelectric wafers, an eddy-current differential proximity sensor, and a strain-gauge force sensor.

mechanical impedance, Z_L, of the rest of the structure. Uncertainties in the knowledge of the structure make the use of the complex conjugate impractical, and instead, the control system synthesizes a suboptimal Z_m, the real (damping) part of which equals $|Z_L|$, the modulus of the impedance of the rest of the structure.

The second of the two new techniques is a scheme for the placement of the active and passive damping members. The problem of where to place each member of each type is one of combinatorial optimization. The criterion for optimization is maximization of a weighted sum of the passive-damping and active-damping contributions to the rate of dissipation of vibrational energy. The weighting factors are selected on the basis of design requirements and engineering experience. In this technique, one seeks a suboptimal solution by use of a simulated-annealing algorithm, which is one of class of heuristic, iterative algorithms that have been used in other optimation problems and that are named to reflect the fact that some aspects of them resemble some aspects of a mathematical model of annealing. In simulated annealing, one accepts nonimproving solutions according to probabilities determined from the Boltzmann function in the hope of escaping from or avoiding local optima and approaching the global optimum.

This work was done by Gun-Shing Chen, John A. Garba, and Ben K. Wada of Caltech for **NASA's Jet Propulsion Laboratory.** *NPO-17889/TN*

FOR ADDITIONAL INFORMATION: *Contact: Director, Technology Transfer Division, P.O. Box 8757, BWI Airport, MD 21240; (301) 621-0100 Ext. 241*
REFER TO THE NUMBER LISTED AT THE END OF THIS ARTICLE

Integrated Analysis Capability Program

This modular software system facilitates multidisciplinary analyses of structures and other systems.

The Integrated Analysis Capability (IAC) software system is intended to provide a highly effective, interactive analysis tool for the integrated design of large structures. With the goal of supporting the unique needs of engineering analysis groups concerned with interdisciplinary problems, IAC was developed to serve as a software interface between computer programs from the fields of structures, thermodynamics, controls, and the dynamics of systems on the one hand and an executive software system and data base on the other hand to yield a highly efficient multi-disciplinary system. Special attention is given to such users' requirements as handling data and online assistance with operational features and the ability to add new modules of the user's choice at a future date.

IAC contains an executive software system, a data base, general software utilities, interfaces to various engineering programs, and a software framework for building interfaces to other programs. IAC has shown itself to be effective in the automatic transfer of data among analysis programs. IAC 2.5, designed to be compatible as far as possible with level 1.5, contains a major upgrade in executive and data-base management system capabilities and includes interfaces to enable analyses of thermal problems, structures, optics, and the dynamics of control interactions.

The IAC software system is modular: (1) The executive module contains an input command processor, an extensive data-management system, and driver code to execute the application modules. (2) Technical modules provide "stand-alone" computational capability as well as support for various solution paths or coupled analyses. (3) Graphics and model-generation interfaces are supplied for building and viewing models. Advanced graphics capabilities are provided within such analysis modules as INCA and NASTRAN. (4) Interface modules provide for the required flow of data between IAC and other modules. (5) User modules can be arbitrary executable programs or job-control-language procedures with no predefined relationship to IAC. (6) Special-purpose modules are included: for example, MIMIC (Model Integration via Mesh Interpolation Coefficients), which transforms field values from one model to another; LINK, which simplifies incorporation of user-specific modules into IAC modules; and DATAPAC, a statistical-analysis package of the National Institute of Standards and Technology (formerly, the National Bureau of Standards).

The IAC data base contains structured files that provide a common basis for communication between modules and the executive system and can contain such unstructured files as NASTRAN checkpoint files, DISCOS plot files, object code, and the like. The user can define groups of data and relations between them. A full data-manipulation and query system operates with the data base.

The current interface modules comprise five groups:

1. Structural Analysis — IAC contains a NASTRAN interface for stand-alone analysis or certain structural/control/thermal combinations. IAC provides enhanced structural capabilities for normal-vibrational-mode and static-deformation analysis via special DMAP sequences. IAC 2.5 contains several specialized interfaces from NASTRAN in support of multidisciplinary analysis.
2. Thermal Analysis — IAC supports finite-element and finite-difference techniques for steady-state or transient analysis. There are interfaces for the NASTRAN thermal analyzer, SINDA/SINFLO, and TRASYS II. There is also an interface between the IAC data base and FEMNET, which converts finite-element structural-analysis models to finite-difference thermal-analysis models.
3. System Dynamics — There is a full interface between the IAC data-management capability and the DISCOS simulation program, which allows for either nonlinear time-domain analysis or linear frequency-domain analysis.
4. Control Analysis — Interfaces for the ORACLS, SAMSAN, NBOD2, and INCA programs provide for a wide range of techniques for the analysis and synthesis of control systems. Level 2.5 includes EIGEN, which provides the capability to obtain the eigenvalues of systems of large order, and BOPACE, which provides geometric capabilities and capabilities for finite-element analysis in the case of a nonlinear material. Also included in IAC level 2.5 is SAMSAN 3.1, an engineering analysis program that contains a general-purpose library of over 600 subroutines for numerical analysis.
5. Graphics — The graphics package IPLOT is included in IAC. IPLOT generates vector displays of tabular data in the form of curves, charts, correlation tables, and the like. Either DI3000 or PLOT-10 graphics software is required for full graphic capability.

In addition to these analysis software tools, IAC 2.5 contains an IGES interface, which enables the user to read arbitrary IGES files into an IAC data base and to edit and put out new IGES files.

IAC is available by license for 10 years to approved U.S. licensees. The licensed program product includes one set of supporting documentation. Additional copies may be purchased separately.

IAC is written in FORTRAN 77 and has been implemented on a DEC VAX-series computer operating under VMS. IAC can be executed by multiple concurrent users in batch or interactive mode. The program is structured to enable users to delete easily those program capabilities and "how-to" examples they do not want, to reduce the size of the program. The basic central-memory requirement for IAC is approximately 750 KB. The following programs are also available from COSMIC as separate packages: NASTRAN, SINDA/SINFLO, TRASYS II, DISCOS, ORACLS, SAMSAN, NBOD2, and INCA. The development of level 2.5 of IAC was completed in 1989.

This program was written by R.G. Vos, D.L. Beste, and J. Greg. of Boeing Aerospace Corporation and H.P. Frisch of **Goddard Space Flight Center.**
GSC-13341/TN

FOR ADDITIONAL INFORMATION

CONTACT

COSMIC®
112 Barrow Hall
University of Georgia
Athens, GA 30602

(404) 542-3265

Numerical-Optimization Program

The ADS computer program is suitable for such applications as minimum-weight design.

The Automated Design Synthesis (ADS) computer program is a general-purpose numerical-optimization program for design engineering. Significant applications have already been found for this program in the synthesis of structures (minimum-weight design).

ADS provides a wide range of options for the solution of constrained and unconstrained function minimization problems. The user makes choices at each of three software levels to tailor the method of solution to fit the particular minimization problem. The three basic software levels are Strategy, which represents the overall minimization strategy; Optimizer, which represents the particular minimization algorithm; and One-Dimensional Search, which represents the method of applying the minimization technique. ADS relies on the user to formulate the problem and make appropriate selections from the solution options.

Strategy options in ADS include sequential unconstrained minimization using the exterior-penalty-function method; sequential unconstrained minimization using the linear-, quadratic-, or cubic-extended-interior-penalty-function method; the augmented Lagrange-multiplier method; sequential linear programming; the method of centers (method of inscribed hyperspheres); and sequential quadratic programming. Optimizer options include the Fletcher–Reeves algorithm for unconstrained minimization, either the Davidon–Fletcher–Powell (DFP) or Broydon–Fletcher-Goldfarb–Shanno (BFGS) variable-metric method for unconstrained minimization, and the regular or modified method of feasible directions (MFD) for constrained minimization. One-Dimensional Search options include constrained or unconstrained function minimization using only a golden-section method or a golden-section method followed by polynomial interpolation, and constrained or unconstrained function minimization using polynomial interpolation and/or extrapolation with or without first finding bounds on the solution.

ADS is invoked by a calling program supplied by the user. ADS returns control to the calling program when information on a function or gradient is needed. This provides considerable flexibility in capabilities for organizing programs and restarting execution of them. ADS can be used in four principal modes: (1) default control parameters and finite-difference gradients, (2) override default parameters (use finite-difference gradients) (3) default parameters and gradients supplied by the user, and (4) override default parameters and gradients supplied by the user. These options provide the user more control over the problem-solving procedure than would otherwise be available.

The ADS program is written in FORTRAN 77 and developed on a CDC CYBER 170-series computer. The program requires approximately 155K (octal) of 60-bit-word memory. The CDC version of ADS was developed in 1984 and updated in 1985. The VAX version is a port of the 1985 CDC version.

This program was written by Garret N. Vanderplaats of the Naval Postgraduate School for **Langley Research Center.**
LAR-14500/TN

FOR ADDITIONAL INFORMATION

CONTACT

COSMIC®
112 Barrow Hall
University of Georgia
Athens, GA 30602

(404) 542-3265

Program Calibrates Strain Gauges

Time required for acceptance tests of hardware is reduced.

Strain data are required for the processing of such pieces of aerospace hardware as the three bolts used to attach the external fuel tank to the Space Shuttle orbiter. The acquisition of these data has traditionally required a time-consuming and inefficient manual process that includes setting up a strain-gauge indicator, reading and recording strain data, and tabulating and plotting strain data versus a load or other parameter. The time and personnel requirements of the traditional method led researchers to develop a computer program to increase the efficiency of the acceptance test performed on these bolts.

The data-acquisition system reads the output from a Wheatstone full-bridge strain-gauge circuit and calculates strain by use of the shunt calibration technique. The program nearly instantaneously tabulates and plots strain data against load-cell outputs, thus saving hours of manual work per test run. The comparative speed and efficiency of this technique was empirically proven by a calibration test of one of the external-tank/orbiter attachment bolts. The use of the program dramatically reduced personnel and time requirements. Researchers verified the accuracy and integrity of the program by comparing its output strain data to those of a calibrated strain-gauge indicator formerly used in the manual method. The program can also be modified to acquire strain data for other specimens wherever full-bridge strain-gauge circuits are used.

The program was developed in 1985 on a Hewlett Packard 9845B Microcomputer. It is written in HP BASIC and is available as a listing only.

This program was written by Gary D. Okazaki of Rockwell International Corp. for **Johnson Space Center.**
MSC-21399/TN

FOR ADDITIONAL INFORMATION

CONTACT
COSMIC®
112 Barrow Hall
University of Georgia
Athens, GA 30602

(404) 542-3265

Tracing and Control of Engineering Requirements

Requirements and progress of an engineering project can be documented in systematic manner.

TRACER (Tracing and Control of Engineering Requirements) is a data-base/word-processing software system created to document and maintain the order of both requirements and descriptions associated with an engineering project. For a project, there is normally generated a set of hierarchical documents in which the requirements of the documents of higher level levy requirements on the documents of the same or lower level. Traditionally, the requirements have been handled almost entirely by manual paper methods. One disadvantage of a typical paper system is that requirements written and changed continuously in different areas lead to misunderstandings and noncompliance.

The purpose of TRACER is to automate the capture, tracing, review, and management of requirements for an engineering project. The engineering project still requires communications, negotiations, interactions, and iterations among people and organizations, but TRACER promotes succinct and precise identification and treatment of real requirements separate from the descriptive prose in a document. TRACER enables the documentation of the requirements and progress of an engineering project in a logical, controllable, traceable manner.

The attributes of TRACER include the presentation of current requirements and status from any linked computer terminal and the ability to differentiate headers and descriptive material from the requirements. Related requirements can be linked and traced. The program also enables the printing of portions of documents, individual approval and release of requirements, and the tracing of requirements down into the specification of equipment. Requirement "links" can be made "pending" and invisible to others until the pending links are made "binding." Individuals affected by linked requirements can be notified of significant changes with acknowledgement of the changes required. An unlimited number of documents can be created for a project, and an ASCII-import feature enables the incorporation of existing documents. TRACER can automatically renumber section headers when inserting or deleting sections of a document and can generate signoff forms for any approval process as well as a table of contents.

TRACER is implemented on an IBM PC under PC-DOS. The program requires 640 KB of random-access memory, a hard disk, and PC-DOS version 3.3 or higher. It was written with CLIPPER. The executable program is also provided with the distribution.

IBM PC and PC-DOS are registered trademarks of International Business Machines. CLIPPER is a trademark of Nantucket Corp.

This program was written by Philip R. Turner, Richard L. Stoller, Ted Neville, and Karen A. Boyle of Caltech for **NASA's Jet Propulsion Laboratory.**
NPO-18215/TN

FOR ADDITIONAL INFORMATION

CONTACT
COSMIC®
112 Barrow Hall
University of Georgia
Athens, GA 30602

(404) 542-3265

U.S. Navy Fact Sheet

Licensing Opportunity

Naval Ocean Systems Center

Liquid Level and Volume Sensor

This device utilizes an optical attenuation technique to measure liquid levels and volumes without contaminating the liquid under observation. It provides an accurate, extended measurement range (from empty to full) - without contacting either the fluid or its container - via a single light source, detector, and associated electronics. The device is applicable to transparent and translucent fluids in containers of similar optical transmission characteristics. Figure 1 is a schematic diagram of the device.

The function of the optical source is to emit a constant output within a specific wavelength band. Examples are: white source with appropriate filters or monochrometer; or a laser diode. The source wavelength is chosen to match the spectral properties of the fluid to be measured. Sources are commercially available to match absortion characteristics of most fluids, including the 1300 nanometers required for water based fluid measurements. The source may be used direct, through a lens, or remotely located from the measurement area by coupling into an optical fiber. The detector can be similarly configured. Analysis circuitry used to convert detector output to liquid level or volume measurements is comprised of standard off-the-shelf

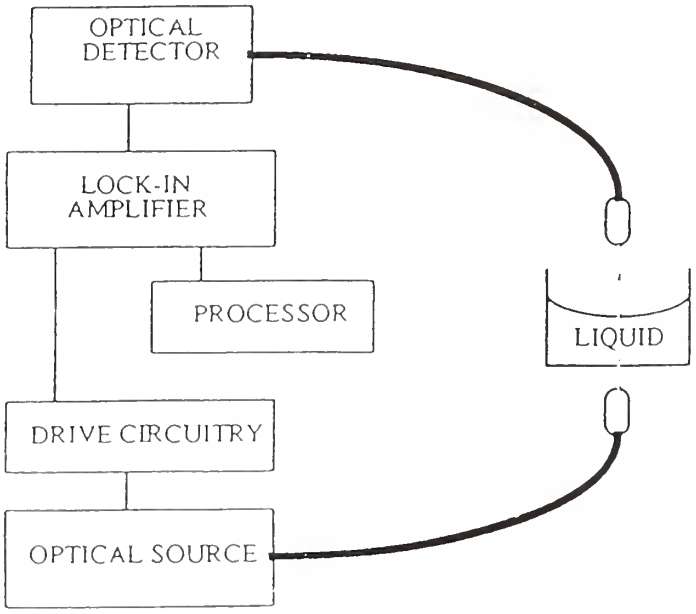

Figure 1. Schematic of Liquid Level & Volume Sensor

components. It processes the detector output to determine the attenuation of the optical beam for subsequent correlation to the parametric measurements. Features of the device include:

- non-contact/non-contaminating technique for liquid volume and level measurements.
- single sensor for accurate, continuous measurements (empty to full range).
- low technical risk.
- off-the-shelf equipment and parts.

Potential users of this device include medical and chemical laboratories, and manufacturing facilities having production lines for filling liquid containers.

Descriptive Literature: U.S. Patent Application # 561413 - "Liquid Level and Volume Measurement Device"

FOR ADDITIONAL INFORMATION: Ramsey D. Johnson, Code D4T, Naval Surface Warfare Center, 10901 New Hampshire Avenue, Silver Spring, MD 20903-5000; Phone: (301)394-1505, Autovon: 290-1505.

National Renewable Energy Laboratory

Snapshots of Room Temperature and Airflow

SERI engineers have found a new way to visualize airflow through a room. This innovative technique could someday help architects and engineers to create more comfortable, energy-efficient indoor environments.

Researchers from SERI and Colorado State University are using the technique to see how cold air flows from thermal storage systems, which could be used to reduce energy demand in a commercial building. This research project is being sponsored by the Electric Power Research Institute.

To visualize air flow, researchers placed a thin fiberglass screen at right angles to the cold-air jet. As air flows through the thin mesh, an infrared thermal imaging system produces a colorful pattern of air-temperature distribution in two dimensions. Researchers can also develop a three-dimensional picture by placing the screen in different positions across the room.

This method has significant advantages over conventional techniques for studying room airflow. It does not require the use of particulates such as chemical smoke, nitrous oxide, or condensable vapors. An overall picture of temperature distribution and flow patterns can be obtained instantaneously. And, unlike other methods, researchers can actually see the three-dimensional airflow that causes cold drafts and other undesirable energy patterns.

SERI researchers Vahab Hassani (left) and Rob Farrington set up a unique infrared imaging system to study airflow.

For Additional Information:

Steve Rubin
National Renewable Energy Laboratory
1617 Cole Boulevard
Golden, CO 80401-3393
(303) 231-7303

Refer to Volume XII, Number 2/TN

NAVY
Domestic Technology Transfer Fact Sheet

Three-Point Bend Tests Performed

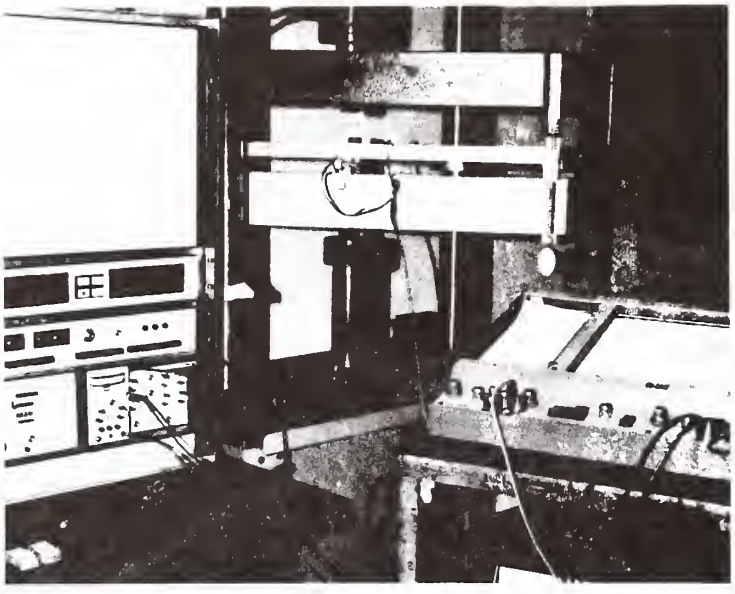

Figure 1. Test Setup

The fracture for notched beams in three-point bending was experimentally determined by the Naval Civil Engineering Laboratory (NCEL), Port Hueneme,California. The series of tests were conducted on a total of 32 beams and a finite element analysis carried out using a nonlinear model

The conclusions were as follows:

- The experiment setup (Figure 1) led to more reliable and consistent values of concrete fracture energy and measured crack length.
- Gf (calculated by current crack size and ligament area) did not present any substantial advantage over Gf (determined by RILEM guidelines).
- Finite element analysis yielded accurate representations of the fracture behavior when coupled with a bilinear stress versus crack width relation.
- Gf is dependent upon size and geometry. The fracture energy increases with increasing size.

For Additional Information:

Backup material on this effort is available from:

Navy Domestic Technology Fact Sheet Reader Reply Service
Code E211
Naval Surface Weapons Center
Dahlgren, VA 22448-5000
(703) 663-8921

Refer to 161104/TN

NASA Tech Brief
National Aeronautics and
Space Administration

Experiments on Schemes for Adaptive-Wall Wind Tunnels

Ways to reduce testing time for adaptation are discused.

A report discusses an experimental investigation of the various convergence schemes for an adaptive-wall wind tunnel. In such a wind tunnel, the shape of the walls is changed, or controlled auxiliary flows are introduced through holes in the walls to compensate for the interference of the walls on the flow about the test model in such a way that the flow at the model approximates the flow that would be obtained if the walls were not present. Measurements of flow variables (e.g., pressures and/or velocities) at a small number of selected positions are used to adjust the auxiliary flows or other compensating mechanisms. A convergence scheme is an iterative or one-step scheme by which the adjustments make the conditions in the compensated flow impinging on the model converge on the free-stream conditions.

At present, ventilated adaptive-wall wind tunnels require complicated instrumentation and excessive testing time to perform adaptations. The purpose of the research described in the report was to establish faster convergence schemes with simpler instrumentation. To simplify the instrumentation, it was proposed to use the distribution of pressure on the side wall as the flow variable. As one of the alternatives to reduce the testing time, a one-step convergence scheme was proposed.

To explore the relative merits of different convergence schemes, the iterative and the one-step methods were implemented with normal and streamwise velocity components measured by a two-component laser Doppler velocimeter and also with resultant velocity distributions calculated from measurements of static pressures on the side wall. Emphasis was given to the convergence schemes with two-level compatibility assessment, which requires the measurement of one flow variable at two levels (unlike the one-level method, in which two flow variables have to be measured at one control level). Measurements were performed at mach numbers from 0.5 to 0.75 and at angles of attack from 0° to 4°.

In the iterative and the one-step methods, influence coefficients were employed for a systematic estimation of the pressure corrections. Different coefficients were used for suction and blowing. One aspect of the investigation was the determination of the practical limitations and the effectiveness of the influence coefficients at various mach numbers and angles of attack.

The results show that the side-wall-pressure measurements can, indeed, be used as the flow variables and that they yield the same unconfined-flow conditions as those obtained by measuring streamwise and perpendicular components of velocity with a laser Doppler velocimeter. The results justify the use of influence coefficients in the one-step and iterative convergence schemes. They also show that with the one-step convergence scheme, satisfactory adaptation can be obtained when the number of iterations is reduced to one (or sometimes two).

This work was done by Z.Z. Celik of Stanford University and S. Bodapati of the Navy–NASA Joint Institute for Aeronautics for **Ames Research Center**. *"Experimental Investigations of the Various Convergence Schemes for an Adaptive Wall Wind Tunnel."* *ARC-12116/TN*

FOR ADDITIONAL INFORMATION: *Contact: Director, Technology Transfer Division, P.O. Box 8757, BWI Airport, MD 21240; (301) 621-0100 Ext. 241*
REFER TO THE NUMBER LISTED AT THE END OF THIS ARTICLE

NASA Tech Brief
National Aeronautics and
Space Administration

New Sensors for Flow Velocity and Acoustics

Development programs promise more accurate measurements.

A paper describes two sensor-development programs at the Fluid Mechanics Laboratory at NASA Ames Research Center. One of the programs, for digital image velocimetry (DIV) sensors, is in progress. The other program, for advanced acoustic sensors for wind tunnels, has just been started.

DIV measures, in real time, the instantaneous velocity fields of time-varying flow or of a collection of objects moving with varying velocities. DIV uses high-speed video photography, image processing, and digital Fourier transformation to create an image of seed particles or moving objects from linearly superposed frames taken at fixed intervals. The velocities of the particles or objects are determined from the separations between subsequent images of them.

DIV differs from other techniques for measuring the velocity fields of fluids (such as particle-image velocimetry and laser-speckle velocimetry) in that its single-exposure images can be isolated from the combined image. Single-exposure images can be used to eliminate uncertainties caused by overlaps and undesirable distributions of particles.

The advanced acoustic sensors for wind tunnels are being developed to reduce the effects of interference from wind noise, noise from interactions between flows and sensors, flow-induced vibrations of sensors, deflections of acoustic waves by boundary layers induced by sensors, and reflections from walls and sensor supports. The advanced sensors include adaptive arrays of optical fibers in which signal processors automatically adjust the sensitivities of the arrays to enhance directivities and spectral responses.

A representative array includes a source of light, optical-fiber interferometers, and a photodetector connected to a signal processor. Sound modulates the phase of the light in the fibers. The modulated light is combined with unmodulated reference light, and the resulting interference signal is detected and sent to the signal processor, which extracts information about the acoustic signal.

This work was done by Y.C. Cho of **Ames Research Center.** *"Sensor Development Program at NASA Ames Research Center."* *ARC-12577/TN*

FOR ADDITIONAL INFORMATION: *Contact: Director, Technology Transfer Division, P.O. Box 8757, BWI Airport, MD 21240; (301) 621-0100 Ext. 241*
REFER TO THE NUMBER LISTED AT THE END OF THIS ARTICLE

Environmental Science & Technology

0376 Hazardous and Industrial Waste Minimization

0377 Detoxifying Groundwater At a Superfund Site

Technology Assessment
U.S. Air Force

Hazardous and Industrial Waste Minimization

This Industrial Modernization Incentives Program (IMIP) project will be implemented at East Hartford, Middletown, Southington and North Haven, Connecticut and North Berwick, Maine.

This project reduces hazardous waste generation through either source reduction, rejuvenation or recycling. Source reduction minimizes waste generation at the point of origin. Rejuvenation restores useful life of the material. Recycling is the use or reuse of a waste as an effective substitute for another product. In addition, the program will evaluate the potential for the sale of the waste or by-products beyond its useful life. This project addresses the following four waste streams: metal finishing wastes, soluble oils, solvents, and sludge from electro-chemical machining operations.

This project is in the final stages of Phase II development and as such, final results and recommendations for alternative technologies and equipment are not yet available. Preliminary results are available from Pratt & Whitney

This project enables industry and the Department of Defense to lower operating costs, enhance product quality, reduce environmental impact and limit contingent liability for waste disposal.

Hazardous waste minimization would be appropriate anywhere in the manufacturing cycle.

Important to the success of this project are:

- Involvement of all facilities scheduled for implementation
- Total "Team" involvement in development
  - — Manufacturing
  - — Procurement
  - — Planning
  - — Design
  - — QA
  - — EPA
  - — Government

Phase II, Development — Sep 89 - Aug 92.
Phase III, Implementation — Jun 92 - Jun 94.

TECHNICAL DOCUMENTATION

Projected final report available from the Defense Technical Information Center (DTIC), Dec 92.

FOR ADDITIONAL INFORMATION: Wright Laboratory, WL/MTX (Robert Reifenberg), Wright-Patterson AFB, OH 45433-6523; (513) 255-7362. Refer to MT91001MH.

National Renewable Energy Laboratory

Detoxifying Groundwater At a Superfund Site

A new method for cleaning up contaminated groundwater has scored high marks in its first field test at Lawrence Livermore National Laboratory (LLNL), a designated Superfund site. This is also the first use of solar detoxification in an actual hazardous-waste environment.

For this multi laboratory project, SERI engineers developed a system consisting of two strings of solar troughs, each 120 feet long. The troughs focus sunlight on narrow, transparent tubes containing contaminated groundwater and a special photocatalyst. High-energy, ultraviolet photons in sunlight interact with the catalyst to turn toxic chemicals into harmless byproducts.

In early runs of the system, groundwater contaminated with trichloroethylene (TCE) was pumped through the reactor tubes at the rate of five gallons a minute. Analysis showed that sunlight reduces TCE levels below detection limits (less than 0.5 parts per billion).

The solar troughs were built by Solar Kinetics Inc. of Dallas, Tex. Support equipment was designed and mounted on a portable equipment skid fabricated by the ECOVA Co. of Belleview, Wash.

"Our goal is to develop a solar-driven system that is economically competitive with other methods of cleaning up polluted water," said SERI project manager Alan Laxson. "Using solar detoxification, groundwater can be cleaned up onsite—you won't have to collect the toxic chemicals on carbon and transport them for treatment."

Improvements to the prototype system will increase flow rates to 30 gallons per minute. Information collected from the experiments will be used to reduce system cost and to

SERI researcher Mark Mehos draws a sample of solar-treated groundwater for analysis. Initial tests showed that trichloroethylene could be reduced to levels well below those required for drinking water.

develop industrial-size units.

Groundwater at the LLNL site was tainted by TCE and other toxins as a result of airplane-engine maintenance during World War II. Specialists at SERI and Sandia National Laboratories in Albuquerque, N. Mex., are now participating in the cleanup studies.

For Additional Information:

Steve Rubin
National Renewable Energy Laboratory
1617 Cole Boulevard
Golden, CO 80401-3393
(303) 231-7303

Refer to Volume XII, Number 2/TN

Manufacturing, Machinery & Tools

0378 Manufacturing Technology for Large Aircraft Composite Primary Structure (Fuselage)

0379 Robotic Engine Manifold Cleaning Cell and Hazardous Chemical Rejuvenation

0380 New Gold Electroplating Process for Microelectronics Safer

0381 Air Driven Grinding and Polishing Tool Developed (Licensing Opportunity)

0382 Long-Lived Electrode for Arc Welding in Vacuum—Pressurized gas reduces the vaporization of the electrode.

0383 Low-Leakage Inlet Swirl Brake—Vanes change the direction of flow while giving rise to relatively low static pressure. (Licensing Opportunity)

0384 Smaller Coaxial-View Welding Torch—This torch resembles an ordinary torch without optics. (Licensing Opportunity)

0385 Testbed for Telerobotic Servicing—Various combinations of operator control and robot autonomy can be evaluated.

0386 Trailing Shield for Welding on Pipes—Weld beads remain covered with inert gas until safely cooled. (Licensing Opportunity)

Testing & Instrumentation

0387 Dynamic Tester for Rotor Seals and Bearings—A simplified apparatus measures performance under vibration. (Licensing Opportunity)

0388 Monitoring Bearing Vibrations for Signs of Damage—Real-time spectral analysis is performed to detect telltale changes in vibrations. (Licensing Opportunity)

Wright-Patterson Air Force Base

Manufacturing Technology for Large Aircraft Composite Primary Structure (Fuselage)

The purpose of this program was to establish and validate new, low cost manufacturing technology for the construction of large aircraft composite fuselage structures.

This program was accomplished in four phases. A six-member team produced manufacturing test hardware using various manufacturing methods and technologies during the first two phases of this program. These test components were compared for manufacturing cost, quality, strength, and weight . In Phases III and IV, two optimum frame fabrication techniques, one stiffener technique, and one skin-panel technique were selected to fabricate full-size verification and demonstration hardware. Three one-piece, filament wound CV-22 aft fuselage sections were fabricated and assembled as part of the Phase IV demonstrating considerable labor savings as compared to traditional assembly operations.

This program was based on the CV-22 Osprey tiltrotor aircraft and demonstrated the technology required to produce large aircraft composite fuselage structures at costs significantly lower than those incurred in current production programs. Overall direct labor cost savings for individual components of the V-22 fabricated on this program ranged from 53 to 60 percent. Actual labor hour comparisons for Boeing fuselage assembly were 296 labor hours using conventional methods as compared to 35 labor hours for the redesigned fuselage. The innovative fabrication techniques demonstrated by this program have broad applicability to future large aircraft fuselage structures. More importantly, they have contributed significantly to making composite structures competitive with aluminum for cost-driven structural applications.

Contract: F33615-83-C-5024, Project Engineer: Robert Neff, WL/MTP, (513) 255-7279.

Wright-Patterson Air Force Base

Robotic Engine Manifold Cleaning Cell and Hazardous Chemical Rejuvenation

An important part of aircraft maintenance is the removal of carbon (coke) deposits that accumulate on engine manifold parts. These deposits build up and restrict fuel flow into the combustion chamber, severely affecting engine performance and efficiency. The manifolds are cleaned to remove the coke deposits using chemical oxidation with a hot concentrated solution of potassium permanganate and sodium hydroxide pumped through the parts. This cleaning activity is a large scale activity at the Oklahoma City Air Logistics Center (ALC), but remains essentially a hands-on operation. This effort was undertaken to reduce the manual intervention required for this effort and to use the cleaning solution more efficiently with less waste and associated disposal costs.

A robotic engine manifold cleaning cell developed by General Atomics has been designed and developed to remedy all the shortcomings of the current process. The process is an automated high-pressure chemical wash and rinse process, with a permanganate rejuvenation system to maintain the cleaning solution at peak cleaning effectiveness and to eliminate disposal of this hazardous solution. The cleaning cell and rejuvenation systems have been installed and implemented in the Oklahoma City ALC Accessories Division engine manifold cleaning shop.

This system will eliminate all hazardous manual operations and all hazardous waste associated with the current cleaning system and will reduce material cost by 95 percent. The new system is expected to save over $2 million each year.

Contract: F33615-87-C-5271, Project Engineer: David See, WL/MTPM, (513) 255-3612.

Department of Energy

Technology Application

Sandia National Laboratory

New Gold Electroplating Process for Microelectronics Safer

Researchers at Sandia National Laboratories have developed a process that allows intricate electroplating of gold on microelectronic devices while using a solution safer than conventional cyanide-based plating solutions.

Gold has several properties that make it desirable for use in microelectronics manufacturing. As a noble metal, it is extremely corrosion resistant. Gold also has high electrical conductivity and forms good electrical contacts, and its high melting point makes it thermally stable.

But standard gold-plating solutions are cyanide-based and can release large amounts of poisonous cyanide gas if the solution becomes too acidic. For this reason, the Environmental Protection Agency has classified the gold cyanide solutions as acutely hazardous, and special safety precautions must be taken.

In the 1970s, a gold sulfite electroplating solution was developed that contains no cyanide and is not hazardous. But until recently this solution's use for microelectronics applications has primarily been limited to protective coverings rather than circuitry. Now, Sandia researchers have applied this gold sulfite solution to form precise gold patterns for semiconductor devices.

"We have successfully plated extremely fine lines using this method," says Walter Worobey, the principal Sandia investigator who developed the new process. "The fabricated gold patterns on substrates had lines and spaces two micrometers wide with the gold four micrometers thick."

The sulfite solution also has been used by Worobey and co-researcher Dennis Rieger to fabricate miniature gold bridges to form crossovers on gallium arsenide substrates. These crossovers allow conductors to cross on the surface of electronic devices without touching or electrically shorting out.

Tests at Sandia have shown that in these applications plating efficiency was close to 100 percent and the plated gold's density approached that of pure gold.

Sandia's expertise in photolithography played a major role in selecting the materials and defining the precision patterns required. An important factor in the procedure was ensuring that the photoresist used to define the precision channels for the gold did not degrade in the alkaline sulfite solution during the electroplating process.

Worobey and Rieger, who are staff members in Sandia's Electronic Interconnections, Packaging, and Calibration Department, are continuing to refine this technology.

"Increased use of this solution promises to not only significantly reduce potential environmental pollution and health risks in electroplating but also simplify waste disposal and handling. All of these benefits add up to reduced production costs," says Worobey. *Technical Contacts: Walter Worobey (505) 845-8965 and Dennis Rieger (505) 844-5554.*

Air Driven Grinding and Polishing Tool Developed

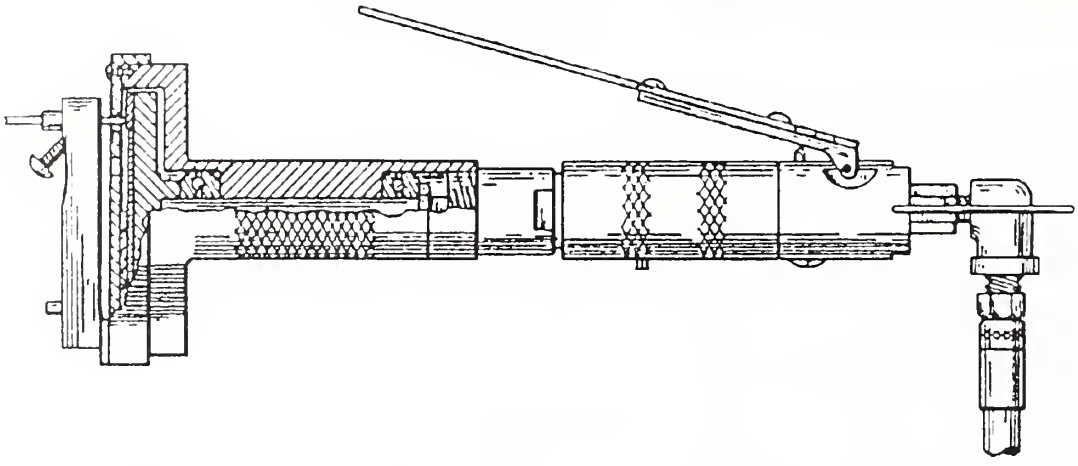

Figure 2. Air driven grinding and polishing tool

The Naval Ocean Systems Center (NOSC), San Diego, California, has developed a portable, hand-held fiber optic grinding and polishing tool specifically designed for fiber optic terminals (Figure 2). The tool is air driven to eliminate the danger of electrical arcing that can cause explosions in field installation, such as onboard aircraft and vessels. A smoother light-emitting surface is achieved in the tool in that the angular orientation between the end of the workpiece and the engaging abrasive surface is constantly changed during the grinding and polishing operation. The overlapping abrasive cuts produce a smoother and flatter workpiece surface.

For Additional Information:

Backup material on this effort is available from:

Navy Domestic Technology Fact Sheet Reader Reply Service
Code E211
Naval Surface Weapons Center
Dahlgren, VA 22448-5000
(703) 663-8921

Refer to 161106/TN

NASA Tech Brief
National Aeronautics and Space Administration
Marshall Space Flight Center, Alabama

Long-Lived Electrode for Arc Welding in Vacuum

Pressurized gas reduces the vaporization of the electrode.

An improved electrode for gas/tungsten arc welding in vacuum is essentially a hollow cylinder along which an inert gas flows. The interior of the cylinder provides a large surface area for the emission of electrons to form the welding arc. The flow of pressurized inert gas inhibits vaporization of the hot electrode material. Both features combine to reduce the erosion of the electrode. Consequently, the electrode lasts considerably longer in a vacuum than does a conventional electrode.

The outer end of the electrode has a small orifice to release the inert gas and the arc (see figure). The electrode is held in a nonconductive cup, which confines the origin of the arc to the orifice; this prevents extraneous corona discharge to other spots on the outside of the welding torch.

For welding in a vacuum chamber, the diameter of the orifice is 0.005 to 0.010 in. (0.13 to 0.25 mm), and the volume of the cylindrical cavity in the electrode is about 0.75 $in.^3$ (about 6.9 cm^3). These dimensions ensure the emission of an adequate number of electrons for the arc while limiting the flow of inert gas into the vacuum chamber so as not to exceed the capacity of the vacuum pump.

This work was done by Jack L. Weeks and Richard M. Poorman of Rockwell International Corp. for **Marshall Space Flight Center.**

This invention is owned by NASA, and a patent application has been filed. Inquiries concerning nonexclusive or exclusive license for its commercial development should be addressed to the Patent Counsel, Marshall Space Flight Center. Refer to MFS-29766/TN.

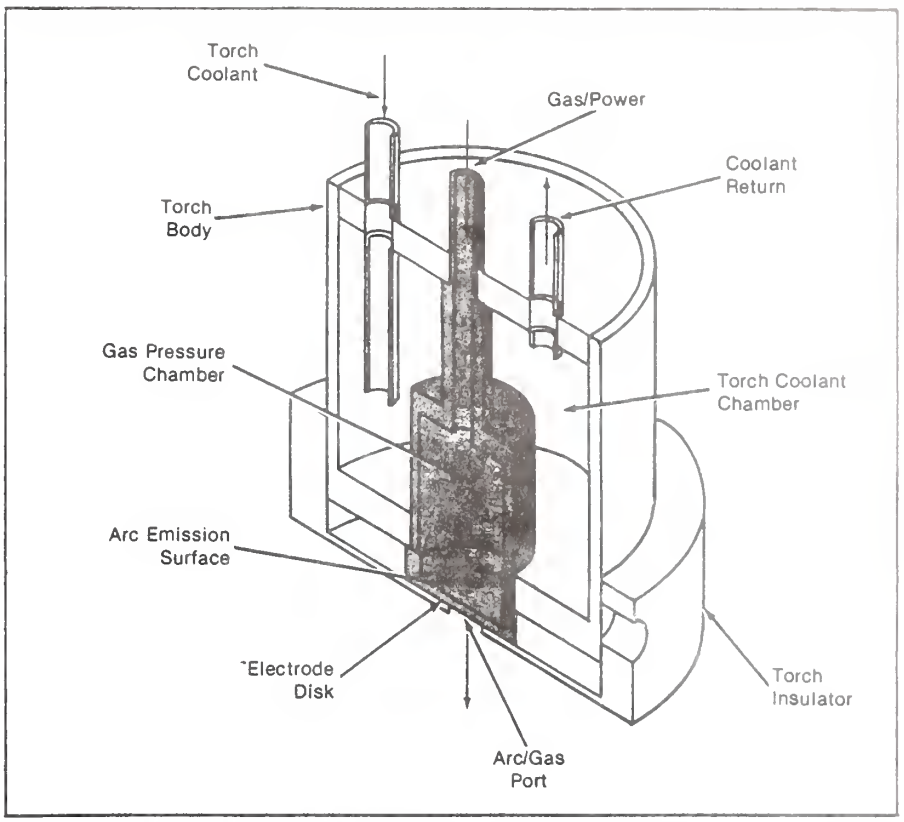

The Electrode for Welding in a Vacuum is a hollow tungsten cylinder. An insulator holds the electrode in the welding torch. Inert gas flows into the cylinder along the central tube at the top. The inert gas flows out through the orifice in the bottom end of the electrode.

FOR ADDITIONAL INFORMATION: *Contact: Director, Technology Transfer Division, P.O. Box 8757, BWI Airport, MD 21240; (301) 621-0100 Ext. 241*

REFER TO THE NUMBER LISTED AT THE END OF THIS ARTICLE

NASA Tech Brief
National Aeronautics and Space Administration
Marshall Space Flight Center, Alabama

Licensing Opportunity

Low-Leakage Inlet Swirl Brake

Vanes change the direction of flow while giving rise to relatively low static pressure.

An improved swirl brake offers both lower rotordynamic instability and lower static-pressure rise. In general, a swirl brake is a device that changes the direction of flow into a fluid seal in a turbomachine from circumferential to partly or entirely axial. Such a device is needed because high inlet circumferential velocities have been shown by experiment to give rise to rotor-destabilizing forces.

The problem in designing a swirl brake is to obtain a low whirl-frequency ratio without causing an excessive buildup of static pressure at the inlet. This problem arises because the ratio of destabilizing to stabilizing forces increases or decreases with the whirl-frequency ratio and because an increase in static pressure caused by diversion of the flow can give rise to an undesired increase in seal leakage. A two-dimensional finite-element solution of the Navier–Stokes equations was used to optimize the design. The angle of the turning vanes in the swirl brake (see figure) was chosen to eliminate the circumferential component of inlet flow. The turning vanes cause the flow to converge so that the increased velocity of flow results in a lower static pressure.

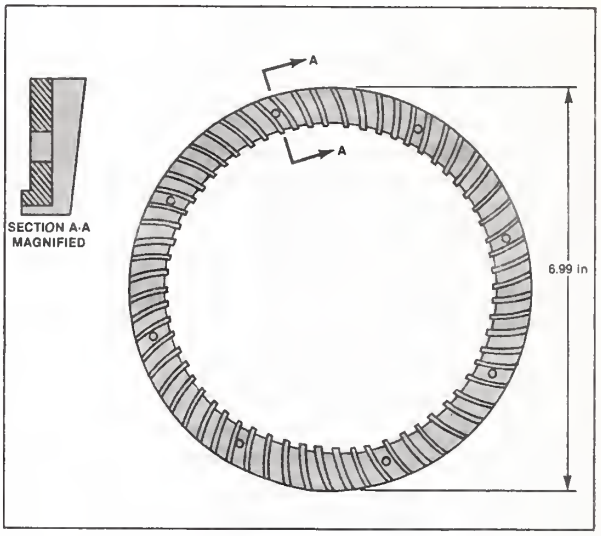

Sixty-Four Vanes are evenly spaced around a ring. The vanes convert inlet flow from circumferential to axial.

This work was done by Joseph K. Scharrer of Rockwell International Corp. for **Marshall Space Flight Center**.

Inquiries concerning rights for the commercial use of this invention should be addressed to the Patent Counsel, Marshall Space Flight Center. Refer to MFS-29608/TN.

George C. Marshall Space Flight Center
Technology Utilization Officer Ismail Akbay
Code AT01
Marshall Space Flight Center,
AL 35812
(205) 544-2223

Patent Counsel Leon D. Wofford, Jr.
Mail Code CC01
Marshall Space Flight Center,
AL 35812
(205) 544-0024

FOR ADDITIONAL INFORMATION: *Contact: Director, Technology Transfer Division, P.O. Box 8757, BWI Airport, MD 21240; (301) 621-0100 Ext. 241*
REFER TO THE NUMBER LISTED AT THE END OF THIS ARTICLE

NASA Tech Brief
National Aeronautics and Space Administration
Marshall Space Flight Center, Alabama

Licensing Opportunity

Smaller Coaxial-View Welding Torch

This torch resembles an ordinary torch without optics.

A coaxial-view torch for gas/tungsten arc welding has only two-thirds the length and width of its predecessor. The shape and size of the new torch are similar to those of a commercial arc-welding torch (Linde HW-27 or equivalent), even though it contains a lens system (see Figure 1). In addition, the collet that holds the electrode has unique design that allows greater passage of light than earlier designs did.

Because the redesigned torch is so much smaller, it can be used in small spaces that were previously inaccessible. In addition, because it is so like the commercial version, it can be introduced into production welding operations with a minimum of disturbance.

The torch, mounted on a welding robot (see Figure 2), forms an image of the weld seam and of the molten pool around the electrode axis. The image is used for remote monitoring by an operator or for closed-loop computer control of the robot.

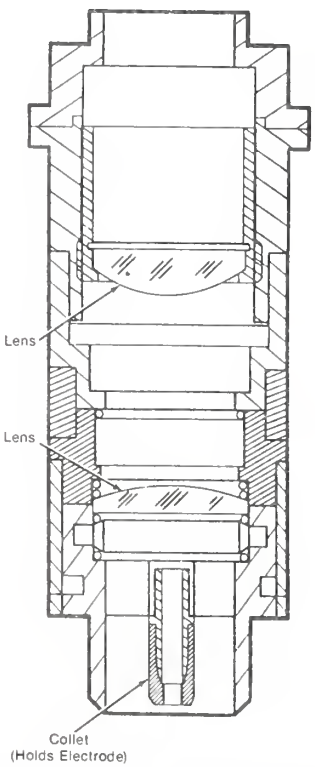

Figure 1. The **Optics in the Welding Torch** are concentric with the electrode. The principal virtue of this design is its relative smallness.

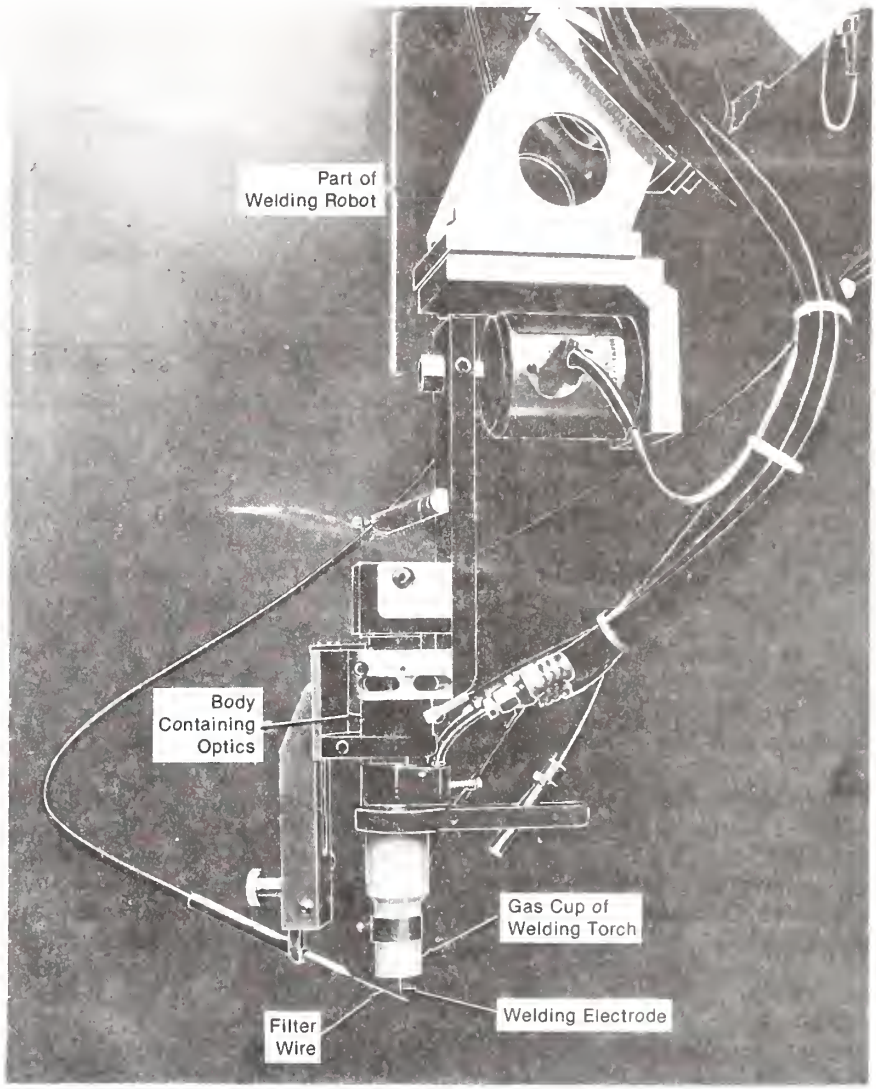

Figure 2. The **Welding Torch**, with its integral optical system, is mounted on one end of a welding robot.

The optical components in the torch are self-aligning, standard-sized parts. These components can be changed easily to obtain different magnifications.

This work was done by Kenneth J. Gangl of Rockwell International Corp. for **Marshall Space Flight Center.**

Inquiries concerning rights for the commercial use of this invention should be addressed to the Patent Counsel, Marshall Space Flight Center. Refer to MFS-29744/TN.

George C. Marshall Space Flight Center
Technology Utilization Officer: Ismail Akbay
Code AT01
Marshall Space Flight Center,
AL 35812
(205) 544-2223

Patent Counsel:
Leon D. Wofford, Jr.
Mail Code CC01
Marshall Space Flight Center,
AL 35812
(205) 544-0024

NASA Tech Brief
National Aeronautics and Space Administration
NASA's Jet Propulsion Laboratory, Pasadena, California

Testbed for Telerobotic Servicing

Various combinations of operator control and robot autonomy can be evaluated.

A telerobot testbed is used to evaluate technologies for remote servicing, including assembly, maintenance, and repair. This type of servicing will be used on the Space Station and on the Space Shuttle and satellites in orbit. It could also be used in hazardous and underwater environments on Earth.

With the testbed, the benefits of individual technologies in the overall servicing system can be quantified and recommendations can be made for their use. The testbed operates in several different modes:

- Direct teleoperation with and without force reflection;
- Shared control, in which the human operator controls some aspects of the operation and the remote robot controls other aspects semiautonomously;
- Traded control, in which the human operator plans gross motion and maneuvering of the remote end effector and the robot then performs the task semiautonomously under the supervision of the operator, who can intervene at any time;
- Operator designate, in which the operator, using a video model, registers the location of an object and otherwise identifies the object for the robot for later autonomous robot operations; and
- Relative update, in which the operator points out two objects, such as the workpiece and the robot end effector, and the system calculates the distance between them for use by the robot in carrying out a task autonomously.

The testbed enables the study of the advantages and disadvantages of the modes and the problems encountered in implementing them. The best technologies for implementing these modes can be chosen. It provides delays that simulate the transmission delays between the control stations on the ground and orbiting spacecraft.

The testbed includes five major equipment subsystems (see figure), each consisting of such commercially available equipment as video cameras, computers, and robot arms. One of these subsystems is the operator control station, which provides an efficient, user-friendly interface between an operator and the telerobot, including keyboards, video monitors, hand controllers, mice, and voice inputs. The station provides graphical displays of force and torque measurements. It also provides displays and function switches for a second operator, who observes the telerobot operator and the operation of the system.

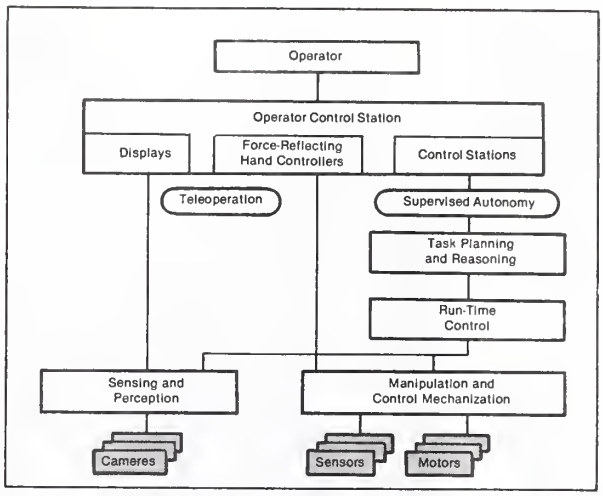

The **Telerobot Testbed** accommodates both human-controlled teleoperation and supervised robot autonomy with five subsystems.

The task-planning-and-reasoning subsystem does the high-level planning of tasks and gross motions. It provides menus and a kinematic-simulator capability, which can be used to preview the effects of an operator's command so that collisions can be avoided.

The run-time control subsystem plans fine motions and controls the execution of autonomous operations by the telerobot. It maintains a current data base on the kinematic, dynamic, and inertial properties of the manipulator arms and the objects in the workspace.

The sensing-and-perception subsystem contains the cameras and machine-vision software. It includes a tracker that supplies information about the positions and orientations of objects.

The manipulation-and-control-mechanization subsystem includes one robot arm for cameras and two robot arms for the manipulation of objects, all with six degrees of freedom. This subsystem also includes computers and sensors for force reflection and for autonomous and shared control.

In a contemplated demonstration of its capabilities, the testbed will be used to move a module and place it in a truss structure. First, the operator will remove the module from a platform between the robot arms and insert it into the truss by use of force-reflecting teleoperation. Next, the operator will repeat the task, using the operator-designate function to locate the truss and the place of insertion, the relative-update function to determine the distance between the end effector and a grapple lug on the module, and traded control to move the arm near the insertion slot and turn control over to the robot. Finally, the operator will repeat the task using shared control and a 2-second transmission delay.

This work was done by Jacob R. Matijevic of Caltech for **NASA's Jet Propulsion Laboratory**. *NPO-18061/TN*

FOR ADDITIONAL INFORMATION: *Contact: Director, Technology Transfer Division, P.O. Box 8757, BWI Airport, MD 21240; (301) 621-0100 Ext. 241*
REFER TO THE NUMBER LISTED AT THE END OF THIS ARTICLE

NASA Tech Brief
National Aeronautics and Space Administration
Marshall Space Flight Center, Alabama

Licensing Opportunity

Trailing Shield for Welding on Pipes

Weld beads remain covered with inert gas until safely cooled.

A trailing shield ensures that a layer of inert gas covers the hot, newly formed bead between two tubes or pipes joined by plasma arc welding. The inert gas protects the weld bead from oxidation by the air until it is cooler and less vulnerable to oxidation. The trailing shield is intended especially for use on nickel-base alloy pipes, on which weld beads remain hot enough to oxidize after the primary inert-gas purge from the welding-torch cup has passed.

Unlike previous shields, the new shield does not require a silicone-cloth skirt to keep outside air from entering the gap between the edges of the shield and the workpiece. Instead, the internal contour of the shield creates a steady flow of inert gas to the bead so that no air can reach it. It provides better protection against oxidation than does a skirted shield.

The new shield is a segment of curved, open-walled aluminum pipe that trails the welding-torch cup (see figure). The segment is contoured to match the circumference of the pipes to be welded while maintaining a uniform 0.125-in. (3.2-mm) gap. The inert gas enters the shield through a sintered stainless-steel tube. The cross section of the shield is shaped to direct the gas to the workpiece in tight turbulent swirls. The gas leaves the shield through the gaps at the edges, excluding exterior air.

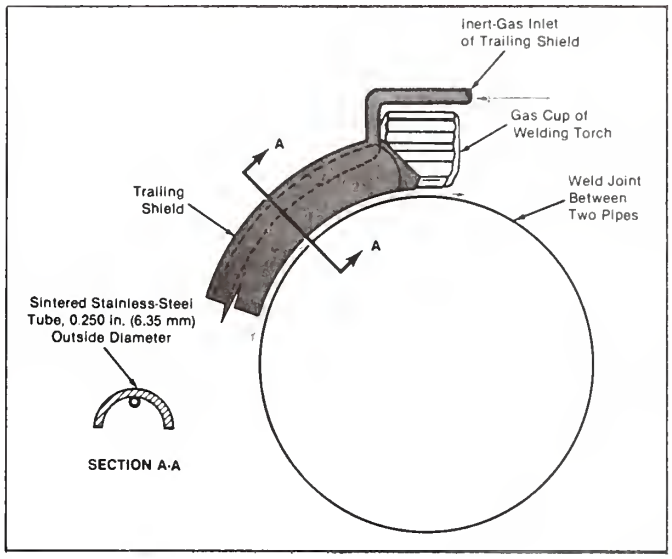

The Tubular Shield Partially Encircles a pair of pipes at a weld joint between them. Inert gas diffuses into the shield through a porous tube, covering the hot weld joint. The shield follows the welding torch as it advances.

This work was done by John B. Coby, Jr., and Kenneth J. Gangl of Rockwell International Corp. for **Marshall Space Flight Center.**

Inquiries concerning rights for the commercial use of this invention should be addressed to the Patent Counsel, Marshall Space Flight Center. Refer to MFS-29743/TN.

George C. Marshall Space Flight Center
Technology Utilization Officer: Ismail Akbay
Code AT01
Marshall Space Flight Center,
AL 35812
(205) 544-2223
Patent Counsel:
Leon D. Wofford, Jr.
Mail Code CC01
Marshall Space Flight Center,
AL 35812
(205) 544-0024

FOR ADDITIONAL INFORMATION: *Contact: Director, Technology Transfer Division, P.O. Box 8757, BWI Airport, MD 21240; (301) 621-0100 Ext. 241*
REFER TO THE NUMBER LISTED AT THE END OF THIS ARTICLE

NASA Tech Brief
National Aeronautics and Space Administration
Marshall Space Flight Center, Alabama

Licensing Opportunity

Dynamic Tester for Rotor Seals and Bearings

A simplified apparatus measures performance under vibration.

A testing apparatus measures some of the dynamic parameters of rotor seals and bearings. It tests damping seals, damping bearings, conventional seals (such as labyrinth seals), and conventional bearings (such as ball bearings). It can be used with a variety of pumped liquids, from water to liquid oxygen or hydrogen.

Designed primarily to test the bearings and seals of turbopumps, the tester rotates the shaft at high speed while liquid flows much as it would in a real turbopump. Meanwhile, the tester subjects the bearings and seals to vibration. It measures pressures at various points to determine leakage and dynamic parameters that depend on pressure. It also measures the deflections of the components.

The version illustrated in the figure contains a set of four damping seals and two damping bearings to be tested. The liquid enters a hollow shaft under high pressure from both ends. The liquid flows out of the shaft along several paths, including through a reaction turbine, which generates a torque that drives the shaft without axial thrust. Small discharges of liquid at opposite ends of the shaft negate any residual axial load.

The four damping seals to be tested are formed by the liquid that flows between the shaft and a grooved bushing that surrounds the shaft. The liquid flows into the damping seals through radial holes in the shaft. A pair of rods tangent to the bushing (only one is shown in the figure) vibrates the seals at frequencies different from the rotational frequency. Strain gauges on the rods measure the forces applied by the vibrator and the torque on the test seals from fluid-rotation drag.

Pairs of orthogonal proximity probes on opposite ends of the shaft measure the deflections and vibrations of the shaft. Similar pairs of probes on opposite ends of the bushing measure the vibrations and deflections of the seal.

An array of pressure gauges at critical locations measures inlet and discharge pressures. The back pressure in cavity A controls the shaft speed. The back pressure in cavity B controls the pressure drop across the test seals.

Flowmeters measure the discharge of liquid from cavities A, B, and C, which are separated by labyrinth seals. The flow from chamber A is used to calculate the turbine torque. The flows from chambers B and C are used to determine the leakage through the damping seals and the damping bearings.

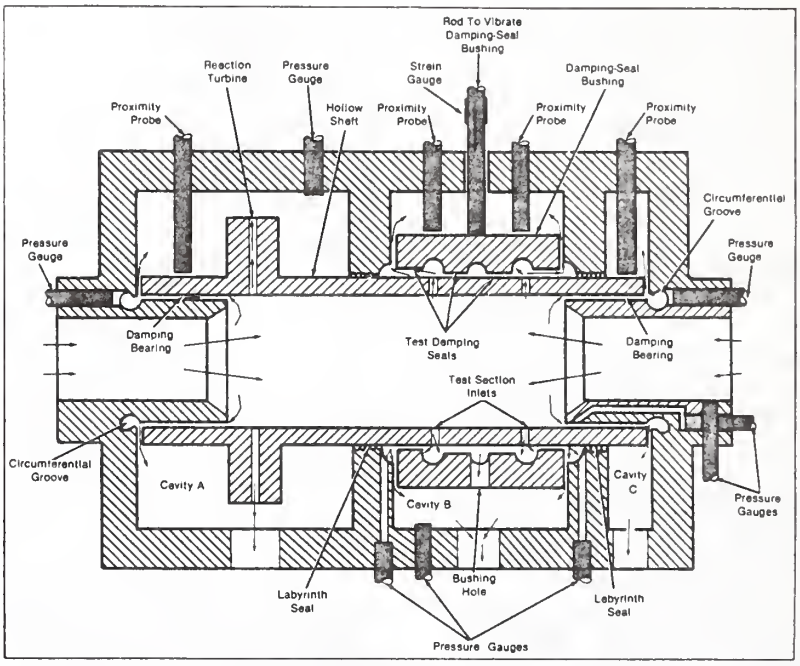

High-Pressure Liquid Flows by diverse routes through the tester. Flow through the reaction turbine drives the hollow shaft. Flow through the radial holes in the shaft to the inner surface of the bushing forms the damping bearings. Flows at the ends of the shaft balance residual axial thrust.

Because the tester contains no rolling-element bearings, it is highly reliable at high speeds. The shortness of its shaft eliminates resonances in the testing-speed range. It is simpler than previous testers were: it uses only one liquid; it has no gears, drive motors, or quill shafts; a single back-pressure valve controls shaft speed. Instrumentation is inserted from outside for ease of access and maintenance; electrical connectors are outside the housing, away from the test liquid. Because it produces no axial thrust, rubbing is eliminated and special hydrostatic thrust bearings are unnecessary.

The bearings can be machined off-center in the bushing to determine the effects of eccentricity. Because four bearings are mounted, their eccentricities can be arranged symmetrically with respect to the midsection of the bushing; this eliminates excessive loads on the damping bearings.

This work was done by George L. von Pragenau of **Marshall Space Flight Center.**

Inquiries concerning rights for the commercial use of this invention should be addressed to the Patent Counsel, Marshall Space Flight Center. Refer to MFS-28493/TN.

George C. Marshall Space Flight Center
Technology Utilization Officer: Ismail Akbay
Code AT01
Marshall Space Flight Center,
AL 35812
(205) 544-2223
Patent Counsel:
Leon D. Wofford, Jr.
Mail Code CC01
Marshall Space Flight Center,
AL 35812
(205) 544-0024

NASA Tech Brief
National Aeronautics and Space Administration
Marshall Space Flight Center, Alabama

Licensing Opportunity

Monitoring Bearing Vibrations for Signs of Damage

Real-time spectral analysis is performed to detect telltale changes in vibrations.

Real-time spectral analysis of vibrations is being developed for use in monitoring the conditions of critical bearings in rotating machinery. The underlying concept is simple and fairly well established: the appearance and growth of vibrations at frequencies associated with the rotations of various parts of a bearing system indicate wear, damage, and imperfections of manufacture. These frequencies include the fundamental and harmonics of the frequency of rotation of the ball cage, the frequency of passage of the balls, and the frequency of rotation of the shaft.

Vibrations that originate in a ball-bearing assembly can be sensed by strain gauges mounted on the outer race. Heretofore, the outputs of strain gauges have been recorded and analyzed after testing the machinery. In the developmental technique, the output of a strain gauge is processed by commercially available spectrum-analyzing equipment to obtain a power spectral density plot of the vibrations in real time (see figure).

A change in the plot — typically, an increase in amplitude at a particular frequency — indicates a particular type of damage. Once this concept is developed into a reliable technique for the detection of incipient failures, it may become permissible to disassemble the machinery less frequently for inspection and/or replacement of bearings.

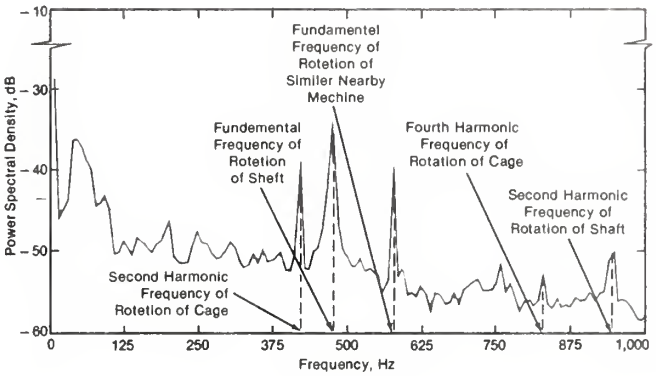

This **Instantaneous Power Spectral Density** was computed from the output of a vibration-sensing strain gauge in a high-pressure oxygen turbopump of the type used in the Space Shuttle. The spectrum includes vibrations synchronous with the rotation of a similar nearby machine—a high-pressure fuel turbopump.

This work was done by Carol L. Martinez of Rockwell International Corp. for **Marshall Space Flight Center.**

Inquiries concerning rights for the commercial use of this invention should be addressed to the Patent Counsel, Marshall Space Flight Center. Refer to MFS-29734/TN.

George C. Marshall Space Flight Center
Technology Utilization Officer Ismail Akbay
Code AT01
Marshall Space Flight Center,
AL 35812
(205) 544-2223
Patent Counsel Leon D. Wofford, Jr.
Mail Code CC01
Marshall Space Flight Center,
AL 35812
(205) 544-0024

FOR ADDITIONAL INFORMATION: *Contact: Director, Technology Transfer Division, P.O. Box 8757, BWI Airport, MD 21240; (301) 621-0100 Ext. 241*
REFER TO THE NUMBER LISTED AT THE END OF THIS ARTICLE

Materials

0389 Powders Hold Promise for Capturing Market Share—Modified high pressure gas atomization.

0390 New Polymer Technology

0391 Imide/Arylene Ether Copolymers—Films cast from solution are tough and flexible, and exhibit useful thermal and mechanical properties. (Licensing Opportunity)

0392 Deposition of Diamondlike Films by ECR Microwave Plasma—Negative dc self-bias induced by radio-frequency bias appears to be essential. (Licensing Opportunity)

0393 Making Thin Laminae of Frozen Alloy Slurries—These laminae, interspersed with fiber mats, can be used to make metal/fiber composites. (Licensing Opportunity)

Other Items of Interest

0380 New Gold Electroplating Process for Microelectronics Safer

Powders Hold Promise for Capturing Market Share

Modified high pressure gas atomization.

Ames Laboratory metallurgists have invented a more efficient, cost-efficient and safer way to produce powders of neodymium-iron-boron alloys, meriting a 1991 R&D 100 Award. The powders are used to make super-powerful Nd-Fe-B permanent magnets that command a high volume consumer market forecast to reach $2.7 billion by the year 2000.

The market is being driven by the need for smaller and more powerful magnet components in motors and generators, acoustical devices, computer and communications equipment and everyday items. Although Nd-Fe-B magnets are 10 to 40 times stronger than competing ferrite magnets, technological barriers in powder processing have prevented U.S. magnet producers from capturing more of the Nd-Fe-B market, which has been largely dominated by foreign manufacturers. Current powder-making methods must contend with explosion hazards, contamination, microstructural inhomogeneities and long processing times, all of which lower cost effectiveness.

The Ames-developed process is based on high pressure gas atomization, using a unique supersonic nozzle to blast a falling stream of molten metal with very cold argon gas traveling up to three times the speed of sound. Extremely fine, homogeneous, spherical droplets are formed and cool rapidly as they fall to a collection point. They are frozen in a microstructure of nanometer scale, which imparts optimum isotropic magnetic properties to the material. Thus, in one step, powder is directly produced from alloy, an improvement over existing methods that require separate melting and chopping/grinding steps to produce powder.

Another key feature of the process is a protective coating step that makes the magnetic material less explosive, less subject to contamination and 40 times more resistant to environmental attack and corrosion than other powders.

Ames-produced powders are especially well-suited to fill the market niche for polymer-bonded magnets; the small, spherical particle size allows more "packing" into a polymer, resulting in a stronger magnet. Two principal applications are in DC servo motors and stepper motors. Stepper motors, used in computer disk drives and automobile fuel pumps, are presently made by gluing magnet pieces together. But the reduced viscosity of the Ames powder-binder mixture would allow manufacturers to use injection molding techniques to form single-piece magnets.

The basic research work for this technology was funded under the Department of Energy; the applied research was funded by the Department of Commerce through Iowa State University's Center for Advanced Technology Development, which also provided business development direction. The technology for making these powders has been patented and is licensed to Ames Specialty Metals, a small company in Ames, Iowa that specializes in goods and services for the magnet industry.

The inventors also received a 1991 Federal Laboratories Consortium Special Award for Excellence in Technology Transfer.

Literature: "Boost in atomizer pressure shaves powder-particle size," *Advanced Materials and Processes,* July 1991, p. 30.

Patent/License Status: Application filed.

Potential Applications/Spinoffs: Hot isotatic pressing or metal injection molding.

FOR ADDITIONAL INFORMATION: For more information on this technology, contact Daniel E. Williams, Office of Research and Technology Application, Ames Laboratory, 199 Office and Laboratory, Iowa State University, Ames, Iowa 50011; (515)294-2635.

U.S. Navy Fact Sheet

Naval Weapons Center

New Polymer Technology

Naval Weapons Center chemists are working on the synthesis of a robust, polyconjugated, electrically conducting polymer that would be transparent in the visible region of the EM spectrum. This new polymer would have many applications, including coatings for sensor protection and anti-static materials.

For over a decade, conducting polymers (synthetic metals) such as polyacetylene and poly para phenylene vinylene (PPV) have been studied in great detail. Interest has recently developed in their optical properties, which include nonlinear optical properties and transparency of the conducting polymer in the visible portion of the EM spectrum. These polymers have applications in windows for visible sensors that reflect RF radiation, coatings for vidicon windows to bleed off static electricity, components of carpet fibers to prevent electrostatic buildup, and transparent electrodes for liquid crystal displays.

Coated substrates are being tested for transparency in the visible region and for opacity to RF and IR radiation. NWC's approach is to build upon the successful arylene vinylene polymer chemistry in conducting polymers and second-order nonlinear optical polymers. A particularly interesting area of research involves shifting the absorption bands of the oxidized polymer (conducting) out of the visible region by shifting the absorption of the neutral polymer (insulating) into the IR.

Another recent development has been to attach flexible side groups to these polymers to make them soluble and processable by melt extrusion and film casting. Inorganie conducting polymers have also been synthesized. This technique may offer unique (transparent) polymeric materials. Other areas of investigation and research include monomer and precursor polymer synthesis, polymer analysis, film fabrication, and absorption and conductivity measurements.

Cooperative Research and Development Agreements (CRADAs) may be established for any aspect of the Center's visibly transparent, electrically conducting polymers project, including investigation and development of additional polymerization methods.

For details on CRADAs, contact Elaine A. Wunderlich, (619) 939-1579.

NASA Tech Brief
National Aeronautics and Space Administration
Langley Research Center, Hampton, Virginia

Licensing Opportunity

Imide/Arylene Ether Copolymers

Films cast from solution are tough and flexible, and exhibit useful thermal and mechanical properties.

New imide/arylene ether copolymers have been prepared by reacting anhydride-terminated poly(amic acids) with amine-terminated poly(arylene ethers) in polar aprotic solvents. Each resulting copolymer may have one glass-transition temperature or two, depending on the chemical structure and/or compatibility of the block units. Most of the copolymers form tough, solvent-resistant films with high tensile properties.

Polyimides are condensation polymers commonly synthesized by the reaction of aromatic dianhydrides with aromatic diamines. The intermediate poly(amic acids) are either thermally or chemically cyclodehydrated to form the polyimides. Wholly aromatic linear polyimides are known for their exceptional thermal, thermo-oxidative, and chemical resistance, but are generally difficult to process as structural adhesives or composite matrices. Several polyimides are commercially available as films, moldings, adhesives, and composite matrices.

Poly(arylene ethers) are condensation polymers commonly synthesized by nucleophilic displacement of activated aromatic halides in polar aprotic solvents by alkali metal phenates. Poly(arylene ethers) are known for their good mechanical properties, good thermo-oxidative stabilities, relative ease of processing, and solubility in common organic solvents. Several poly(arylene ethers) are commercially available and are used as films, moldings, adhesives, and composite matrices.

In an attempt to take advantage of the attractive features of both types of polymers, a series of block copolymers that contain polyimide and poly(arylene ether) segments were synthesized. A wide variety of imide and arylene ether repeat units can be used to yield copolymers with specific desired properties. Furthermore, the length of the blocks, for both the imide and the arylene ether, is easily controlled. By varying the length of the blocks, one can alter the properties of the copolymer to produce materials with the desired physical and mechanical properties.

The imide/arylene ether copolymers were synthesized from the reaction of anhydride-terminated poly(amic acids) and amine-terminated poly(arylene ethers). After curing, the resulting block copolymers had glass-transition temperatures from 165 °C to 270 °C. Some had two glass transitions, corresponding to the arylene ether segment and to the imide segment, indicating a phase separation in the films due to incompatibility of block segments of higher molecular weight. Solution-cast, unoriented films of the copolymers were tough and flexible with tensile strength, tensile moduli, and elongation at break up to 16,200 psi (112 MPa), 431,000 psi (2.97 GPa), and 23 percent, respectively, at 25 °C. Depending on the glass-transition temperatures of the arylene ether segments, some block copolymers maintained good mechanical properties at 177 °C.

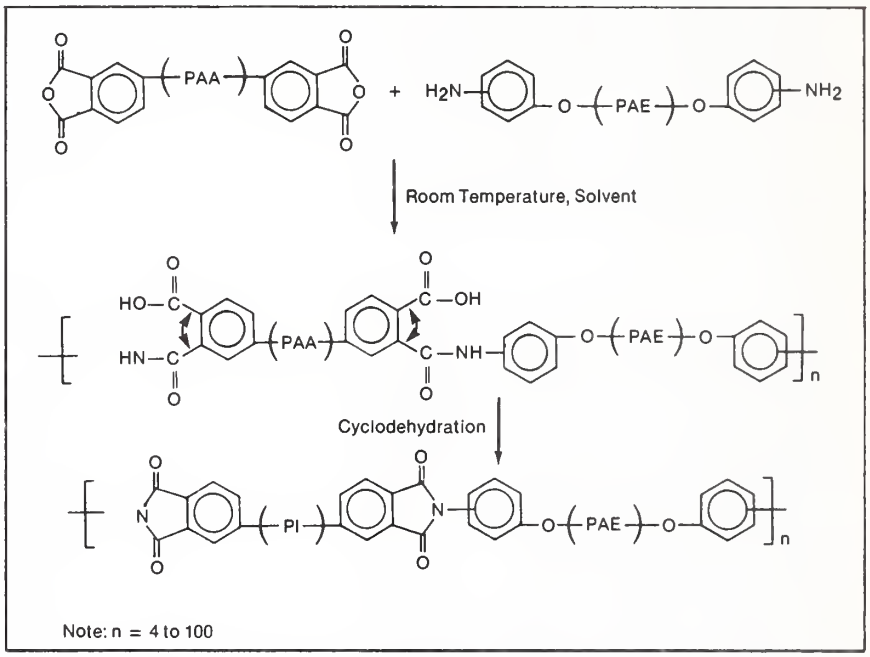

Imide/Arylene Ether Block Copolymers are synthesized by reacting anhydride-terminated poly(amic acids) with amine-terminated poly(arylene ethers) in polar aprotic solvents.

The general reaction sequence for the block copolymers is represented by the equation shown in the figure, wherein PAA represents a poly(amic acid) synthesized by reacting excess dianhydride with a diamine, and PAE represents a poly(arylene ether) synthesized by reacting an activated aromatic dihalide with a bisphenol. The solvent for copolymer preparation is preferably N,N-dimethylacetamide, but can be N-methylpyrrolidinone, *m*-cresol, N,N-dimethylformamide, dimethyl sulfoxide, or any of such ether solvents as diglyme. Cyclodehydration is accomplished chemically or by heating the intermediate poly(amic acid) at temperatures exceeding 150 °C.

Films were prepared from the new copolymers and found to have useful thermal and mechanical properties. The new materials are potentially useful as films, moldings, adhesives, or composite matrices. Because of the flexible arylene ether blocks, these copolymers are easier to process than polyimides are.

This work was done Brian J. Jensen and Paul M. Hergenrother of **Langley Research Center** *and Robert G. Bass of Virginia Commonwealth University.*

This invention is owned by NASA, and a patent application has been filed. Inquiries concerning nonexclusive or exclusive license for its commercial development should be addressed to the Patent Counsel, Langley Research Center. Refer to LAR-14159/TN.

Langley Research Ctr.
Technology Utilization
Officer John Samos
Mail Stop 139A
Hampton, VA 23665
Patent Counsel
George F. Helfrich
Mail Code 279
Hampton, VA 23665
(804) 864-3523

NASA Tech Brief
National Aeronautics and Space Administration
NASA's Jet Propulsion Laboratory, Pasadena, California

Licensing Opportunity

Deposition of Diamondlike Films by ECR Microwave Plasma

Negative dc self-bias induced by radio-frequency bias appears to be essential.

Hard, amorphous hydrogenated carbon (a-C:H) films of diamondlike quality have been deposited at room temperature on silicon, optical glass, and quartz through the decomposition of CH_4 in an electron-cyclotron-resonance (ECR) microwave plasma of CH_4 diluted with H_2. This technique could provide hard, abrasion-resistant coatings for lenses and other optical components. In addition, a-C:H diamondlike films are chemically inert and posses high electrical resistivity and breakdown fields, valuable properties in microelectronics applications.

The apparatus used in experiments on the deposition technique is shown schematically in Figure 1. The ECR plasma is generated by 2.45-GHz microwaves transmitted in a rectangular waveguide and coupled to the plasma chamber via a symmetric mode coupler and a quartz window. Electron resonance at 2.45 GHz occurs at a magnetic field of 875 gauss. Two coaxial coils mounted approximately 33 cm apart supply the confining magnetic field in a magnetic-mirror configuration.

Directly below and connected to the plasma chamber is the deposition chamber, within which the deposition substrate is mounted on a stage. The substrate stage is approximately 15 cm below the aperture leading to the plasma chamber and is electrically isolated from the system ground. The CH_4 enters through a circular gas ring in the deposition chamber. All depositions were made at a microwave power of 360 W on substrates that had been prepared by ultrasonic cleaning in acetone, isopropyl alcohol, then deionized water, for 5 min. each.

In the experiments, it was found that the application of no bias or of external negative dc bias to the substrate stage failed to produce hard a-C:H films under a wide range of deposition conditions: the films, deposited at rates of 2 to 3 Å/s, were mechanically soft and had optical energy-band gaps (E_g's) of approximately 2.8 eV. The films had broad fluorescence in the wavelength range of 450 to 650 nm that prevented the measurement of their Raman spectra. Apparently, because of charging of the substrates and films (since both are excellent insulators), external dc bias is not sufficient to obtain the incident ions at the kinetic energies of 10 to 50 eV that are necessary to produce hard, diamondlike films.

In contrast, hard films were produced when a 13.56-MHz radiofrequency bias was applied to the substrate stage, giving rise to a self-induced negative dc bias. Raman spectra indicate the deposition of films of two distinct types (see Figure 2): one exhibiting well defined bands at 1,360 and 1,580 cm^{-1} (the graphitic D and G

Figure 1. This **Electron-Cyclotron-Resonance (ECR) Microwave Plasma** system deposits a-C:H films on a variety of optical substrates.

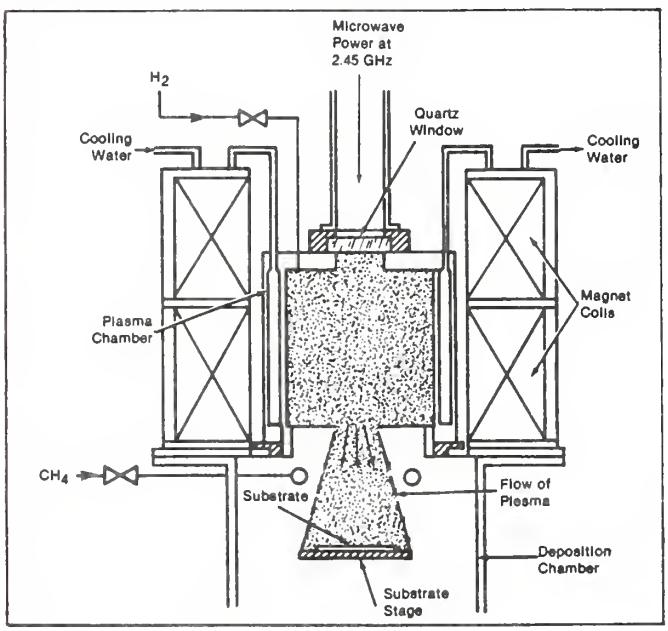

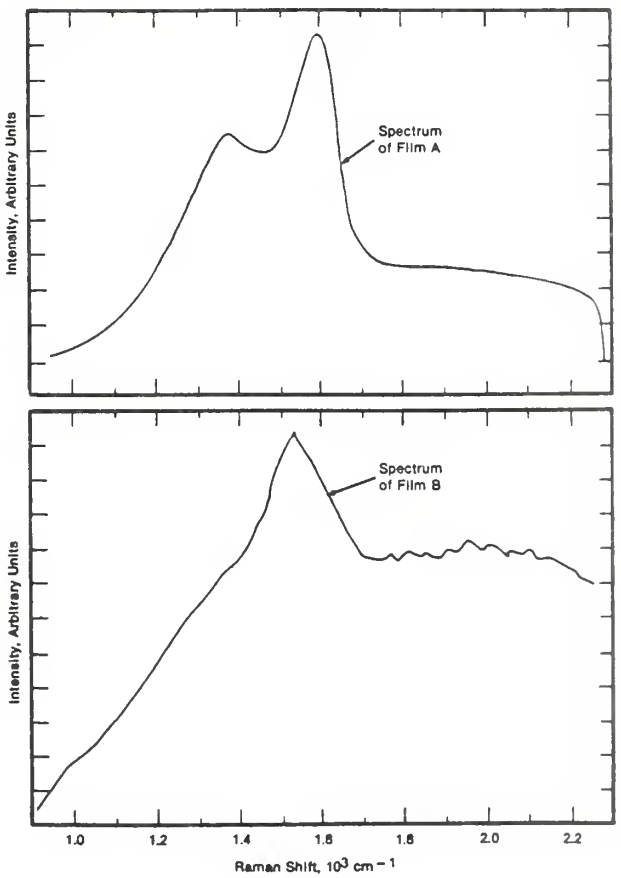

Figure 2. **Two Types of Raman Spectra** were exhibited by diamondlike films deposited with a radiofrequency-induced negative self-bias (V_{sb}) of the substrate stage. Film A was deposited with V_{sb} = -3 V at 30 W radio-frequency power. Film B was deposited at 5 W and V_{sb} = -100 V.

bands), another displaying a broad Raman peak centered at approximately 1,500 cm^{-1}. The E_g's of these films ranged from 1.0 to 1.6 eV, and their electrical resistivities were greater than 10^{12} Ω•cm.

A comparison of the Raman spectra and optical gaps indicates that there is more than one hard diamondlike film molecular structure for a given E_g. Moreover, the characteristics of a film depend on the profile of the magnetic field used during deposition: decreasing the mirror magnetic field was found to increase the E_g by increasing the kinetic energy of the ions extracted from the confinement region between the two coils. Decreasing the pressure in the chamber was found to increase E_g. This seems reasonable inasmuch as a decrease in pressure should result in an increased energy of incident ions because less energy would be lost in collisions. These latter results follow a trend opposite to that observed in radiofrequency-plasma depositions, in which increasing the self-bias (and, thereby, the energy of incident ions) reduces E_g.

This work was done by Frederick S. Pool and Yuh-Han Shing of Caltech for **NASA's Jet Propulsion Laboratory.**

Inquiries concerning rights for the commercial use of this invention should be addressed to the Patent Counsel, NASA Resident Office-JPL. Refer to NPO-18094/TN.

Jet Propulsion Lab.
NASA Resident Office
Technology Utilization Officer Gordon S. Chapman
Mail Stop 180-801
4800 Oak Grove Drive
Pasadena, CA 91109
(818) 354-4849
Patent Counsel Paul F. McCaul
Mail Code 180-801
4800 Oak Grove Drive
Pasadena, CA 91109
(818) 354-2734
Technology Utilization Mgr. for JPL Norman L. Chalfin
Mail Stop 156-211
4800 Oak Grove Drive
Pasadena, CA 91109
(818) 354-2240

FOR ADDITIONAL INFORMATION: *Contact: Director, Technology Transfer Division, P.O. Box 8757, BWI Airport, MD 21240; (301) 621-0100 Ext. 241*
REFER TO THE NUMBER LISTED AT THE END OF THIS ARTICLE

NASA Tech Brief
National Aeronautics and Space Administration
Langley Research Center, Hampton, Virginia

Licensing Opportunity

Making Thin Laminae of Frozen Alloy Slurries

These laminae, interspersed with fiber mats, can be used to make metal/fiber composites.

There is interest in consolidating metal-matrix/ceramic-fiber composite materials in thin layers. This would involve the lamination of very thin metal layers between layers of fibers, within each of which the fibers would be parallel. The first choice for the metal layers would be thin foils, but some of the brittle intermetallic alloys (e.g., titanium aluminides) that are of interest for this purpose are not now available as foils, while such techniques as plasma spraying and spraying or coating with polymer binders raise concern regarding contamination. A new technique that involves the use of sheets of frozen alloy powder overcomes the foregoing limitations.

In developing the new technique, the primary objective was to develop a method to distribute uniformly-thin powder-metal-alloy layers between alternate fiber layers prior to consolidation. In one demonstration, a blend of two fine (200-mesh) titanium aluminide (65Ti/24Al/11Nb and 51Ti/48Al/1V, where the numbers denote weight percentages) powders was used. A slurry was made by mixing small amounts of deionized water with the powder blend to obtain a mudlike slurry. The slurry was then transferred onto a stainless-steel sheet to which thin rails had been spotwelded (see Figure 1). The rails controlled the thickness of the powder as it was smoothed with a doctor blade. This operation was performed with the stainless-steel sheet resting on a sheet of glass. Next, the entire assembly consisting of the sheet of glass and the stainless-steel sheet covered with the slurry was placed in a freezer to freeze the water in the slurry.

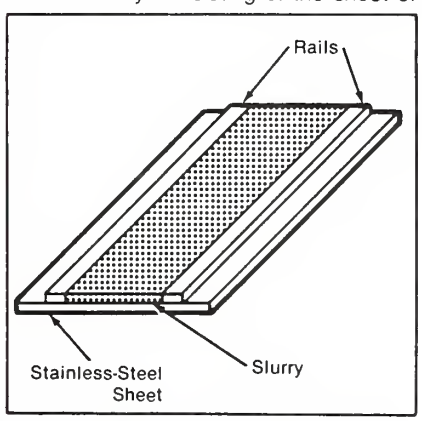

Figure 1. The **Slurry Was Spread Out** and leveled between the rails, then frozen. The sheet of frozen slurry was then removed from the stainless-steel sheet and used as one of the layers of a composite layup.

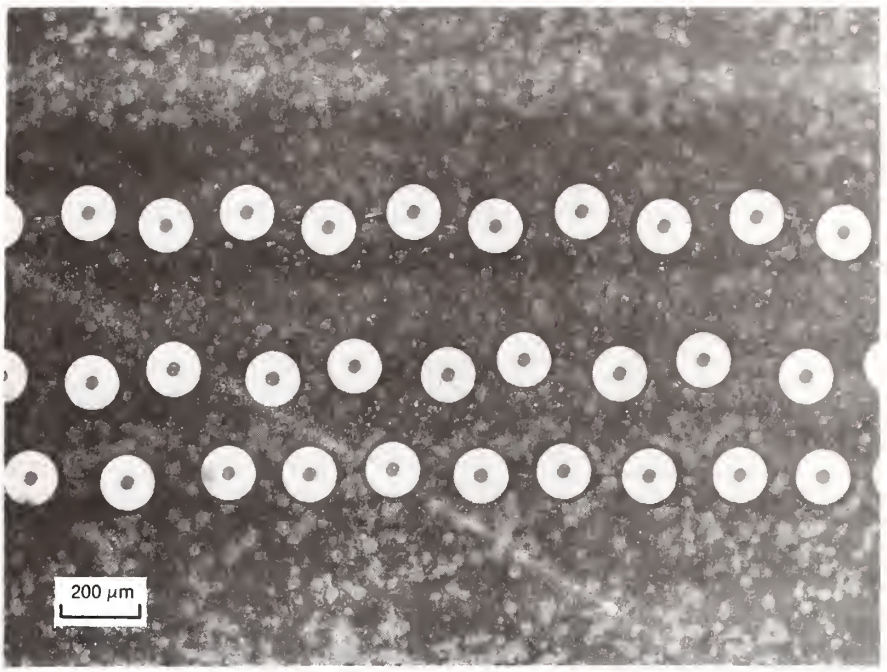

Figure 2. This is a **Magnified Cross Section** of the titanium-alloy/silicon carbide-fiber composite made by the technique described in the text.

When composite layup is required in production, assemblies like the one described above are to be removed from a freezer, and the stainless-steel sheets are to be flexed slightly to separate the frozen alloy-powder sheets from them. The frozen alloy-powder sheets can then be placed in an appropriate stack between reinforcing fibers. The stack is then to be vacuum-outgassed at a temperature of 400 to 500 °C to remove the water. Finally, the stack of alloy-powder and fiber layers is to be consolidated. In an alternative version of the process, one could embed a fiber mat inside the slurry prior to freezing to obtain sheets that could be consolidated directly into a composite.

In the demonstration, a composite of the blended titanium aluminide powders and silicon carbide fibers (see Figure 2) was prepared by the new technique and consolidated. Consolidation was performed in a constrained die in which some flow of the matrix was allowed only along (not across) the fibers. Such constrained deformation is believed to improve the quality of the alloy matrix by elimination of prior particle boundaries between the powder particles deformed in the process. In the microstructure of the resulting composite, the layers of alloy matrix between rows of fibers were found to be of uniform thickness and well bonded.

In addition to aerospace applications, this technique, appropriately modified, could have potential in the manufacture of future automobile engines or components that include molded ceramics.

This work was done by A.K. Ghosh, L.M. Holmes, R.B. Houston, and G.M. Ecer of Rockwell International Corp. for **Langley Research Center.**

Inquiries concerning rights for the commercial use of this invention should be addressed to the Patent Counsel, Langley Research Center. Refer to LAR-14111/TN.

Langley Research Ctr.
Technology Utilization Officer: Joseph J. Mathis, Jr.
Head, TU & AO Office
Mail Stop 200
10 West Taylor Road
Hampton, VA 23665-5225
(804) 864-2484

Patent Counsel:
Dr. George F. Helfrich
Mail Stop 143
9A Ames Road
Hampton, VA 23665-5225
(804) 864-3221

Medicine & Biology

0394 Electrostatic Discharge

0395 Boosting Immunity in the Elderly

0396 Patients Prefer Extraction

0397 3D-Mouse for Point-and-Direct Telerobotics

0398 Evaluation of DeVAR-IV with a Quadriplegic Employee

0399 An ATPase From Halobacterium Saccharovorum—The purification and subunit structure of a halobacterial enzyme are described.

0400 Deconditioning Under Prolonged, Repeated Bed Rest—Recovery takes longer than previously thought, and effects seem to be cumulative.

0401 Numerical Simulation of Flow Through an Artificial Heart—Research in both artificial hearts and fluid dynamics benefits from computational studies.

Testing & Instrumentation

0402 New Sensors with Biological Properties

0403 Non-Invasive Electromyography

Sandia National Laboratory

Electrostatic Discharge

A simulator that mimics the severe static electric discharge that can be triggered by a human body has been developed at Sandia National Laboratories.

The simulator, called the Severe Human Body Electrostatic Discharge Tester (SSET), was designed to test semiconductors, explosive devices and electronic systems, which can malfunction or be destroyed if subjected to such a shock.

Static electricity is an accumulation of charge on an insulated object. It can be produced when a person walks across a carpeted floor, gets out of a car or stands outdoors in the wind. When accumulated charge is suddenly transferred to another object or person, either through direct contact or a spark, it is called electrostatic discharge (ESD).

The ESD from a person or object is a potential threat to semiconductors,explosives and electronic systems. It can temporarily interfere with the operation of systems or components or cause permanent damage, possibly impairing their reliability and safe operation.

The effects of ESD can generate significant losses in terms of life, property and dollars. For example, in the electronics industry, losses associated with ESD are estimated at between a half billion and five billion dollars annually. The unintentional detonation of explosives (fireworks, industrial explosives) can cause significant loss of life and property damage.

With the costs so high, Sandia researchers have devoted considerable attention to assessing the vulnerability of components and systems to the ESD threat. To do that, experimental tests are performed by applying a known, simulated discharge that mimics the actual event as closely as possible. When a high degree of reliability or safety is needed, a "severe" ESD simulation is used. The simulator developed at Sandia was designed to simulate a severe environment and can replicate a human body ESD up to 35 kV.

When human beings acquire charge, the potential difference between the body and the ground will normally rise to between 6 and 12 kilovolts (kV). However, under dry conditions (10 to 20 percent relative humidity), a person can develop and sustain voltages of about 35 kV or slightly greater. Normally, it is difficult to achieve and sustain voltages of greater that 25 kV due to the "corona" effect in which some of the accumulated charge spontaneously disperses, lowering the voltage.

Sandia researchers have also investigated factors influencing ESD effects such as maximum sustainable voltages, humidity, individual height, etc. They have assembled a database from scientific literature of documented measurements of human body electrical parameters (voltage, capacitance, resistance and inductance) that have been developed into an electrical model of the human body.

The model, developed by Sandian Dick Fisher, uses the extremes of the documented data to define a severe human body ESD model that is intended for use in qualification testing of systems with stringent safety and/or reliability requirements. The model exhibits the distinctive characteristics of an actual human body ESD waveform, having an extremely fast rise time to peak current (approximately one nanosecond), and an initial voltage of 25 kV. It also specifies that current be injected directly into a test object

without a spark, which replicates the most severe stress created by an ESD.

The model was used to develop the SSET. Although a wide variety of ESD simulators exist commercially, none could adequately address all the requirements identified in the severe human body model.

Although the SSET is intended primarily to simulate a severe human body ESD event, the flexibility of the design allows for other ESD sources to be simulated by modifying the pulse-forming network. To date, the SSET has been used to test and evaluate a variety of components, including diodes, explosives, electro-explosive devices, electrical filters and transient suppressors to the severe human body requirement.

Sandia researchers are currently using the SSET and other types of pulse sources to investigate the effects of human body and other forms of ESD on electronics and explosives.

For more information, contact John Barnum, (505) 844-4367.

Research Technology
Agricultural Research Service
U.S. Department of Agriculture

Boosting Immunity in the Elderly

In study after study spanning decades, laboratory animals have maintained strong immune systems and lived substantially longer when raised on far fewer calories than they would normally eat. But why this works has been a mystery.

Now a clue as to how lifelong calorie restriction improves immune function in aging mice could point the way to improving older people's ability to fight infection and nip would-be cancers in the bud.

Researchers at ARS' Human Nutrition Research Center on Aging at Tufts found that mice who were raised on about 80 percent of their normal calorie intake synthesized significantly less prostaglandin E2 (PGE2). This hormone-like substance is known to suppress immune function, explains nutritional immunologist Simin Nikbin Meydani. So reducing the hormone helps to boost immune function.

Restricting food intake for extended periods is not practical for lean people. But Meydani says, "It is possible to reduce PGE2 levels through other dietary modifications, such as increasing vitamin E intake."

In fact, Meydani reported success in improving immune function in senior citizens with vitamin E supplements last year before she knew the results of the mouse study. (See *Agricultural Research*, Feb. 1989, pp. 12-13.)

She expects that a reduction in PGE2 is only part of the answer, but it's a beginning. Now, she says, researchers can design studies to see how individual nutrients known to alter PGE2 synthesis affect the immune system in elderly people.

The eyes of older people could also benefit from follow-up studies. Colleague Allen Taylor, who heads the Nutrition and Vision Research Laboratory at the center, found that calorie restriction significantly delayed cataracts in the test mice—which are from a strain that develops cataracts much as older people do. He says this is the first study that demonstrates the delay of senile-type cataracts in a living animal.

Simin N. Meydani and Allen Taylor are at the USDA-ARS Human Nutrition Research Center on Aging at Tufts, 711 Washington Street, Boston, MA 02111. Phone (617) 556-3129 and 556-3155. ◆

NAVY
Domestic Technology Transfer Fact Sheet

Patients Prefer Extraction

The Naval Dental Research Institute (NDRI), Great Lakes, Illinois, conducted a study to determine the personal preference of asymptomatic third molar removal in military patients. From 1 to 30 days after the extraction of one or more third molars, 100 returning patients were asked to respond to hypothetical questions concerning the extraction of asymptomatic third molars. The study showed that immediate removal was preferred. When respondents chose to delay treatment until there was a problem, no likelihood group would tolerate more than 2.77 additional days of post-extraction pain before changing their preference to immediate extraction. The results indicate general acceptance of the strategy of preventive third molar removal among a sample of military patients who have undergone pre-treatment counseling and the surgical procedure.

For Additional Information:

Backup material on this effort is available from:

Navy Domestic Technology Fact Sheet Reader Reply Service
Code E211
Naval Surface Weapons Center
Dahlgren, VA 22448-5000
(703) 663-8921

Refer to 161103/TN

3D-Mouse for Point-and-Direct Telerobotics

Problem Directing a telerobot to perform tasks involving unknown objects in an unstructured environment is difficult for any human operator. The problem is compounded for disabled individuals such as quadriplegics. Existing human-machine tools do not allow arbitrary objects and locations to be designated in real three-dimensional environments.

Significance A three-space pointing tool could give disabled individuals several capabilities, including the ability to quickly direct a telerobot to perform new or customized tasks in any environment. Without such an interface, operating a telerobot is either highly structured and unforgiving (autonomous robotics), or a tedious movement-by-movement endeavor on the part of the human operator (telemanipulation).

Background In 1986, the author programmed a PUMA 250 robotic arm to perform several routines for quadriplegics, including hair brushing, face washing, eating, drinking and tooth brushing. The research effort was successful and became a basis for an evaluation project testing quadriplegics using a desk top robot with similar prepackaged routines [1].

Apparent, however, was that disabled robot operators should eventually be able to interactively reprogram the robot to do new tasks without having to hire a robot engineer each time items were moved or new tasks required. Verbal telemanipulation did allow some interactive fine tuning. But any new routine had to be developed by experts.

An interface that allows the disabled individual to simply say to the robot "go there," or "that is the new mouth position" would enable customization for a wide variety of tasks. The robot, therefore, should be equipped with a pointing system to let the user designate any location in an unstructured environment to accomplish this objective.

Hypothesis The hypothesis of this demonstration research is that a class of Point-and-Direct telerobots can be implemented for operation in robotically unstructured environments by creating the equivalent of a computer mouse for the three-dimensional case.

Approach Preliminary testing of the new 3D-mouse concept involved observing six quadriplegics as they directed a surrogate mobile robot. While videotape recorders documented activities, the author manually panned and tilted a mobile video camera on a tripod in accordance with head motions made by the test subject.

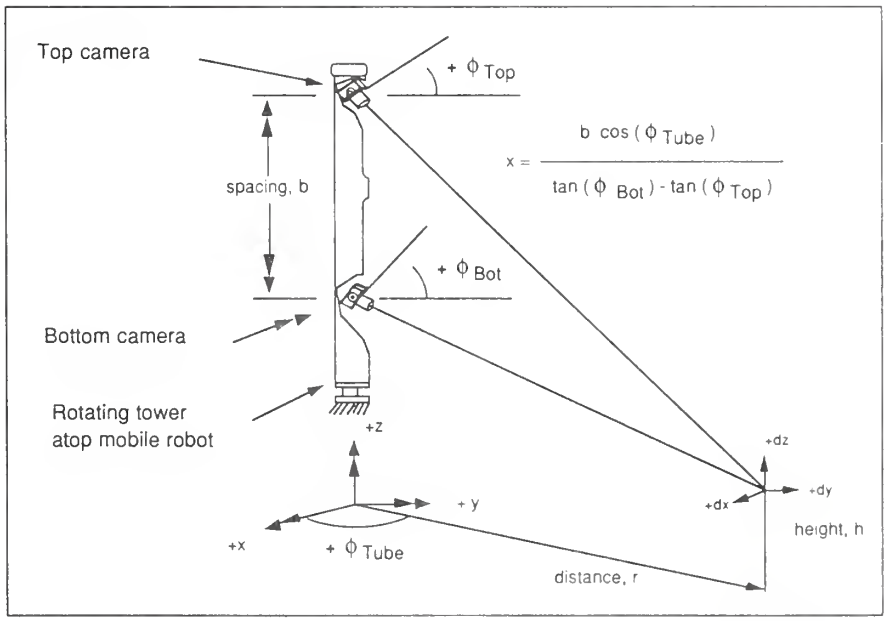

Figure 1. The 3-D Mouse is mounted on a mobile robot and can be used to designate points and objects in a workspace.

Subsequently, a 3D-mouse was built and mounted on a real mobile robot. The 3D-mouse system itself (see Figure 1) consists of two remotely controllable cameras spaced verti-

cally inside a tower. The miniature camera heads pan together but tilt separately. Triangulation is used to determine x, y, and z coordinates of the unique location at which both camera centers aim.

At a remote console, where a pair of video monitors display the live camera views, the operator controls where the cameras point and aligns crosshairs in the center of each monitor with an object or location that is in view. The operator, disabled in this case, uses chin-cup joysticks to operate the remote cameras (see Figure 2). A radio control unit similar to those used to fly model airplanes transmits signals to the camera motors on the robot.

Status A 3-D Mouse, developed for this research, consists of two miniature cameras that are remotely panned and tilted using PWM radio joystick control. The operator's workstation includes two monitors that show the camera views. When both cameras point to an object, and the operator says "that" or "there," the camera encoder angles are read and the proper arm and base destinations are calculated and entered into an evolving telerobot trajectory plan for subsequent execution.

The viability of the workspace-mouse system, as integrated on the mobile robot, was verified by several demonstrations. In one demonstration, miscellaneous items (a measuring tape, a spool of electrical wire, and electrical tape) were randomly placed in a work environment. Using the two-camera 3D-mouse system, an operator pointed to each and then to an open toolbox saying, "put that, that, and that there." The robot successfully moved itself as required to manipulate the objects, placing each into the tool box. A series of subsequent demonstrations also verified the concept.

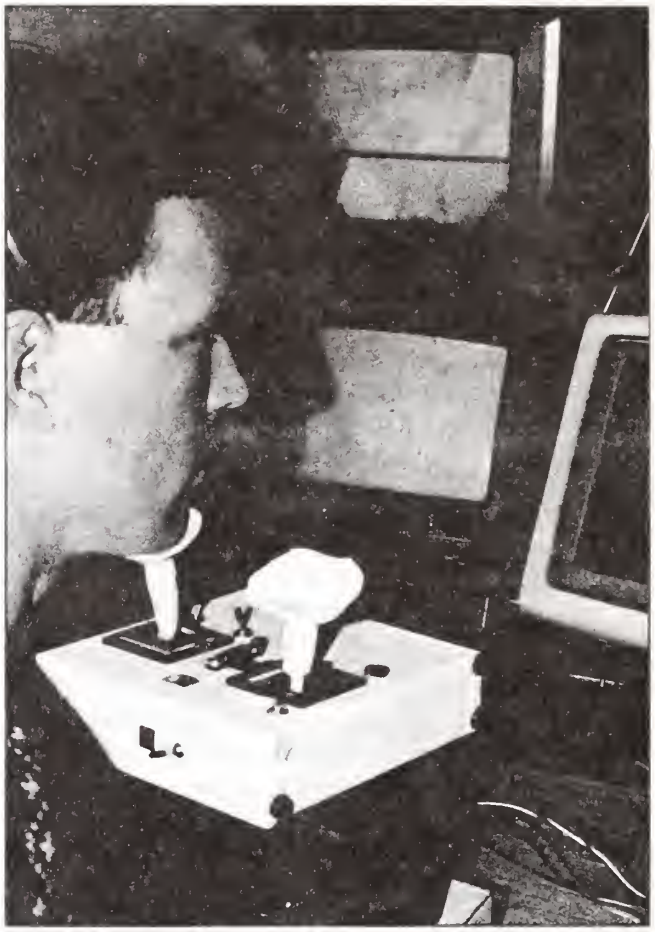

Figure 2. Operating a workspace-mouse: a triangulation algorithm locates an object when remote control camera crosshairs are aligned.

Reference

1. Lees D, Crigler B, Van der Loos HFM, Leifer LJ. Design of a second generation desk-top robotic aid. *Proc RESNA 10th Ann Conf*, San Jose, CA, 796-798, 1987.

Publications

Cannon DJ, Leifer LJ. Speed and accuracy for a telerobotic human/machine system: experiments with a target-threshold control theory model for Fits' law. *IEEE Intl Conf Systems, Man and Cybernetics*, 677-679, 1990.

Cannon DJ. A workspace mouse concept. *Proc RESNA 13th Ann Conf*, Washington, DC, 1990.

Support

RR&D Center core resources

FOR ADDITIONAL INFORMATION: Contact the author listed at (415) 493-5000, ext. 4480. Rehabilitation and Research Center, VA Medical Center/153, 3801 Miranda Avenue, Palo Alto, CA 94304.

Evaluation of DeVAR-IV with a Quadriplegic Employee

Problem Individuals with high-level quadriplegia are faced with a myriad of problems when returning to employment. One major barrier is the person's inability to perform required daily living and vocational tasks, thereby requiring the constant assistance of a full-time human attendant in the workplace. Unfortunately, qualified and reliable attendants are costly and difficult to locate and retain. The Palo Alto VA RR&D Center chose to address the need for attendant assistance by providing an alternative means for performing daily living support in the work environment through the development of the Desktop Vocational Assistance Robot (DeVAR). DeVAR was placed in the worksite of a high-level quadriplegic employee at Pacific Gas & Electric Company (PG&E) for evaluation purposes for one year (see Figure 1).

Significance This first installation of the DeVAR system outside the clinical laboratory setting is significant in being the first study of the quality and reliability of DeVAR over time with one user. Previous studies emphasized the measurement of subjective reactions to the technology by a number of individuals in a laboratory setting.

Background Studies done at the Palo Alto VA Spinal Cord Injury Center (SCIC) with early prototypes of the robotic workstation focused on performing daily living tasks. These studies demonstrated the feasibility of robotics technology in performing tasks, and revealed a high acceptance rate of disabled users toward this type of technology to replace human assistance. Based on feedback and requests from disabled individuals, corporate employers, and third-part reimbursement sources, DeVAR was designed to assist quadriplegics in returning to work by replacing the need for a human attendant for an extended period of time.

Hypothesis By replacing the attendant for a continuous period of time, DeVAR can offer the quadriplegic employee independence in performing daily living and vocational tasks and control over the worksite environment. In order to be considered for reimbursement by insurance companies, the attendant must be replaced for a minimum of four continuous hours, corresponding to one attendant workshift.

Approach To determine the design specifications of the DeVAR system before installing it into the workplace, an activity analysis of the typical week in the life of a disabled employee, referred to as RY, was performed by the occupational therapist. RY had sustained a C4,5 level quadiplegia from a fall in 1984. He returned to full-time work as a senior analyst programmer for PG&E in San Francisco; however, he was completely dependent upon a full-time attendant to perform all manipulation tasks. Due to his extensive needs and computer expertise, RY was found to

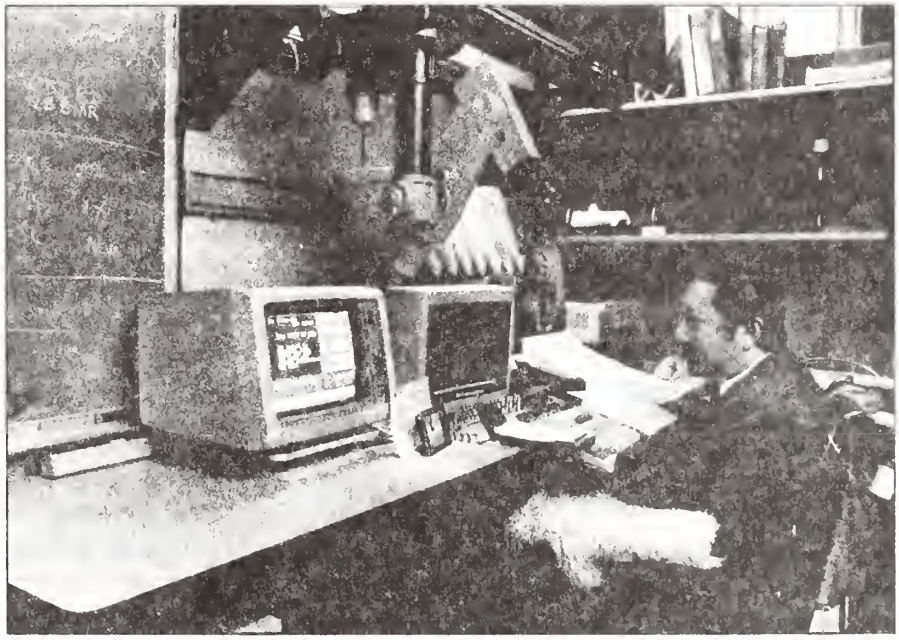

Figure 1. Disabled employee uses DeVAR to perform dailiy living and vocational tasks in the office setting.

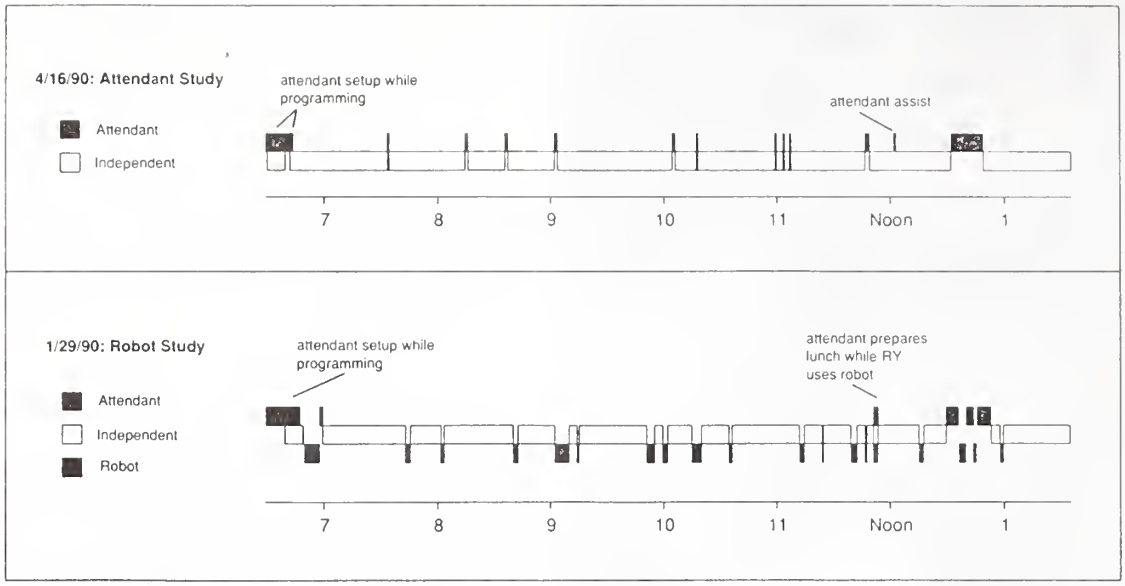

Figure 2. Typical daily task distribution, from 6:30 AM to 1:00 PM.

be an excellent candidate for the first extended placement of the DeVAR system. DeVAR was programmed to perform a combination of daily living (get a drink of water, give medications, scratch nose, serve lunch) and vocational tasks. The system was installed at PG&E in August, 1989 and has been used by RY on a daily basis since that time.

A single subject B-A (B=with robot assistance, A=with attendant assistance) study was designed to measure the functional independence level of RY and compare the use of a robotic assistant versus a human attendant in providing daily living and vocational assistance. The study was conducted in two parts. In the first half, RY was asked to use the robot for a period of six 10-hour days to perform the majority of his daily living and vocational tasks. The attendant was used only for set-ups performed at the beginning and end of the day and once after lunch, emergencies, and tasks outside the office. In the second half of the study, RY used only the attendant for a period of four 10-hour days.

Status This study showed that RY's attendant could be replaced for two 5-hour periods during the work day. It did not show that the attendant could be completely replaced, since human handling, set-ups, and emergency tasks are too difficult to automate with a robot. Figure 2 shows a typical morning of robot and attendant use, showing RY's independent working hours, the robot use, and attendant activities. A recommended scenario for providing this infrequent but necessary assistance is for corporate sponsors to hire an attendant who could serve one or more disabled employees when needed, but who would otherwise be employed by the company in a lower level job, such as mail delivery.

The DeVAR system will continue to stay at PG&E with RY for the first half of 1991 for data collection purposes. Negotiations are underway for permanent placement of a DeVAR system in this setting.

This first successful implementation of the DeVAR system in the worksite of a specific individual demonstrates the potential for robotic technology to replace attendant care in a vocational setting for an extended period of time and offer independence to the disabled employee.

Acknowledgements The authors would like to thank RY and Pacific Gas & Electric Company for their support and assistance.

Publications

Hammel J, Hall K, Lees DS, Van der Loos HFM, Leifer LJ, Perkash I. Clinical evaluation of a desk-top robotic assistant. *J Rehab Res & Develop*, 26: 1-16, 1989.

Van der Loos HFM, Hammel J, Lees DS, Chang D, Perkash I, Leifer LJ. A voice-controlled robot system as a quadriplegic programmer's assistant. *Proc RESNA 13th Ann Conf*, Washington, DC, 1990.

Van der Loos HFM, Hammel J. Designing rehabilitation robots as household and office equipment. *Proc First Intl Conf Rehabilitation Robotics*, Wilmington, DE, 1990.

Support

VA RR&D Merit Review (1985-present)
VA Spinal Cord Injury Center resources
RR&D Center core resources

FOR ADDITIONAL INFORMATION: Contact the author listed at (415) 493-5000, ext. 4480. Rehabilitation and Research Center, VA Medical Center/153, 3801 Miranda Avenue, Palo Alto, CA 94304.

NASA Tech Brief
National Aeronautics and
Space Administration

An ATPase From *Halobacterium Saccharovorum*

The purification and subunit structure of a halobacterial enzyme are described.

A report describes the purification and the determination of the subunit structure of a membrane-bound adenosinetriphosphatase (ATPase) from the archaebacterium *Halobacterium saccharovorum*. In analyzing the molecular structure, the authors took advantage of the observation that cold inactivates the enzyme and causes it to dissociate into subunits. The dissociation, which is irreversible, was shown to be the cause of the inactivation.

Membranes were prepared from *H. saccharovorum*. The enzyme was extracted from the membrane by use of detergent in two steps. The first step resulted in the extraction of about 54 percent of the membrane protein and left about 75 percent of the ATPase activity still associated with the membranes. In the second step, 7 percent of the remaining protein and essentially all of the remaining ATPase activity were extracted, although only 60 percent of that activity was recovered after gel filtration.

The enzyme was then solubilized by use of sodium deoxycholate and Zwittergent 3-10 and separated into fractions by hydrophobic and ammonium sulfate-mediated chromatography. After ammonium sulfate-mediated chromatography, a seventy-fold purification had been achieved, with retention of 13 percent of the initial ATPase activity. Gel-permeation chromatography and polyacrylamid-gel electrophoresis indicate that the native enzyme has a molecular mass of 350 kDa and includes two major (87 and 60 kDa) and two minor (29 and 20 kDa) subunits. It appears to be the unlike any ATPase described previously.

This work was done by L.I. Hochstein of **Ames Research Center** *and H. Kristjansson and W. Altekar of the National Research Council. "The Purification and Subunit Structure of a Membrane-Bound ATPase from the Archaebacterium* Halobacterium Saccharovorum."
ARC-11855/TN

FOR ADDITIONAL INFORMATION: *Contact: Director, Technology Transfer Division, P.O. Box 8757, BWI Airport, MD 21240; (301) 621-0100 Ext. 241*
REFER TO THE NUMBER LISTED AT THE END OF THIS ARTICLE

NASA Tech Brief
National Aeronautics and
Space Administration

Deconditioning Under Prolonged, Repeated Bed Rest

Recovery takes longer than previously thought, and effects seem to be cumulative.

Cardiovascular deconditioning from prolonged bed rest is not counteracted by mild exercise and requires at least 3 weeks for recovery, a report contends. Deconditioning involves more than a simple decrease in the volume of plasma; neurohumoral mechanisms, loss of mass of skeletal muscles, and a general decrease of the body's metabolic needs seem to be major contributors.

The conclusions are based on a study of seven subjects who rested in bed for three 2-week periods and spent 3 weeks in ambulatory recovery between rest periods. The subjects were males, aged 19 to 21, who were participants in a college physical-education program. The study was intended to examine the recovery process and its applicability to future Space Shuttle crewmembers, who may be asked to fly another mission after an interval of only 2 or 3 weeks.

The subjects exercised isometrically and aerobically every day during bed rest and recovery. Each man operated an ergometer at 68 percent of his maximum oxygen intake for 30 minutes, morning and afternoon, and did isometric leg exercises for another 30 minutes twice a day.

Subjects were exposed to suction on the lower parts of their bodies several times during the study while their heart rates and arterial blood pressures were measured. The data suggest that deconditioning effects may be cumulative. For example, the heart rate increased an average of 13.3, 35.1, and 51 percent for each of the three pre-bed-rest measurements under a suction of 40 mm of mercury (5.3 kPa).

The heart rate and the left ventricular end-diastolic volume index, both measured under suction, proved to be the parameters that exhibited the greatest changes. While the volumes of bodily fluids returned to their normal levels within 2 days after bed rest ended, both the heart rate and the left ventricular end-diastolic volume index had not returned to normal after 3 weeks. Apparently, the exercises performed by the subjects did little or nothing to prevent deconditioning.

This work was done by Harold Sandler, Richard L. Popp, and Donald C. Harrison of the Stanford University School of Medicine for **Ames Research Center.** *"The Hemodynamic Effects of Repeated Bed Rest Exposure."*
ARC-12172/TN

FOR ADDITIONAL INFORMATION: *Contact: Director, Technology Transfer Division, P.O. Box 8757, BWI Airport, MD 21240; (301) 621-0100 Ext. 241*
REFER TO THE NUMBER LISTED AT THE END OF THIS ARTICLE

NASA Tech Brief
National Aeronautics and Space Administration
Ames Research Center, Moffett Field, California

Numerical Simulation of Flow Through an Artificial Heart

Research in both artificial hearts and fluid dynamics benefits from computational studies.

An algorithm that implements the Navier–Stokes equations of flow has been extended to simulate the flow of viscous, incompressible blood through an artificial heart. The ability to compute the details of such flow is important for two reasons: (1) internal flows with moving boundaries are of academic interest in their own right, and (2) many of the deficiencies of artificial hearts are attributable to the dynamics of flow. For example, high turbulent stresses can damage red blood cells.

Although blood is viscoelastic, in the initial formulation of the algorithm it is approximated by a Newtonian fluid to simplify the calculations. Later, as a first step toward the full simulation of non-Newtonian behavior, viscosity can be allowed to vary in space and time, and non-Newtonian effects can be represented by a simplified constitutive mathematical model of viscous stresses.

The Navier–Stokes equations are cast in primitive-variable form, using pressure and velocity as dependant variables. The equations are transformed into generalized curvilinear coordinates. The coordinate grid is formulated to conform to the pump chamber and to the piston, and to contain a constant number of grid points as it expands and contracts with the motion of the piston. To avoid further complications in this initial formulation, the motion of the valves is neglected, and the motion of the piston is altered so that it does not cross the valve openings.

The transformed equations of flow are treated via an artificial-compressibility, flux-difference-split, upwind-differencing numerical-integration scheme for convective fluxes. The resulting system of equations is more-nearly diagonally dominant than it would be if a central-difference scheme were used. The system of equations is solved by use of an unfactored line-relaxation scheme, which proves to have good stability and convergence characteristics. Time accuracy is maintained by iteratively solving the equations at each physical time step.

Despite the simplifying assumptions, the results of an early numerical simulation show some of the complicated features of the flow, and agree at least qualitatively with the experiment (see figure). To simulate the operation of the artificial heart in all its complexity, it will be necessary to eliminate the simplifying assumptions and incorporate more-advanced grid techniques and multiple zones to accommodate the valves. Furthermore, because simulations of this type now require much computer time, computers of increased speed and more-efficient algorithms could contribute greatly to progress in this field.

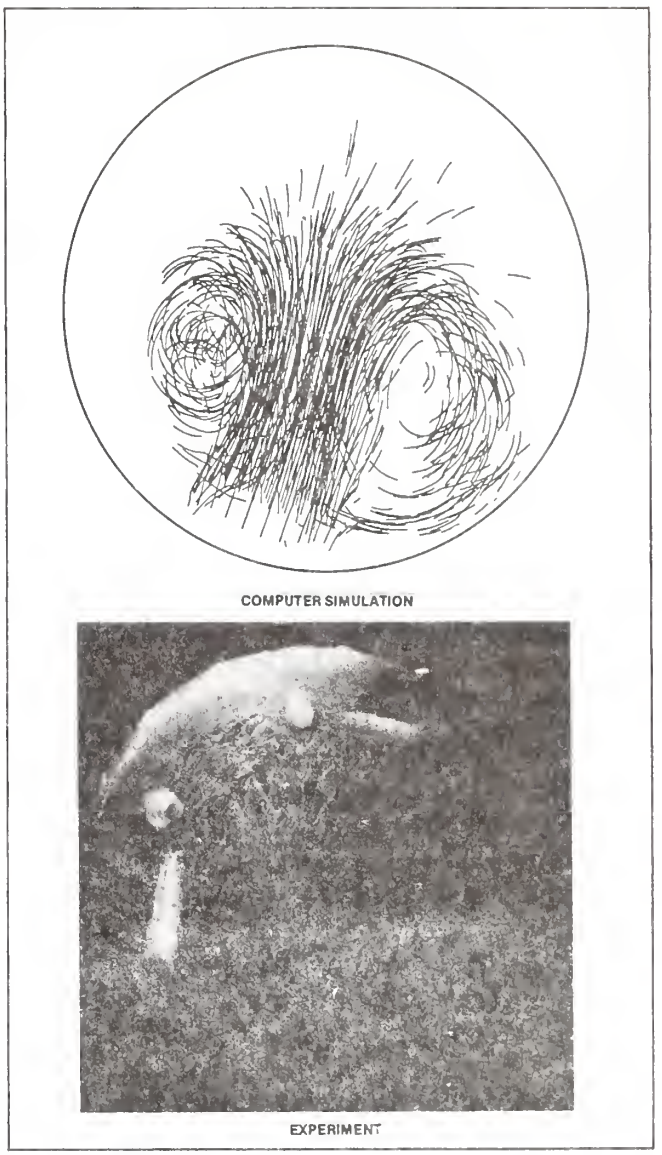

Two Distinct Vortexes form in the flow entering an artificial heart through its inflow valve as the piston nears its lowest position.

This work was done by Stuart Rogers, Paul Kutler, and Dochan Kwak of **Ames Research Center** *and Cetin Kiris of Stanford University. Further information may be found in NASA TM-102183 [N89-24111], "Numerical Simulation of Flow Through an Artificial Heart."*

Copies may be purchased [prepayment required] from the National Technical Information Service, Springfield, Virginia 22161, Telephone No. (703) 487-4650. Rush orders may be placed for an extra fee by calling (800) 336-4700.
ARC-12478/TN

Lawrence Berkeley Laboratory

New Sensors with Biological Properties

In a fusion of the fields of materials science, chemistry, and biotechnology, Lawrence Berkeley Laboratory scientists are creating sensors able to lock onto and detect targeted biological molecules and organisms.

The sensors have a broad range of potential applications. Doctors could know within moments precisely which bacterial or viral strain has infected a patient. Researchers could screen for new enzymes. And technicians could sample air and water for particular contaminants.

The best medical sensors currently available rely on cumbersome, time-consuming assay techniques to detect specific pathogens. When dealing with low concentrations of pathogens, they often are inaccurate. Conversely, the new sensors will detect low concentrations and provide immediate results. They will allow a doctor to make an on-the-spot diagnosis and a patient to receive the added benefit of more immediate medical care.

The new biologically sensitive films are possible due to recent advances in materials science. Researchers create the films with a micro-fabrication process called molecular self-assembly. The degree of molecular organization can extend beyond that achieved by etching with the photolithographic technologies used to create silicon semiconductors. The films are generated by manipulating the interactions between molecules, exploiting phenomena that range from van der Waals' interactions to entropy.

In an important advance, the team has fabricated an array of molecules that bind to different pathogens as well as to an assortment of biological receptors including complex carbohydrates and peptides.

Their invention relies on a film containing "ligands" on its surface. Ligands are molecular structures that compose one-half of a biological lock and key mechanism. They are shaped so that only agents with a complementing structure can bind to them. Through molecular self-assembly, films can be fabricated so that a virus, bacteria, antibody, or enzyme, each of which has a uniquely shaped binding site, will attach to a matching ligand structure.

FOR ADDITIONAL INFORMATION: Public Information Department, ATTN: Lynn Yarris, Lawrence Berkeley Laboratory, Berkeley, CA 94720; Telephone (415)486-5375.

Non-Invasive Electromyography

Problem Diagnostic electromyography (EMG) is an important tool in the evaluation of patients with known or suspected neuromuscular injuries or diseases. Most clinical applications of diagnostic EMG require that data be collected using intramuscular needle electrodes. The procedure is somewhat painful and is not well tolerated by all individuals.

Significance The purpose of this project is to develop accurate methods for recording and analyzing EMG activity using surface (skin) electrodes. The use of noninvasive electrodes will reduce the discomfort of the EMG examination, making diagnostic evaluation and serial EMG monitoring (*e.g.*, of response to therapy for neuromuscular disability) more feasible, particularly for those individuals with low pain tolerance and for children.

Background Surface EMG recordings have generally been considered unsuitable for electrodiagnosis, even of superficially situated muscles, because of the attenuation and distortion suffered by the myoelectric signals as they pass through the subcutaneous tissues and the skin. Recently, however, new types of surface electrodes have been developed that are capable of detecting the fundamental electrophysiological components of the EMG signal – the discharges of individual groups of muscle fibers known as motor-unit action potentials (MUAPs). These electrodes consist of arrays of very small (1-mm diameter), very closely spaced (2.5-5.0 mm) metal contacts, or closely spaced needles that penetrate only the outermost layer of the skin. The signals recorded by the various contacts can be combined in such a way as to accentuate the more superficial MUAPs while suppressing the deeper ones.

Hypothesis We predict that computer-based signal-processing techniques can be used to decompose surface-recorded EMGs into their component MUAP trains, and that these surface MUAPs will be shown to contain information relevant to neuromuscular diagnosis and evaluation.

Approach EMG signals will be recorded from the skin surface by an array of small contacts. Signals from adjacent contacts will be subtracted to accentuate the MUAPs. The signals will be decomposed into trains of individual MUAPs using a modified version of our ADEMG program (a program originally developed to analyze needle-recorded EMGs, see Report 34). The ability to record the MUAP waveform at many points on the skin surface simultaneously will allow estimation of properties that cannot be easily measured using needle electrodes, including the size and conduction velocity of the motor unit and the location and spatial extent of the motor endplates.

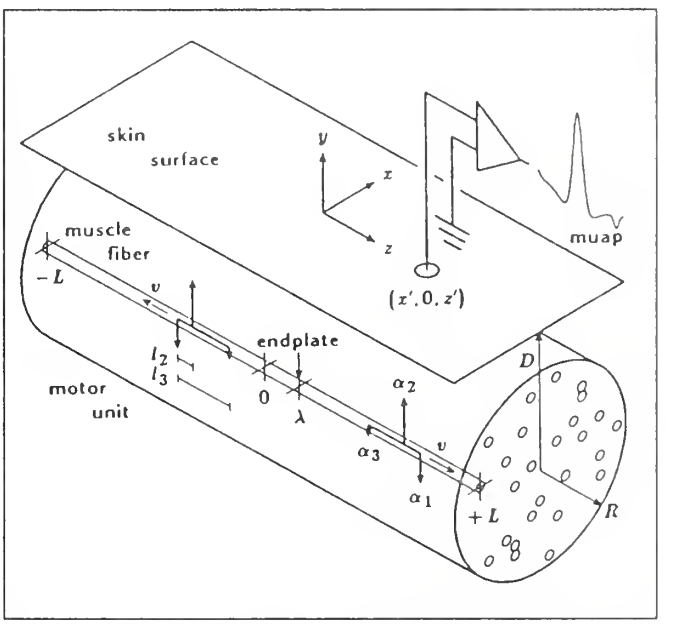

Figure 1. Diagram of the single muscle fiber and the motor unit.

Status We have developed a prototype hand-held surface EMG electrode whose features include detachable heads for either flat or needle-type contact arrays, a metal shield to ground the electromyographer and suppress noise, and an on-board buffer amplifier. With this electrode it is possible to record EMG signals from some superficial muscles, such

as abductor pollicis brevis, in which the individual MUAPs are clearly distinguishable and can be identified using the ADEMG method.

In order to investigate the influence of the size and shape of the surface electrode on the electrical properties of the recorded signal, we measured the electrical impedance of electrodes ranging in size from 0.02 to 0.125 inches in diameter and having cylindrical, hemispherical, and conical shapes. Each electrode was pressed against the skin over the abductor pollicis brevis or the brachial biceps with a constant force (50 g). The skin had been rubbed with an alcohol wipe. The impedance between the test electrode and a large ground electrode on the forearm was measured as a function of frequency from 10 to 1000 Hz.

We found impedance to decrease with frequency for all electrodes. As a function of size, impedance was less for the larger electrodes, because of increased contact area, and for the smaller electrodes, because of increased contact pressure. Conical electrodes had lower impedances than cylindrical and hemispherical ones at low frequencies, but roughly the same impedances at high frequencies. We conclude that small electrodes with tips sharp enough to indent but not pierce the skin have sufficiently low impedances to be practical for surface recording.

In conjunction with this experimental work, we have also developed a theoretical model of the surface-recorded MUAP in terms of the gross anatomical properties of the motor unit (Figure 1). The MUAP is modeled as arising from six current sources (two tripoles) which are diffused throughout a volume defined by the motor unit's cross section and the length of its endplate zone. To account for the MUAP's initiation and termination, the space and time domains are treated separately. The results of the model agree qualitatively with actual surface MUAPs, and quantitatively with results from a more complex model in which each muscle-fiber action potential is modeled individually. These results suggest that surface-recorded MUAPs can be used to estimate anatomical motor-unit properties such as size and depth.

Publications

McGill KC, Dorfman LJ, Howard JE, Valainis EV. Decomposition analysis of the surface electromyogram. *Proc 9th Ann Conf IEEE Eng Med Biol Soc*, Boston, MA, 2001-2003, 1987.

McGill KC, Huynh A. A model of the surface-recorded motor-unit action potential. *Proc 10th Ann Intl Conf IEEE Eng Med Biol Soc*, 1697-1699, 1988.

Support

VA RR&D Merit Review
RR&D Center core resources
Muscular Dystrophy Association

FOR ADDITIONAL INFORMATION: Contact the author listed at (415) 493-5000, ext. 4480. Rehabilitation and Research Center, VA Medical Center/153, 3801 Miranda Avenue, Palo Alto, CA 94304.

Physical Sciences

0404 Please Release Me—But Slowly

Software

0405 Calculating Thermophysical Properties of 12 Fluids—Properties are expressed via equations of state.

0406 Designing Catalytic Monoliths for Closed-Cycle CO2 Lasers—The LASCAT program enables a designer to determine quickly the consequences of changes in design.

Testing & Instrumentation

0407 Wavefront Dividing Infrared Interferometer

0408 Ionizable-Substance Detector—The detector nondisruptively monitors the concentration of an ionizable substance in a stream. (Licensing Opportunity)

Other Items of Interest

0346 Multiaperture Spectrometer—Advantages would be a convenient two-dimensional spectral image, fewer components, and greater efficiency.

0347 Spaceborne Microwave Imagers—Principles and practices are described.

Research Technology
Agricultural Research Service
U.S. Department of Agriculture

Please Release Me--But Slowly

There's a family of compounds called cyclodextrins that are adept at letting go.

The three compounds, differing in molecular ring size and made from cornstarch, serve as "hosts" or traps for other substances, which they slowly release.

The substances that have been encapsulated in this way include pharmaceuticals, pesticides, perfumes, cosmetics, and foods. Their gradual release can be triggered in several ways, including exposure to moisture.

Cyclodextrins are ideal for shielding drugs or nutrients from premature deterioration caused by oxygen and for masking undesirable flavors.

Until now, however, it hasn't been practical to encapsulate certain products. Although cornstarch is inexpensive, cyclodextrins have been costly to make and purify, says ARS chemist Jacob A. Rendleman, Jr., of the National Center for Agricultural Utilization Research, Peoria, Illinois.

Especially costly is gamma-cyclodextrin with a "donut hole" larger than those of alpha- and beta-cyclodextrins. Its cavity is easily capable of binding cyclic molecules that have 12 or more atoms in their rings.

Prices for gamma-cyclodextrin have been about 100-fold greater than those of beta-cyclodextrin over the past 10 years, but they are drifting downward with prospects of market competition, according to an industry spokesperson.

Rendleman's studies may lead to cheaper production and increased use of gamma-cyclodextrin. Until he recently found a way to convert up to 50 percent of starch into gamma-cyclodextrin, a typical yield was 5 percent unless processes were involved that require toxic or more expensive materials.

Currently, worldwide sales of beta-cyclodextrin are estimated at 2 million pounds, mostly for encapsulating food additives in Japan. But the fastest market growth - estimated at 20 to 30 percent annually - is in pharmaceuticals, where 3 to 5 percent of the specialty product is used.

BRUCE FRITZ

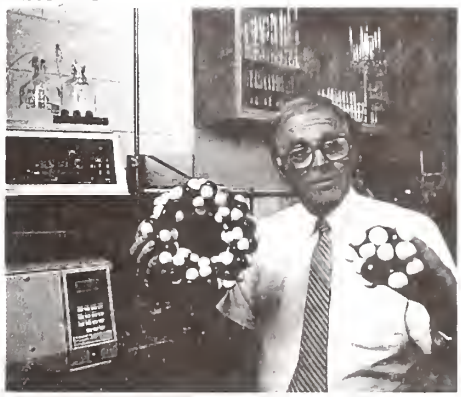

Chemist Jacob Rendleman uses molecular models to determine the best shape and size for a molecule to bind snugly within the cavity of the donut-shaped gamma-cyclodextrins. (K-4208-1)

Cyclodextrins are formed when an enzyme from the bacterium *Bacillus macerans* breaks up starch and reassembles it into the donut-shaped molecules. Biosynthesis begins to shut down with increasing concentration of product in the reaction medium.

Rendleman enhanced the yield of the gamma form by adding a nontoxic 12-carbon-ring compound called cyclododecanone to the reaction medium where it captured and insolubilized the cyclodextrin as it was formed.

Then, in a process called azeotropic distillation, he separated cyclodextrin from the cyclododecanone - which could then be reused.

FOR ADDITIONAL INFORMATION: Jacob A. Rendleman, Jr., is at the USDA-ARS National Center for Agricultural Utilization Research, 1815 N. University St. Peoria, IL 61604. Phone (309) 685-4011.

Calculating Thermophysical Properties of 12 Fluids

Properties are expressed via equations of state.

MIPROPS is a set of computer programs that gives the thermophysical and transport properties of selected fluids. Although these programs are written in FORTRAN 77 for implementation on microcomputers, they are direct translations of interactive FORTRAN IV programs that were originally developed for large mainframe computers. MIPROPS calculates the properties of fluids in both the liquid and vapor states over a wide range of temperatures and pressures. The fluids included are helium, hydrogen, nitrogen, oxygen, argon, nitrogen trifluoride, methane, ethylene, ethane, propane, isobutane, and normal butane.

All of the programs except the helium program incorporate the same equation of state. A separate program was necessary for helium, as the mathematical model for the thermodynamic surface of helium is of a different form. The input variables are any two of pressure, density, or temperature for the single-phase regions, and either pressure or temperature for the saturated-liquid or saturated-vapor states. The output is pressure, density, temperature, internal energy, enthalpy, entropy, specific heat capacities, and speed of sound. In addition, viscosity, thermal conductivity, and dielectric constants are calculated for most of the fluids. The user can select either a single point or a table of output values for a specified temperature range, and can display the data in either engineering or metric units.

This machine-independent FORTRAN 77 program was implemented on an IBM PC XT computer with an MS-DOS 3.21 operating system. It has a memory requirement of approximately 100K bytes. The program was developed in 1986.

This program was written by T.F. Cleghorn and R.D. McCarty of **Johnson Space Center.** *MSC-21664/TN*

FOR ADDITIONAL INFORMATION

CONTACT

COSMIC®
112 Barrow Hall
University of Georgia
Athens, GA 30602

(404) 542-3265

Designing Catalytic Monoliths for Closed-Cycle CO_2 Lasers

The LASCAT program enables a designer to determine quickly the consequences of changes in design.

Pulsed carbon dioxide lasers are useful in many areas, including aeronautics, research in outer space, and monitoring weather. Most applications require closed-cycle carbon dioxide lasers, which are more portable and self-sustaining than are open-cycle lasers. Without a fresh supply of carbon dioxide and provisions for disposal of byproducts, a closed-cycle laser must recycle the carbon monoxide and oxygen gas produced by the lasing of carbon dioxide. The recombination of the carbon monoxide and oxygen to form a constant supply of carbon dioxide requires an active catalyst, which must be carefully designed to optimize the performance of the laser in accordance with design requirements specific to the application. The LASCAT (Design of Catalytic Monoliths for Closed-Cycle Carbon Dioxide Lasers) computer program aids in the design of a catalyst in a monolith by simulating the effects of design decisions on the performance of the laser.

In a portable laser system, considerations of size, weight, and cost are critical. LASCAT provides the opportunity for the designer to explore tradeoffs among the activity and dimensions of the catalyst, the dimensions of the monolith, the pressure drop caused by the flow of gas through the monolith, the conversion of oxygen, and other variables. The program uses a flexible, simplified model of the catalyst in the monolith to determine the bulk-average gas temperature, composition, and pressure of the gas along its length. The user specifies values for the several parameters that define the operating conditions of the catalyst, including the dimensions of the monolith, the gas at the inlet, thermal properties in operation, and properties of the catalyst. LASCAT provides results that indicate whether the experimental design meets such constraints defined by the user as limits on the rate of conversion, maximum temperature of the gas, and the weight of the monolith.

LASCAT is written in FORTRAN 77 and is designed for use with any text or character-based terminal or computer display. The program requires roughly 40 KB of memory. LASCAT was developed in 1989. LASCAT is restricted to use by U. S. citizens only.

This program was written by Keith Guinn, Richard K. Herz, Seth Goldblum, and Ed Noskowski of University of California, San Diego, for **Langley Research Center.** *LAR-14190/TN*

FOR ADDITIONAL INFORMATION

CONTACT

COSMIC®
112 Barrow Hall
University of Georgia
Athens, GA 30602

(404) 542-3265

Brookhaven National Laboratory

Wavefront Dividing Infrared Interferometer

Researchers at Brookhaven National Laboratory have developed a novel instrument that opens up a new class of experiments with synchrotron radiation. Known as a wavefront dividing infrared interferometer, the instrument is installed at Brookhaven's National Synchrotron Light Source (NSLS), the world's largest synchrotron radiation center. An interferometer splits light from a source into two beams, one of which then passes through a sample. When the beams are recombined, an interference pattern results, thereby giving information about the sample.

At the NSLS, the BNL interferometer is coupled to the new infrared beam line, which is the brightest broadband infrared source available today. As a point of reference, the infrared beam line produces radiation that is over 300 times hotter than the surface of the sun. This extreme intensity enables the interferometer to perform efficiently in the spectral region from the mid-infrared to millimeter wavelengths. In the past, this particular region has been difficult to work in because it is an area of low photon energy and, hence, weak signals. The BNL interferometer has a signal-to-noise ratio as much as 1,000 times better than that of conventional instruments. As such, it can measure highly absorbing samples such as high-temperature superconductors, newly discovered materials that have promising applications in such areas as electronics and transportation.

The interferometer can also detect small signals from dilute systems, such as molecules on metal surfaces, which makes possible catalysis and corrosion studies at the molecular level. Further, the spectral region covered by the instrument is of great interest to the chemical, oil, and gas industries, particularly for research on environmental control and monitoring.

When measuring a sample, the BNL interferometer covers in a single scan a wavelength region from 10 micrometers to 1 centimeter. Even though it functions over such a broad wavelength range, the instrument can operate with no change in components, a significant advantage over conventional instruments. In addition, it can completely characterize the optical activity of solids, liquids, and gases. A future refinement of the instrument will enable it to scan samples rapidly, thereby eliminating low-frequency noise.

The instrument was developed by Gwyn Williams, Peter Siddons, and Carol Hirschmugl, all of BNL, along with K. Dieter Möller, a collaborator from Fairleigh Dickinson University in New Jersey.

Literature: G. P. Williams, The Initial Scientific Program at the NSLS Infrared Beam Line, Nuclear Instruments and Methods, vol. A291, pp. 8-12, 1990.

Patent Status: No patent, none pending.

Applications/Spinoffs: The instrument will perform with any synchrotron or other diffraction limited source.

FOR ADDITIONAL INFORMATION: Margaret C. Bogosian, Office of Technology Transfer, Brookhaven National Laboratory, Building 902-C, Upton, New York 11973; Phone: Commercial (516)282-7338 or FTS (516) 666-7338. Refer to BNL/AA-53 R.

Transportation & Components

0409 Developing Software for a Flight-Control System—Integration of design activities reduces the incidence of errors.

0410 Langley Aircraft Landing Dynamics Facility—Aircraft landing-gear systems are tested on actual runways at operational conditions.

0411 Mechanical Backup for Fly-by-Wire Control System—A mechanical device eliminates the need for redundant fly-by-wire subsystems.

0412 Precise Autohover Control for a Helicopter—A control system attempts to maintain a constant horizontal position.

NASA Tech Brief
National Aeronautics and Space Administration
Marshall Space Flight Center, Alabama

Licensing Opportunity

Ionizable-Substance Detector

The detector nondisruptively monitors the concentration of an ionizable substance in a stream.

A device (see figure) that includes all of the conventional components of a fuel cell and electrolyzer can continuously monitor the concentration of an ionizable substance in a stream of fluid without significantly disrupting the flow or the chemical composition. Among the substances that can be monitored are hydrogen, sodium, fluorine, chlorine, oxygen, and bromine. The device can be useful in early detection of fluctuations, malfunctions, or hazards. This device is particularly useful for detecting hydrogen in a stream of water in a closed system that contains oxygen, wherein the concentration of hydrogen must not exceed a given maximum, lest the hydrogen react explosively with the oxygen. The device could also be used to monitor an exhaust stream to comply with environmental-protection requirements.

In the version of the device shown in the figure, an anode includes a catalytic layer capable of ionizing the substance to be detected (in this case, hydrogen). The cathode includes a catalytic layer capable of recombining the ions and free electrons produced at the anode. The two electrodes are separated by an ion-exchange membrane. A feed chamber in intimate contact with the anode introduces the stream that contains the substance to be detected, and a reflow chamber in intimate contact with the cathode removes the stream, including the detected hydrogen or other substance (which regains its original molecular form upon recombination of ions and electrons at the cathode).

A power source that maintains a dc potential across the ion-exchange membrane serves two purposes: (1) to conduct the free electrons produced at the anode to the cathode and (2) to supply the voltage necessary to influence the flow of ions from the anode, through the ion-exchange membrane, to the cathode. In the case of the detection of hydrogen in water, the voltage should not exceed 1.23 V; otherwise, the water could be electrolyzed.

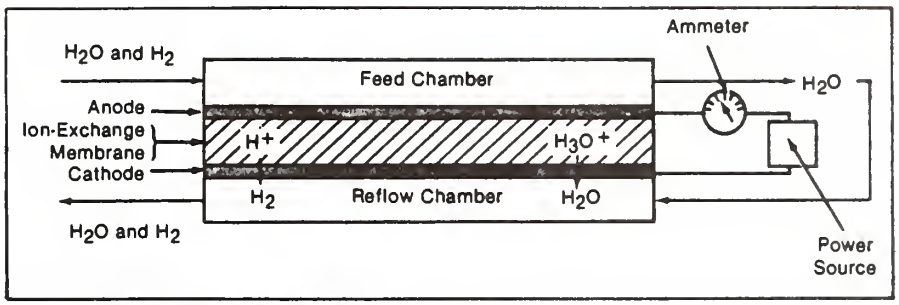

This Ionizable-Substance Detector, which includes all of the conventional components of a fuel cell and electrolyzer, measures the concentration of hydrogen in a stream of water.

As the free-electron current passes from the anode to the cathode, it is measured by an ammeter or other current-measuring device. This current is directly proportional to the amount of hydrogen or other substance being monitored. In practice, the device must be calibrated at a particular pressure, temperature, and rate of flow by use of an alternative analytical technique to measure the amount of substance that passes (in ionic form) through the detector and by comparing this amount with the measured current.

The type of catalyst in this device depends on the substance to be detected and on the operating conditions. The type of ion-exchange membrane depends on the type and size of ion to be transferred, on the operating temperature, and on the chemical effects of the ion on the membrane and vice versa. In the case of the detection of hydrogen, for example, the catalyst must be capable of ionizing the hydrogen and could be ruthenium, rhodium, palladium, iridium, or platinum. The preferred version of such a catalyst is made of platinum black bonded with polytetrafluoroethylene. The preferred ion-exchange membrane is Nafion (or equivalent).

This work was done by William McElroy and William Smith of United Technologies Corp. for **Marshall Space Flight Center.**

Title to this invention has been waived under the provisions of the National Aeronautics and Space Act [42 U.S.C. 2457(f)], to the United Technologies Corp. Inquiries concerning licenses for its commercial development should be addressed to

Stephen E. Davis
United Technologies Corp.
One Riverview Square, 7th Floor
East River Drive
East Hartford, CT 06108

Refer to MFS-28515/TN.

George C. Marshall Space Flight Center
Technology Utilization Officer Ismail Akbay
Code AT01
Marshall Space Flight Center,
AL 35812
(205) 544-2223
Patent Counsel Leon D. Wofford, Jr.
Mail Code CC01
Marshall Space Flight Center,
AL 35812
(205) 544-0024

FOR ADDITIONAL INFORMATION: *Contact: Director, Technology Transfer Division, P.O. Box 8757, BWI Airport, MD 21240; (301) 621-0100 Ext. 241*
REFER TO THE NUMBER LISTED AT THE END OF THIS ARTICLE

NASA Tech Brief
National Aeronautics and Space Administration
Marshall Space Flight Center, Alabama

Developing Software for a Flight-Control System

Integration of design activities reduces the incidence of errors.

An improved process for the development of flight-control software has been devised by integrating the conventional software-development process with the conventional control-system-analysis process. Historically, these latter two processes have been regarded as independent of each other. The integration of them reduces the costs of development dramatically, eliminates the need for reengineering, and almost eliminates production errors. The concept of the integrated design process may be applicable to the design of other control systems and of complicated hardware-and-software systems in general.

In the integrated design process, a control system is designed in three phases. The control concept is designed in the first phase, in which the control engineer sets requirements that have to be satisfied by recourse to noncontrol engineering disciplines. These include such requirements as stiffnesses of structures. The second phase involves the design and validation of the control system. This phase includes the testing of the source version of the control software by a process of computer modeling of the behavior of the entire system of control software, controlling hardware, and controlled hardware. In the third phase, the object code that is to be used in the computer or computers of the control system is generated and validated.

The approach taken in the integrated design process ensures that requirements at each stage are understood fully before engineering proceeds. The control engineer does not have to make ad-hoc modifications to an otherwise final design, and the software engineer has only to integrate the design into the computer or computers in the control system. Design errors and redesign activity are almost eradicated, and large increases in productivity are effected.

The figure illustrates the development of flight-control software by an integrated design process. To meet those engineering requirements that are oriented toward life cycles, software that effects guidance, navigation, and control functions is integrated into the flight software from the beginning. The effect is to eliminate the reengineering of software and provide a clear method of ensuring quality. Also, emphasis is placed upon the integration of subsystems in the design of the control system.

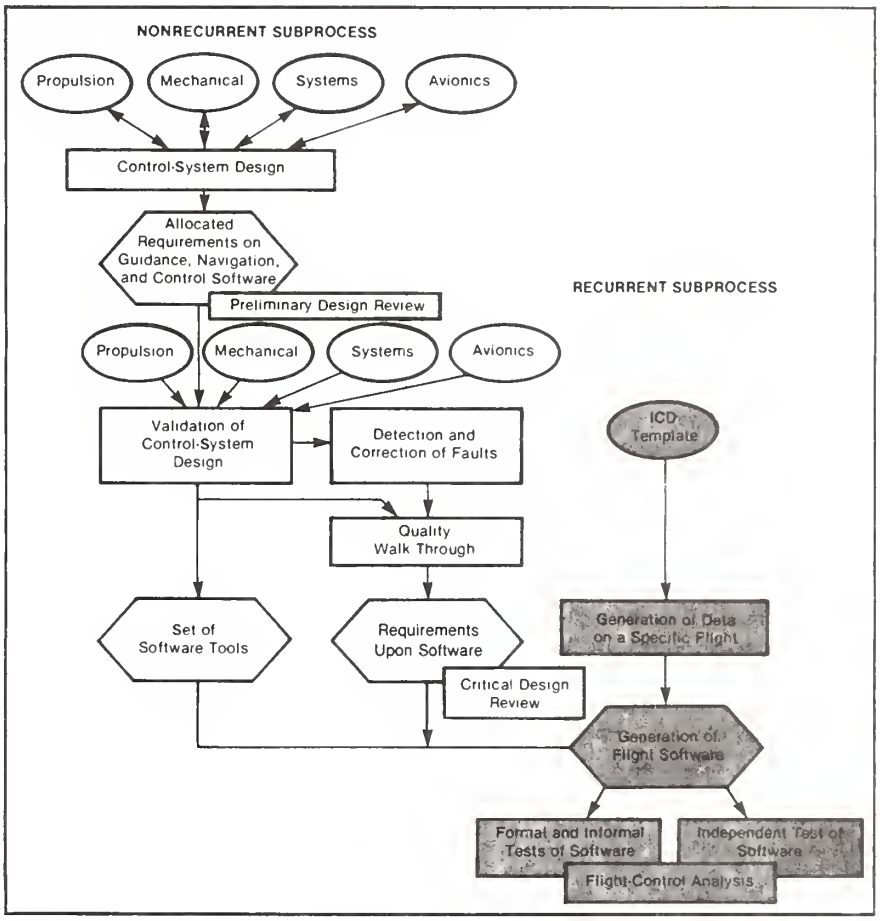

The **Process of Development of Flight Software** includes recurrent and nonrecurrent subprocesses.

The design process starts with a broad conceptual design of the control system (including provisions for guidance and navigation functions). The acceptable design of each subsystem is predicated upon the ease with which the control system can function. For example, a suitably rigid structure facilitates the development of a simple set of control algorithms; this, in turn, facilitates the required automation of the generation of the object code to be used in the computer or computers of the control system. Similarly, in the case of a spacecraft, the layout of the reaction-control subsystem can be instrumental in the design of thrustor-switching logic that provides redundancy of functions; this, in turn, obviates expensive built-in testing for the management of redundancy.

Once the design process reaches preliminary design review, the boundary conditions for a robust guidance, navigation, and control system have been set. The next step is the validation of the design, after which the initial flight source code will have been completed by the control engineer and will be ready for critical design review. At this stage, the software engineer completes the definition of requirements upon software ready for coding.

The nonrecurring component of the design process is completed with the establishment of the common set of software tools. The recurring component of the design process is simply one of generation of macro descriptive language and integration into the flight code to generate the object-code version of the flight software. The common set of software tools is then used to validate performance and post-flight analysis.

This work was done by Jonathan Murray of Martin Marietta Corp. for **Marshall Space Flight Center.**
MFS-28461/TN

FOR ADDITIONAL INFORMATION: *Contact: Director, Technology Transfer Division, P.O. Box 8757, BWI Airport, MD 21240; (301) 621-0100 Ext. 241*
REFER TO THE NUMBER LISTED AT THE END OF THIS ARTICLE

NASA Tech Brief
National Aeronautics and
Space Administration

Langley Aircraft Landing Dynamics Facility

Aircraft landing-gear systems are tested on actual runways at operational conditions.

A NASA Reference Publication reports on NASA Langley Research Center's recent upgrading of the Landing Loads Track (LLT) to improve the capability of low-cost testing of conventional and advanced landing-gear systems. The unique feature of the Langley Aircraft Landing Dynamics Facility (ALDF) is the ability to test aircraft landing-gear systems on actual runway surfaces at operational ground speeds and loading conditions. A historical overview of the original LLT is given, followed by detailed description of systems and operational capabilities of the new ALDF.

The ALDF began operation in 1985. It has the capability of testing full-size aircraft landing-gear systems under closely controlled simulated takeoff and landing conditions on actual runway surfaces. Testing landing-gear systems on the ALDF is advantageous over flight testing for such reasons as safety, economy, control of parameters, and versatility. Virtually any aircraft landing-gear system or subsystem can be accommodated on the ALDF test carriage. Novel landing-gear concepts can also be investigated, and the versatility of the facility enables testing on a variety of runway surfaces under many different simulated weather conditions. The paper gives a brief historical overview of the LLT, the facility that preceded the ALDF, and discusses how the older facility was upgraded to the present ALDF configuration. It describes the main features of the ALDF, including the high-pressure propulsion system, the test carriage, the track, the arresting-gear system, and the data-acquisition system.

This unique facility is capable of testing various types of landing-gear systems at speeds up to 220 kt (113 m/s) on a variety of runway surfaces, under all types of weather conditions. The facility has a track 2,800 ft (853 m) long with a test section 1,800 ft (549 m) long, which allows 5 s of test time at maximum speed. Test articles can be subjected to vertical loads up to 65,000 lb (2.9×10^5 N) or sink rates of 20 ft/s (6 m/s). This facility significantly increases the capability to conduct low-cost tests of conventional and advanced aircraft landing-gear systems. The capabilities facilitate testing at speeds and sizes pertinent to large transport aircraft, fighter aircraft, and the Space Shuttle Orbiter.

This work was done by Pamela A. Davis, Sandy M. Stubbs, and John A. Tanner of **Langley Research Center**. *Further information may be found in NASA RP-1189 [N87-29544], "Langley Aircraft Landing Dynamics Facility."*

Copies may be purchased [prepayment required] from the National Technical Information Service, Springfield, Virginia 22161, Telephone No. (703) 487-4650. Rush orders may be placed for an extra fee by calling (800) 336-4700.
LAR-14038/TN

FOR ADDITIONAL INFORMATION: *Contact: Director, Technology Transfer Division, P.O. Box 8757, BWI Airport, MD 21240; (301) 621-0100 Ext. 241*
REFER TO THE NUMBER LISTED AT THE END OF THIS ARTICLE

NASA Tech Brief
National Aeronautics and Space Administration
Langley Research Center, Hampton, Virginia

Mechanical Backup for Fly-by-Wire Control System

A mechanical device eliminates the need for redundant fly-by-wire subsystems.

A mechanical backup device for a fly-by-wire aircraft-control system has been designed. In a fly-by-wire control system, the pilot's control wheel is mechanically disconnected from the aerodynamic control surfaces, so that the motions of the aerodynamic surfaces do not affect the position of the pilot's wheel as they do in conventional control systems. However, when the fly-by-wire control system malfunctions, a backup system is needed. In previous fly-by-wire control systems, backup has been supplied by redundant actuators, computers, electronics, and hydraulic systems. This redundancy increased the cost and made fly-by-wire control systems impractical for small, inexpensive, general-aviation airplanes. The new design provides mechanical backup that eliminates the need for this kind of redundancy.

The main components are two linkages, as shown in the figure. One of the linkages is connected to the control column in a conventional, reversible control system. The other linkage slides inside the first linkage and is connected to the pilot's control wheel. In the normal fly-by-wire mode of operation, the two linkages slide independently of each other, and the position on the pilot's linkage is used as an input to the flight computer. The centering and feel of the pilot's control are provided by a spring attached to the pilot's linkage. The other end of the spring is connected to the pilot's trim wheel so that the pilot can position the wheel for hands-off operation.

When a malfunction occurs in the fly-by-wire control system, the pilot moves the control lever (similar to the gear-shift lever on a car) from the "engaged" to the "disengaged" position. A switch on the pilot's lever electrically disengages a conventional magnetic clutch between the actuator and the capstan, thereby mechanically disconnecting the aerodynamic surface from the actuator. The aerodynamic hinge moments then force the linkage connected to the column into a relatively fixed position.

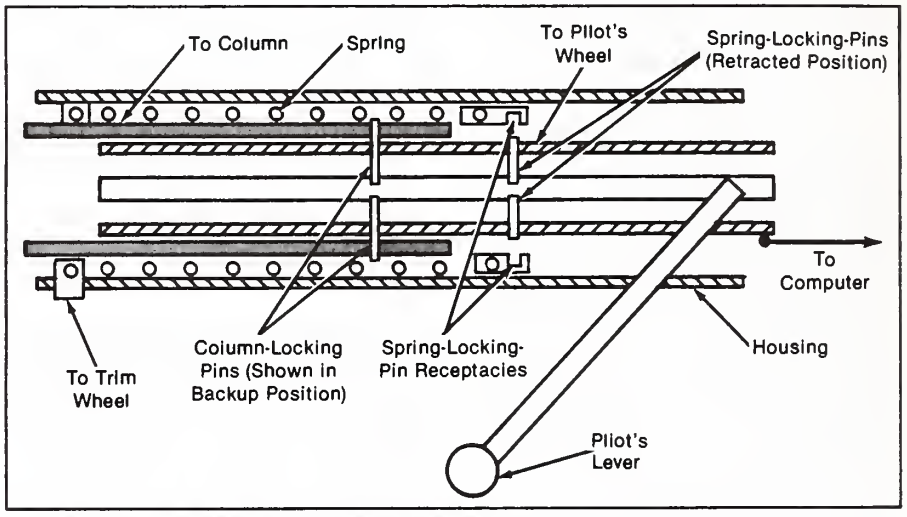

Concentric Linkages Are Principal Elements in providing a conventional, reversible, mechanical backup for a fly-by-wire control system.

In moving to the "disengaged" position, the lever also retracts the spring-locking pins (which previously connected the pilot's linkage to the centering spring) and spring-loads the column-locking pins in the extended direction. The pilot then moves the control wheel until the pins extend into the slot in the nearly stationary column linkage, thus securing the pilot's wheel to the column as shown in the figure. This mechanical arrangement provides a conventional, reversible control system for flying the airplane until a landing can be made.

The system described thus far is for the elevator-(pitch)-control loop. However, the design can easily be extended to include a fly-by-wire control for the aileron (roll). When this backup system is used, the need for multiple levels of redundancy in the fly-by-wire control system is eliminated. In addition to aircraft applications, this design can be used in control systems in which computer control is desirable but safety backup systems are required; for example, in boat rudders, engine controls in boats and automobiles, and controls in construction equipment.

This work was done by Eric C. Stewart of **Langley Research Center.**
LAR-13941/TN

FOR ADDITIONAL INFORMATION: *Contact: Director, Technology Transfer Division, P.O. Box 8757, BWI Airport, MD 21240; (301) 621-0100 Ext. 241*
REFER TO THE NUMBER LISTED AT THE END OF THIS ARTICLE

NASA Tech Brief
National Aeronautics and
Space Administration

Precise Autohover Control for a Helicopter

A control system attempts to maintain a constant horizontal position.

A report describes the development and testing of an experimental precise autohover control system for a helicopter. This work is part of a continuing effort to develop such systems for the next generation of military rotorcraft. The principal design requirement for a precise autohover control system is the ability to maintain a nearly constant horizontal position while operating in a strong wind. The requirement for precision in the maintenance of horizontal position is severe because the helicopter is expected to operate in proximity to obstacles.

The experiments were performed on a CH47 variable-stability research helicopter equipped with a position-measurement subsystem that used acceleration, velocity, and position inputs from accelerometers, rate gyroscopes, Doppler radar, a radar altimeter, and a ground-based laser tracking system. The pilot can actuate a switch to mark the reference horizontal position, which the system then attempts to maintain, even during sudden climbs or descents, or when the helicopter is turned about the vertical axis. In the experimental autohover system, measurements from the laser tracking system were transmitted to the flight computer aboard the helicopter, where they were combined with measurements from the sensors aboard the helicopter to obtain precise position feedback for use by the horizontal-position-holding system.

The report provides a brief description of the helicopter, followed by a more detailed description of the position-measuring subsystem, including the means for filtering out unwanted transients and biases. Then it describes the mathematical model used in the design of the horizontal-position-holding system. Next, the report presents data on the performance of the autohover system in strong winds. It concludes with a discussion of the relationships between the design and the observed performance and discusses the implications for future design efforts.

This work was done by W.S. Hindson and G.E. Tucker of **Ames Research Center**. *"Development and Flight Test of a Precision Autohover Capability for Tactical Rotorcraft."* *ARC-12243/TN*

FOR ADDITIONAL INFORMATION: *Contact: Director, Technology Transfer Division, P.O. Box 8757, BWI Airport, MD 21240; (301) 621-0100 Ext. 241*
REFER TO THE NUMBER LISTED AT THE END OF THIS ARTICLE

*U.S. Government Printing Office: 1992 — 311-885/60006

U.S. DEPARTMENT OF COMMERCE
National Technical Information Service
Springfield, VA 22161

NTIS ORDER FORM

Use this form ONLY to order reports designated as available from NTIS.

TELEPHONE ORDERS (703) 487-4650 FAX (703) 321-8547 TELEX 89-9405

Rush Service
1-800-553-NTIS

For Subscription Questions
(703) 487-4630

For Tracing an Order
(703) 487-4660

For Editorial Questions
(703) 487-4805

If your address label on this Tech Notes is NOT correct, call the NTIS Subscriptions Department on (703) 487-4630.

1 ADDRESS INFORMATION

Last Name .....

Title .....

Company/Organization .....

Address .....

.....

City/State/ZIP .....

Telephone Number .....

2 METHOD OF PAYMENT

☐ Charge my NTIS Deposit Account .... – .....

☐ Check/Money order enclosed payable to NTIS for $ .....

☐ Purchase order **ADD $7.50 per order** (U.S., Canada, and Mexico only)

Purchase order number .....

Charge my ☐ American Express ☐ VISA ☐ MasterCard

Account Number. ..... Exp. .....

Signature .....
(Required to validate order)

3 ORDER SELECTION (Use only for reports stated as available from NTIS)

NTIS Order Number	*Price**	*Quantity*	*Total Price*
..... /NAC	.....	.....	.....
..... /NAC	.....	.....	.....
..... /NAC	.....	.....	.....
..... /NAC	.....	.....	.....
..... /NAC	.....	.....	.....
		Handling fee	$3.00
		Total	.....

NTIS PRICE SCHEDULE *

This schedule converts into actual prices the price codes cited in those Tech Notes having a report available from NTIS.

Price Code	*Price*
A01	$9.00
A02	12.50
A03	17.00
A04 through A05	19.00
A06 through A09	26.00
A10 through A13	35.00
A14 through A17	43.00
A18 through A21	50.00
A22 through A25	59.00
A99	Contact NTIS for price

These prices are for customers in U.S., Canada, and Mexico. Other addresses should write for the price listing, number PR-360-4.

Prices effective October 1, 1991

10/91

U.S. DEPARTMENT OF COMMERCE
National Technical Information Service
Springfield, VA 22161

NTIS ORDER FORM

Use this form ONLY to order reports designated as available from NTIS.

TELEPHONE ORDERS (703) 487-4650 FAX (703) 321-8547 TELEX 89-9405

Rush Service
1-800-553-NTIS

For Subscription Questions
(703) 487-4630

For Tracing an Order
(703) 487-4660

For Editorial Questions
(703) 487-4805

If your address label on this Tech Notes is NOT correct, call the NTIS Subscriptions Department on (703) 487-4630.

1 ADDRESS INFORMATION

Last Name .....

Title .....

Company/Organization .....

Address .....

.....

City/State/ZIP .....

Telephone Number .....

2 METHOD OF PAYMENT

☐ Charge my NTIS Deposit Account .... – .....

☐ Check/Money order enclosed payable to NTIS for $ .....

☐ Purchase order **ADD $7.50 per order** (U.S., Canada, and Mexico only)

Purchase order number .....

Charge my ☐ American Express ☐ VISA ☐ MasterCard

Account Number. ..... Exp. .....

Signature .....
(Required to validate order)

3 ORDER SELECTION (Use only for reports stated as available from NTIS)

NTIS Order Number	*Price**	*Quantity*	*Total Price*
...../NAC	.....	.....	.....
...../NAC	.....	.....	.....
...../NAC	.....	.....	.....
...../NAC	.....	.....	.....
...../NAC	.....	.....	.....

Handling fee ... $3.00

Total .....

NTIS PRICE SCHEDULE *

This schedule converts into actual prices the price codes cited in those Tech Notes having a report available from NTIS.

Price Code	*Price*
A01	$9.00
A02	12.50
A03	17.00
A04 through A05	19.00
A06 through A09	26.00
A10 through A13	35.00
A14 through A17	43.00
A18 through A21	50.00
A22 through A25	59.00
A99	Contact NTIS for price

These prices are for customers in U.S., Canada, and Mexico. Other addresses should write for the price listing, number PR-360-4.

Prices effective October 1, 1991

10/91

- Agriculture & Food
- Computers
- Electrotechnology
- Energy
- Engineering
- Environmental Science & Technology
- Manufacturing, Machinery, & Tools
- Materials
- Medicine & Biology
- Natural Resources Technology & Engineering
- Physical Sciences
- Transportation & Components

Route To:

PENN STATE UNIVERSITY LIBRARIES
A0000720104 40

:PARTMENT OF COMMERCE
al Technical Information Service
ld, Va. 22161

. BUSINESS
or Private Use, $300

AN EQUAL OPPORTUNITY EMPLOYER

BULK RATE
POSTAGE & FEES PAID
NTIS
Permit No. G-292